

Bedeutung von Wirtszellproteasen für die Infektion mit dem Severe Acute Respiratory Syndrome-Coronavirus (SARS-CoV)

Von der Naturwissenschaftlichen Fakultät der Gottfried Wilhelm Leibniz
Universität Hannover zur Erlangung des Grades

DOKTORIN DER NATURWISSENSCHAFTEN
Dr. rer. nat.

genehmigte Dissertation
von
Dipl.-Biol. Ilona Glowacka
geboren am 30. Juni 1981 in Treptow, Polen

2011

Referent: Prof. Dr. Stefan Pöhlmann

Medizinische Hochschule Hannover

Korreferent: Prof. Dr. Thomas Pietschmann

TWINCORE, Zentrum für Experimentelle und Klinische Infektionsforschung
GmbH

Tag der Promotion: 23.02.2011

Schlagwörter: SARS-Coronavirus, Spike-Protein, Cathepsin, Furin, TMPRSS2,
ACE2, proteolytische Spaltung

Keywords: SARS-coronavirus, spike protein, cathepsin, furin, TMPRSS2,
ACE2, proteolytic cleavage

Kurzzusammenfassung

Das hochpathogene *severe acute respiratory syndrome*-Coronavirus (SARS-CoV) infiziert Zellen über die Interaktion seines Oberflächenproteins Spike (SARS-S) mit der Karboxypeptidase *angiotensin-converting enzyme 2* (ACE2). Die Expression von ACE2 schützt vor Lungenpathogenese und wird durch das SARS-S negativ reguliert. Es ist daher möglich, dass die Interaktion vom SARS-S mit ACE2 die SARS-Pathogenese fördert. Das humane Erkältungs-Coronavirus-NL63 verwendet ebenfalls ACE2 für den Zelleintritt, ist aber nur wenig pathogen. Im ersten Teil der Arbeit sollte daher die Hypothese überprüft werden, ob sich das SARS-S und NL63-S in der Interferenz mit der ACE2-Expression unterscheiden, was zur unterschiedlichen Pathogenität dieser Viren beitragen könnte. Ein besonderer Fokus sollte dabei auf die Wirtszellprotease TACE/ADAM17 gelegt werden, da dokumentiert wurde, dass die SARS-S-Bindung an ACE2 die TACE/ADAM17-abhängige Spaltung des Rezeptors induziert.

Die Untersuchungen haben gezeigt, dass rekombinantes SARS-S mit höherer Effizienz an ACE2 bindet als NL63-S. Eine Herabregulierung der ACE2-Expression wurde nur in SARS-CoV- jedoch nicht in HCoV-NL63-infizierten Zellen beobachtet. Die Herabregulierung von ACE2 durch rekombinantes SARS-S wurde durch die Blockierung von TACE/ADAM17 vollständig inhibiert, die Inhibition der Protease hatte jedoch kaum Einfluss auf die virale Vermehrung in Zellkultur. Die verminderte ACE2-Expression im Kontext der SARS-CoV-Infektion ist daher vermutlich auf die SARS-S-induzierte ACE2-Proteolyse zurückzuführen. Dieser Prozess ist für die virale Ausbreitung verzichtbar, könnte jedoch zur viralen Pathogenese beitragen.

Für den erfolgreichen Zelleintritt ist die proteolytische Aktivierung des SARS-S durch Wirtszellproteasen essentiell. Die Wirtszellprotease TMPRSS2 wird in Lungengewebe exprimiert und aktiviert das Influenza-Virus Hämagglutinin, das einen ähnlichen Aufbau zeigt wie das SARS-S. Im zweiten Teil der Arbeit sollte untersucht werden, ob das SARS-S durch TMPRSS2 gespalten wird und, ob die Spaltung das SARS-S aktiviert. Es konnte gezeigt werden, dass das SARS-S in TMPRSS2-koexprimierenden Zellen gespalten wird und dabei eine lösliche Form des S-Proteins entsteht. Das lösliche S-Protein verhindert die Antikörper-Neutralisation von Viren und könnte die Immunkontrolle des Virus in infizierten Personen vermindern. Nach Expression von TMPRSS2 auf Zielzellen wurde die Aktivierung vom SARS-S für die Zell-Zell- und Virus-Zellfusion beobachtet. Schließlich konnte gezeigt werden, dass Typ II Pneumozyten, wichtige SARS-CoV-Zielzellen, ACE2 und TMPRSS2 koexprimieren. TMPRSS2 könnte daher die virale Ausbreitung in infizierten Personen über unterschiedliche Mechanismen fördern.

Abstract

The highly pathogenic severe acute respiratory syndrome-coronavirus (SARS-CoV) infects cells by the interaction of the surface protein spike (SARS-S) with the carboxypeptidase angiotensin-converting enzyme 2 (ACE2). The expression of ACE2 protects from lung injury and is negatively regulated by SARS-S. The interaction of SARS-S with ACE2 might therefore promote SARS pathogenesis. The human coronavirus-NL63 (HCoV-NL63), causative agent of common colds, also employs ACE2 for cell entry, but displays low pathogenicity. In the first part of this study it was analysed whether SARS-S and NL63-S differentially interfere with ACE2 expression, which might account for the differential pathogenicity of these viruses. One focus was on the host cell protease TACE/ADAM17, which was shown to induce ACE2 cleavage upon SARS-S binding.

The analysis revealed that recombinant SARS-S binds ACE2 with higher efficiency than NL63-S. The downregulation of ACE2 expression was detected in SARS-CoV- but not in NL63-infected cells. Furthermore, the downregulation of ACE2 by recombinant SARS-S was abrogated by an inhibitor of TACE/ADAM17, but inhibition of the protease did not modulate viral spread in cell culture. The diminished ACE2 expression in the context of SARS-CoV infection might therefore be due to SARS-S-induced ACE2 proteolysis. This process is dispensable for viral entry, but could contribute to viral pathogenesis.

The proteolytic activation of SARS-S by host cell proteases is essential for infectious cell entry. The host cell protease TMPRSS2, which is expressed in lung tissue, activates the influenza virus hemagglutinin, which exhibits a domain structure similar to SARS-S. Therefore, the second part of this study addressed whether the SARS-S is cleaved by TMPRSS2 and whether cleavage activates SARS-S.

It could be demonstrated that SARS-S is cleaved in TMPRSS2-co-expressing cells and that cleavage generates a soluble form of the S-protein. The soluble S-protein diminished antibody neutralisation of the SARS-S-bearing viruses and could reduce viral control by the humoral immune response in infected patients. In contrast, expression of TMPRSS2 on target cells activated SARS-S for cell-cell and virus-cell fusion. Finally, ACE2 and TMPRSS2 were found to be co-expressed by type II pneumocytes, which represent important SARS-CoV target cells, suggesting that TMPRSS2 could promote the spread of SARS-CoV in infected patients by different mechanisms.

Inhaltsverzeichnis

Kurzzusammenfassung

Abstract

Inhaltsverzeichnis	1
1. Einleitung	3
1.1 Severe Acute Respiratory Syndrome (SARS)	3
1.2 Coronaviridae	5
1.2.1 Allgemein	5
1.2.2 Phylogenetische und Taxonomie	5
1.2.3 Allgemeiner Aufbau und Morphologie	6
1.3 Severe Acute Respiratory Syndrome-Coronavirus	7
1.3.1 Genomaufbau	7
1.3.2 Viraler Vermehrungszyklus	8
1.3.3 Zelleintritt vom SARS-CoV	9
Struktur und Aufbau des Spike-Proteins	9
SARS-Spike ist ein Klasse I Fusionsprotein	10
Die Interaktion vom SARS-S mit <i>angiotensin-converting enzyme 2</i> vermittelt den Zelleintritt	11
SARS-S-getriebene Membranfusion	12
1.3.4 Bedeutung von Wirtszellproteasen für den SARS-CoV-Eintritt	13
Proteolytische Spaltung des SARS-Spike durch Cathepsin L	14
Proteolytische Spaltung des SARS-Spike durch	
Typ II Transmembran-Serinproteasen	15
Proteolytische Spaltung des SARS-Spike durch Furin	17
Proteolyse von ACE2	19
Zusammenfassung	20
2. Zielsetzung	23
3. Manuskripte	24
Publikationsstadium	24
- Differential Downregulation of ACE2 by the Spike Proteins of Severe Acute Respiratory Syndrome Coronavirus and human Coronavirus NL63	25
- Different host cell proteases activate the SARS-coronavirus spike-protein for cell-cell and virus-cell fusion	33

- Evidence that TMPRSS2 activates the SARS-coronavirus spike-protein for membrane fusion and reduces viral control by the humoral immune response	64
4. Diskussion	99
5. Literaturverzeichnis	113
6. Anhang	123
Abkürzungsverzeichnis	131
Danksagung	134
Lebenslauf	135
Publikationen	136
Erklärung	137

1. Einleitung

1.1 Severe Acute Respiratory Syndrome (SARS)

Das *severe acute respiratory syndrome* (SARS) trat erstmals im November 2002 in der südchinesischen Provinz Guangdong auf [Zhong *et al.*, 2003] und breitete sich anschließend in Asien und Kanada aus. SARS war die erste Epidemie des 21. Jahrhunderts. Der Ausbruch dieser atypischen Lungenentzündung wurde durch die Weltgesundheitsorganisation WHO (*World Health Organization*) im Februar 2003 offiziell bestätigt [WHO, 2003]. Die Inkubationszeit betrug 2-10 Tage und es traten hohes Fieber, trockener Husten, Atemnot, Kurzatmigkeit und Kopfschmerzen auf. Ein Arzt aus Guangdong verschleppte die Erkrankung nach Hongkong, wo er in einem Hotel mehrere Menschen infizierte. Diese wiederum verbreiteten die Erkrankung lokal und international, unter anderem nach Toronto, Singapur und Vietnam.

Im März 2003 wurde durch die WHO ein internationales Forschungsnetzwerk zusammengestellt, um die Ursache für SARS zu ergründen. Anhand der Elektronenmikroskopie wurde in mehreren Laboratorien ein neues Coronavirus als verursachendes Agens von SARS identifiziert [Drosten *et al.*, 2003; Ksiazek *et al.*, 2003; Peiris *et al.*, 2003a] und kurz darauf das Genom durch das Verfahren des *high-throughput sequencing* entschlüsselt [Marra *et al.*, 2003; Rota *et al.*, 2003]. Die Bestätigung der Koch'schen Postulate modifiziert nach Rivers [Rivers, 1937] erfolgte am 15. Mai 2003 durch Fouchier und Kollegen [Fouchier *et al.*, 2003]. Die drei untersuchten Kriterien waren: (i) Erzeugung einer Erkrankung im gesunden Wirt, (ii) die Reisolierung des Virus und (iii) die Detektion einer spezifischen Immunantwort gegen das Virus [Fouchier *et al.*, 2003]. Folglicherweise galt das SARS-CoV (SARS-CoV) als Erreger der neuen Lungenerkrankung [Kuiken *et al.*, 2003]. Durch die strikte Isolierung der Patienten, Reiseeinschränkung und die Aufklärung der Öffentlichkeit konnte die Ausbreitung von SARS (Abb. 1) trotz fehlender Behandlungsmöglichkeiten zeitnah eingeschränkt werden. Im Juli 2003 wurden keine Übertragungen zwischen Personen mehr festgestellt und daher wurde die Epidemie durch die WHO für beendet erklärt. Insgesamt wurden 8098 infizierte Patienten registriert, von denen 774 in 29 Ländern an der Krankheit verstarben [Stadler, 2003]. Im März 2003 publizierten Wissenschaftler die Isolierung eines SARS-CoV-verwandten Virus aus Zibetkatzen (*Paguma larvata*) und Marderhunden (*Nyctereutes procyonoides*), welche in Südchina als eine Delikatesse angesehen und auf Tiermärkten verkauft werden. Zudem wurde statistisch belegt, dass Patienten der frühen Phase der Epidemie gehäuft mit exotischen Tieren in Kontakt standen [Xu *et al.*, 2004]. Diese Befunde legten eine

zoonotische Transmission des Virus von den genannten Tierspezies auf den Menschen nahe [Guan et al., 2003].

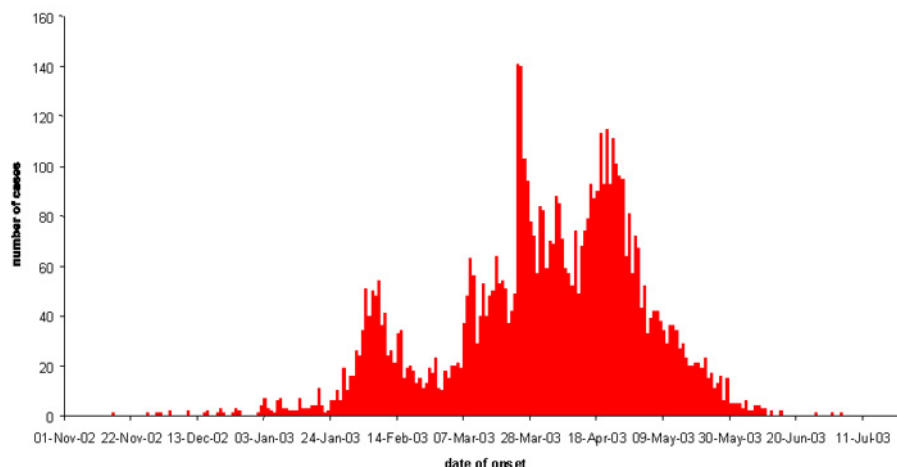


Abbildung 1: Registrierte SARS-Erkrankungen weltweit während der Epidemie von November 2002 bis Juli 2003 [<http://www.who.int/csr/sars/epicurve/epiindex/en/>].

Im Jahr 2005 wurden in mehreren Publikationen Fledermäuse als potentielle Reservoirspezies diskutiert. Beispielsweise wurde in Flughunden der Gattung *Miniopterus spp* ein neues Coronavirus identifiziert, dessen Spike-Protein auf Nukleotidebene zu 41% Sequenzhomologie mit dem SARS-Spike-Protein aufweist [Poon et al., 2005]. Auch Fledermäuse der Gattung *Rhinolophus* wiesen Infektionen mit SARS-ähnlichen Coronaviren auf [Li et al., 2005]. Spezifisch in *Rhinolophus sinicus* (Abb. 2) wurde genetisches Material identifiziert, welches dem humanen SARS-CoV stark ähnelt [Lau et al., 2005]. Aufgrund dieser Beobachtungen wurde postuliert, dass die Interspezies-Transmission in der Genese der SARS-Epidemie über *Rhinolophus sinicus* erfolgte und die Zibetkatze als Zwischenwirt diente [Lau et al., 2005].



Abbildung 2: Potentielle tierische Reservoirspezies und Zwischenwirte vom SARS-CoV. (A) Fledermaus der Spezies *Rhinolophus sinicus* und potentielles Reservoir vom SARS-CoV [http://focosi.altervista.org/Rhinolophus_sinus.jpg]. (B) Schleichkatze der Spezies *Paguma larvata* wird als potentieller Vermehrungswirt des SARS-CoV diskutiert [<http://www.mountain-tai.com.cn/UploadFiles/image/tsdw/huamianli.jpg>].

1.2 Coronaviridae

1.2.1 Allgemein

Coronaviren sind artspezifisch und können Menschen und verschiedene Säugetiere infizieren. Humane Coronaviren wurden 1965 von David Tyrrell und Mark Bynoe in Patienten mit Erkältungssymptomatik entdeckt [Tyrrell und Bynoe, 1965] und 1968 als eigene Virusfamilie definiert [Tyrrell *et al.*, 1968; Siddell *et al.*, 1983].

Viren, die ein RNS-Genom tragen, sind die häufigsten Erreger von Erkältungen. Die humanen Coronaviren 229E und OC43 verursachen beim Menschen Erkrankungen des oberen Respirationstraktes. Ihnen werden bis zu 30% der Fälle von Schnupfen beim Menschen zugeschrieben. Das humane Coronavirus-NL63 (HCoV-NL63), ein weiteres Erkältungsvirus, ist zudem in seltenen Fällen mit akuten Atemwegserkrankungen assoziiert. Charakteristisch dabei ist die Infektion des unteren Respirationstraktes [van der Hoek *et al.*, 2004]. Die tierpathogenen Coronaviren hingegen verursachen hochvirulente Infektionen mit teilweise massiver respiratorischer und gastrointestinaler Symptomatik [Holmes, 2003]. Das SARS-CoV ist der einzige Vertreter der Coronaviren, der beim Menschen Infektionen mit einer Mortalität von ca. 10% verursacht.

1.2.2 Phylogenie und Taxonomie

Die Familie der *Coronaviridae* gehört der Ordnung der Nidovirales an [Gorbalenya *et al.*, 2006]. Die Subfamilie der *Coronavirinae* wurde erst kürzlich durch das *International Committee of Taxonomy of Viruses* (ICTV) vorgeschlagen und in drei Genera (*Alpha-, Beta- und Gammacoronavirus*) unterteilt (Abb. 3). Zu den Alpha- und Betacoronaviren gehören humanpathogenen Viren wie auch Säugetieviren. Zu den Gammacoronaviren zählen vorrangig pathogene Vogelviren [Carstens, 2009]. Die drei Genera weisen auf die Coronavirusgruppen I, II und III hin [Cavanagh, 1997; Gonzalez *et al.*, 2003; Masters, 2006]. Die Alphacoronaviren HCoV-NL63 und HCoV-229E und die Betacoronaviren HCoV-OC43 und HCoV-HUK1 sind typische Vertreter humaner Coronaviren, die respiratorische Erkrankungen verursachen [Larson *et al.*, 1980; Isaacs *et al.*, 1983; van der Hoek *et al.*, 2006; Vabret *et al.*, 2003, 2008]. Das HCoV-NL63 wurde 2004 von van der Hoek und Mitarbeitern beschrieben [van der Hoek *et al.*, 2004] und weist die größte genetische Identität mit dem HCoV-229E auf.

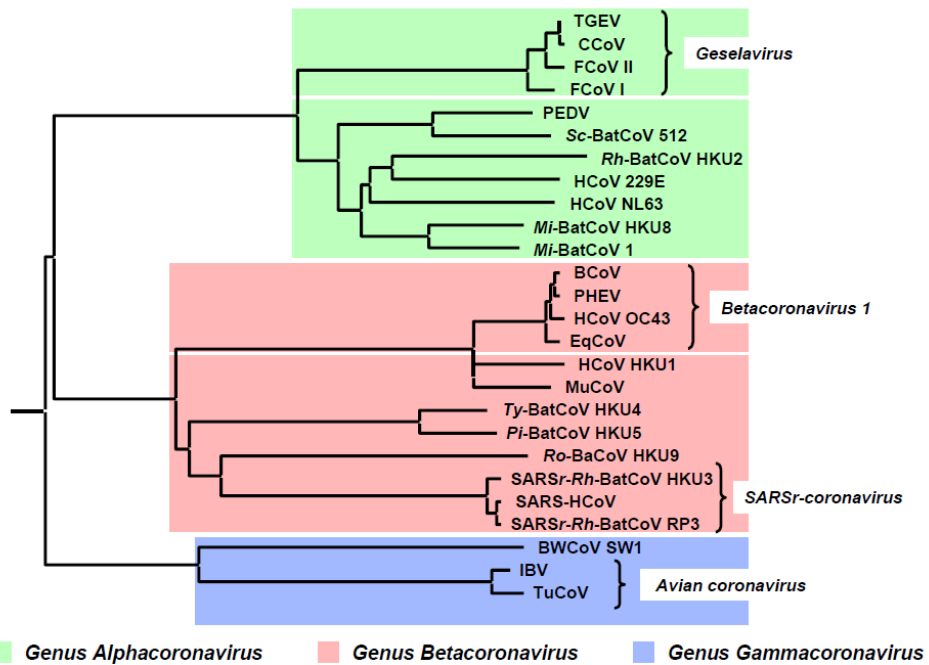


Abbildung 3: Phylogenetische Darstellung der Coronaviren. Die Analyse der Verwandtschaftsverhältnisse erfolgte basierend auf der Aminosäuresequenz der RNS-abhängigen RNS-Polymerase [de Groot et al., 2008].

Anfangs wurde angenommen, dass das SARS-CoV einer neuen Coronavirus-Gruppe angehören würde [Marra et al., 2003; Rota et al., 2003]. Studien der Antikörperreaktivität und der Sequenzvergleiche haben jedoch gezeigt, dass das SARS-CoV als Vertreter der Gruppe II Coronaviren klassifiziert werden muss [Eikmann et al., 2003; Snijder et al., 2003]. Erst kürzlich wurde das SARS-CoV mit dem SARS-verwandten *Rhinophorus* BatCoV zusammengelegt und somit der Spezies SARS-rCoV zugeordnet, die nun den Betacoronaviren angehört (Abb. 3) [Carstens, 2010]. Laut der Klassifizierung des ICTV werden Coronaviren nur dann als separate Spezies betrachtet, wenn sie sich weniger als 90% auf der Aminosäureebene der sieben Nichtstrukturproteine 3, 5, 12, 13, 14, 15 und 16 gleichen [de Groot et al., 2008; Carstens, 2010].

1.2.3 Allgemeiner Aufbau und Morphologie

Coronaviren sind mit einem Durchmesser von 60 bis 160 nm die größten bekannten umhüllten RNS-Viren und pleomorph bzw. sphärisch geformt [Ksiazek et al., 2003; Peiris et al., 2003a]. Das einzelsträngige Plusstrang-RNS-Genom beträgt 27-32 kb und liegt als helikales Nukleokapsid im Inneren des Partikels assoziiert mit den N-Proteinen

vor. Es interagiert mit den in die virale Hüllmembran eingelagerten M-Proteinen. Zwei weitere glykosylierte Proteine sind in die virale Hülle eingebettet: Das Spike (S)-Protein mit einer Größe von ca. 180 bis 200 kDa, das das Erscheinungsbild der Coronaviren im Elektronenmikroskop prägt, und das E-Protein mit einer Größe von 9 bis 12 kDa, das für die Partikelbildung notwendig ist (Abb. 4A) [Stadler *et al.*, 2003]. Die charakteristische Oberflächenmorphologie der Coronaviren wird durch das Spike-Protein erzeugt, das in elektronenmikroskopischen Aufnahmen als „Strahlenkranz“ (lateinisch *corona*) sichtbar ist (Abb. 4B).



Abbildung 4: Morphologie der Coronaviren. (A) Schematische Darstellung des Coronavirusaufbaus mit der Lipidmembran und den inserierten Strukturproteinen (S, M, E) und dem, das RNS-Genom beinhaltenden, Nukleokapsid [Abbildung modifiziert aus Holmes und Enjuanes, 2003]. (B) Elektronenmikroskopische Aufnahme vom SARS-CoV. Die keulenartigen Fortsätze werden durch das Spike-Protein erzeugt [Stadler *et al.*, 2003].

1.3 Severe Acute Respiratory Syndrome-Coronavirus

1.3.1 Genomaufbau

Bei dem SARS-Coronavirus Genom handelt es sich um eine polyzistrone Genomstruktur mit einem einzelsträngigen Plusstrang-RNS, die 29727 Nukleotide (den (3')Poly(A)-Schwanz ausgeschlossen) umfasst [Marra *et al.*, 2003; Rota *et al.*, 2003]. Die RNS ist infektiös und kodiert für insgesamt 14 offene Leserahmen (ORFs) [Thiel *et al.*, 2003]. Zwei große 5'-terminale ORFs, 1a und 1b, stellen das Replikasegen dar, welches die Proteine für die virale RNS-Synthese kodiert. Die restlichen 12 ORFs kodieren die vier Strukturproteine S, M, N und E und acht akzessorische Proteine, deren Funktion teilweise noch unbekannt ist (Abb. 5) [Ziebuhr *et al.*, 2004].

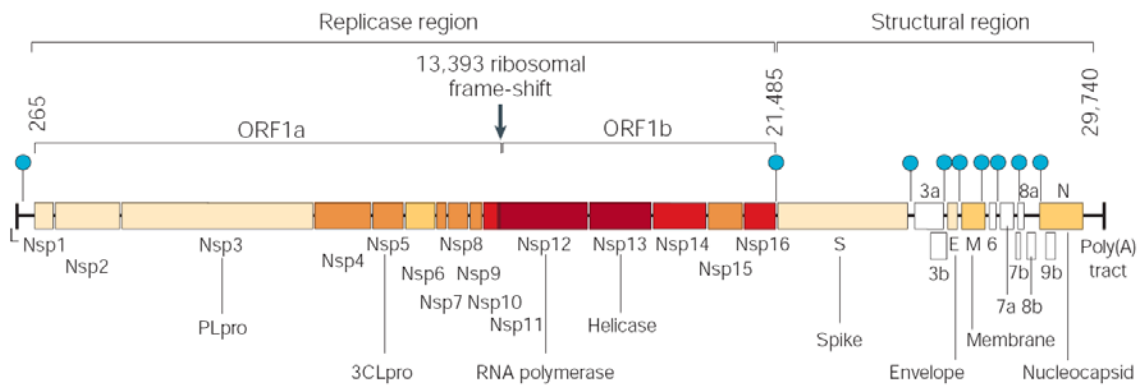


Abbildung 5: Genomaufbau des SARS-CoV. Dargestellt sind die Replikase- und die Strukturregion zusammen mit den Spaltprodukten in ORF1a und ORF1b. Die Position der *leader*-Sequenz (L), der (3')Poly(A)-Schwanz sowie die Stelle der ribosomalen Rasterverschiebung sind eingezzeichnet. Die akzessorischen Proteine sind durch weiße Kästchen gekennzeichnet. Die blauen Punkte stellen die Positionen der neun transkriptionsregulierenden Sequenzen (TRSs) dar, die spezifisch für das SARS-CoV sind (5'ACGAAC3') [Thiel et al., 2003; Stadler et al., 2003].

Die Synthese von acht subgenomischen mRNS-Segmenten ist ein typisches Merkmal der SARS-CoV-Replikation. Zur RNS-Transkription und -Regulierung ist die transkriptionsregulierende Sequenz (TRSs) bei Coronaviren von besonderer Bedeutung. Dieses Motiv ist jedem translatierten ORF vorangestellt [Lai und Holmes, 2001]. Als Thiel und Kollegen 2003 die acht isolierten subgenomischen RNS-Segmente am 5' Ende sequenzierten, identifizierten sie eine konservierte Sequenz (5'ACGAAC3') als mögliches TRSs [Thiel et al., 2003]. Rota et al. hingegen schlugen eine andere TRS vor (5'C UAA AAC3') und Marra et al. wiederum diskutierten 5'AAACGAAC3' als TRS [Marra et al., 2003 Rota et al., 2003]. Letzteres Motiv war jedoch nicht allen SARS-CoV-Genen vorangestellt und Hinweise auf die Funktion wurden noch nicht erbracht.

1.3.2 Viraler Vermehrungszyklus

Das Spike-Protein des SARS-CoV vermittelt die Bindung an den zellulären Rezeptor *angiotensin-converting enzyme 2* (ACE2) [Li et al., 2003] und die nachfolgende Fusion der viralen Membran mit der begrenzenden Membran von Wirtszellendosomen. Das Nukleokapsid wird nach der Membranfusion in das Zytoplasma freigesetzt [Hofmann und Pöhlmann, 2004], wo das Virus die Synthesekapazität der Wirtszelle für seine Vermehrung nutzen kann.

Das SARS-CoV durchläuft seinen Replikationszyklus assoziiert an zytoplasmatische Vesikel, die von einer Doppelmembran umgeben werden [Snijder *et al.*, 2006]. Im ersten Schritt erfolgt die Translation der genomische RNS (mRNS), wobei aufgrund einer ribosomalen Leserasterverschiebung die zwei Polyproteine pp1a und pp1ab als erste Produkte entstehen. Diese werden durch ihre autoproteolytische Aktivität in die einzelnen Replikaseproteine gespalten, die einen Replikations/Transkriptions-Komplex bilden. Innerhalb dieses Komplexes wird das virale Genom als Vorlage zur Herstellung einer negativsträngigen RNS verwendet, welche wiederum als Matrize zur Generierung des positivsträngigen viralen Genoms dient [Ziebuhr, 2004]. Die *leader*-Sequenz am 5' Ende des Genoms wird während der diskontinuierlichen Transkription jeder der acht subgenomischen (sg) RNS vorangestellt. Die Transkription dieser negativsträngigen sg RNS wird am 3' Ende des Genoms initiiert und endet an den TRSs, welche sich stromaufwärts der jeweiligen ORFs befinden [Thiel *et al.*, 2003; Sawicki *et al.*, 2007]. Durch Basenpaarung und anschließende Transkription werden diese Sequenzabschnitte in die komplementäre *leader* TRS generiert [Du *et al.*, 2009; Perlman und Netland, 2009]. Diese negativsträngigen sg RNS dienen als Matrize für die Produktion der sg mRNS, die in die vier Struktur- und die restlichen acht Nichtstrukturproteine translatiert werden. Das N-Protein und die genomische RNS interagieren im Zytoplasma zum Nukleokapsid, das im ER-Golgi intermediären Kompartiment (ERGIC) in virale Partikel verpackt wird, wohin die E-, M- und S-Proteine während der Biogenese transportiert werden. Das N-Protein interagiert mit dem M-Protein, um die Assemblierung der Viruspartikel zu initiieren, gefolgt von der Knospung viraler Partikel in das Lumen des ERGIC [Stertz *et al.*, 2007]. Die Freisetzung der Viruspartikel erfolgt schließlich durch Exozytose.

1.3.3 Zelleintritt vom SARS-CoV

Struktur und Aufbau des Spike-Proteins

Das Spike-Protein des SARS-CoV fungiert als Schlüssel zur Wirtszelle. Es spielt eine wichtige Rolle bei der Virus-Interaktion mit dem Rezeptor ACE2 und bestimmt wesentlich den Zelltropismus des SARS-CoV [Li *et al.*, 2003; Hoffmann *et al.*, 2004a,b]. Mit einer Größe von 1255 Aminosäuren ist das S-Protein das größte Strukturprotein des Virus. Unter dem Elektronenmikroskop ist es deutlich als 20 nm lange, keulenartige Oberflächenprojektion auf der viralen Membran zu erkennen [Stadler *et al.*, 2003]. Das S-Protein ist ein virales Klasse I Fusionsprotein (siehe Abschnitt: SARS-Spike ist ein Klasse I Fusionsprotein) [Bosch *et al.*, 2003; Rota *et al.*, 2003] und besitzt

23 N-Glykosylierungsstellen [Hofmann und Pöhlmann, 2004]. Das N-terminale Signalpeptid (Abb. 6) ist für die Translokation in das raue endoplasmatische Retikulum verantwortlich, wo das S-Protein gefaltet und posttranslational durch mannosereiche Zucker modifiziert wird. Nach dem Transport des S-Proteins in den Golgi-Apparat werden diese teilweise in komplexe Glykane prozessiert [Nal *et al.*, 2005]. Ein dibasisches Motiv im zytoplasmatischen Teil fördert die Akkumulation des S-Proteins im ERGIC und der Golgi-Region [McBride *et al.*, 2007], wo die unreifen Viruspartikel zusammengebaut werden [Stertz *et al.*, 2007; Siu *et al.*, 2008]. Die Bildung neuer Viruspartikel wird durch das M-Protein, das E-Protein und das N-Protein vorangetrieben [Huang *et al.*, 2004; Hsieh *et al.*, 2005; Siu *et al.*, 2008], wobei das M-Protein die Retention des S-Proteins im ERGIC bewirkt [Voss *et al.*, 2009]. In Coronaviren rekrutiert das M-Protein zudem das N- und das E-Protein zum ERGIC und ist für das Verpacken des Nukleokapsids in neue Viruspartikel verantwortlich [Klumperman *et al.*, 1994; Opstelten *et al.*, 1995].

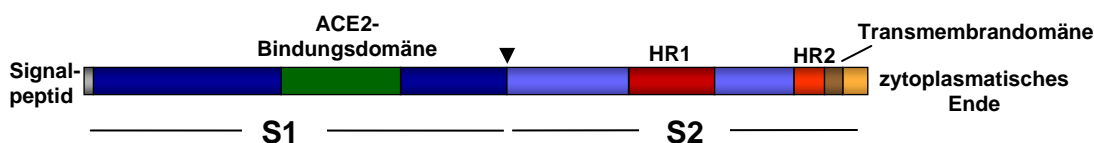


Abbildung 6: Schematische Darstellung des S-Proteins. Das N-terminale Signalpeptid ist für die Translokation ins raue endoplasmatische Retikulum (ER) verantwortlich. Die S1-Domäne beinhaltet die ACE2-Bindungsdomäne, welche für den Viruseintritt in die Wirtszelle wichtig ist. Die S2-Domäne trägt funktionelle Elemente, die für die Membranfusion essentiell sind. Eine mögliche Spaltstelle für Wirtszellproteasen ist durch eine Pfeilspitze gekennzeichnet.

Das SARS-S-Protein zählt zu der Gruppe der Klasse I Fusionsproteine [Bosch *et al.*, 2003] und ist mit Glykoproteinen (GP) anderer umhüllter Viren wie dem gp160 des humanen Immundefizienzvirus-1 (HIV-1), dem GP des Ebola Virus, dem Hämagglutinin des Influenza Virus und dem F-Protein des Simian Virus 5 (SV5) verwandt [Baker *et al.*, 1999; Colman und Lawrence, 2003; Hofmann und Pöhlmann, 2004].

SARS-Spike ist ein Klasse I Fusionsprotein

Virale Fusionsproteine werden aufgrund ihrer charakteristischen Postfusionskonformation in drei Klassen unterteilt (I-III). Klasse I Fusionsproteine zeichnen sich durch den Besitz konservierter α -helikaler Regionen aus; bekannte virale Fusionsproteine der Klasse I sind das gp41 des humanen Immundefizienz-Virus, das Glykoprotein des Ebola Virus und das Hämagglutinin des Influenza Virus [Kielian und Ray, 2006]. Klasse II Fusionsproteine tragen charakteristische β -Faltblattstrukturen und werden bei Flavi- und Alphaviren gefunden. Die Fusionsproteine der Herpes- und

Rhabdoviren werden schließlich der Klasse III zugeordnet und zeichnen sich durch den Besitz markanter α -helikaler Regionen und β -Faltblattstrukturen aus [Kielian, 2006; Backovic und Jardetzky 2009].

Ein weiteres Merkmal der Klasse I Fusionsproteine ist die Ausbildung von Homotrimeren, welche vertikal aus der viralen Membran ragen [Skehel und Wiley, 2000; Harrison, 2005], während Klasse II Fusionsproteine typischerweise als Dimere vorliegen, die parallel zur viralen Membran orientiert sind. Auch die Domänenorganisation von Klasse I Fusionsproteinen ist charakteristisch: Sie besitzen eine N-terminale Oberflächendomäne, die mit dem zellulären Rezeptor interagiert, und eine C-terminale Transmembrandomäne, die die Fusion mit der Wirtszellmembran vermittelt [Kielian und Rey, 2006]. In der Transmembrandomäne befinden sich *heptad repeats* (HRs), die für den Membranfusionsprozess essentiell sind und deren Sequenzen zwischen viralen Fusionsproteinen hoch konserviert sind [Bosch et al., 2003; Hofmann und Pöhlmann, 2004]. Ein weiteres Charakteristikum ist der Erhalt der Trimerstruktur vor wie auch nach der Fusion. Während der Fusion werden die Trimere in die Wirtsmembran inseriert und klappen zur Bildung eines stabähnlichen Moleküls mit dem Fusionspeptid und der Transmembrandomäne zusammen. Diese Struktur wird als *trimer of hairpins* bezeichnet [Eckert und Kim, 2001]. Trotz vieler Gemeinsamkeiten mit den Klasse I Fusionsproteinen gibt es einige Merkmale, die das SARS-S-Protein im Vergleich zu den S-Proteinen anderer Coronaviren [Gallagher und Buchmeier, 2001; de Haan et al., 2004; Qiu et al., 2006] hervorheben, wie die Abwesenheit eines N-terminalen Fusionspeptids in der Oberflächendomäne sowie eine nennenswerte Spaltung des S-Proteins in eine S1- und S2-Untereinheit in infizierten Zellen [Xiao et al., 2003; Yang et al., 2004; Simmons et al., 2004; Yao et al., 2004; Hofmann et al 2004b]. Die proteolytische Spaltung von Coronavirus Spike-Proteinen durch Wirtszellproteasen ist jedoch essentiell für die Spike-Protein-Aktivierung [Gallagher und Buchmeier, 2001].

Die Interaktion vom SARS-S mit *angiotensin-converting enzyme 2* vermittelt den Zelleintritt

Zelluläre Rezeptoren sind für den viralen Zelleintritt unentbehrlich. Im November 2003 identifizierten Li und Kollegen die Karboxypeptidase *angiotensin-converting enzyme 2* (ACE2) als zellulären Rezeptor für das SARS-CoV [Li et al., 2003]. Es wurde gezeigt, dass ACE2 auf der Oberfläche von SARS-CoV-permissiven Vero E6-Zellen an die S1-Einheit vom SARS-S bindet und eine lösliche Form von ACE2 die Bindung vom SARS-S an Vero E6-Zellen blockiert. Zudem repliziert das SARS-CoV effizient in

normalerweise nicht-permissiven Zelllinien, nachdem diese mit einem ACE2-Expressionsplasmid transfiziert wurden [Li *et al.*, 2003; Kuhn *et al.*, 2004; Prabakaran *et al.*, 2004]. Ferner konnte gezeigt werden, dass die endogene Expression von ACE2 mit der Suszeptibilität von Zelllinien gegenüber der SARS-CoV-Infektion korreliert [Nie *et al.*, 2004; Hofmann *et al.*, 2004a]. Darüber hinaus wurde ACE2 auf wichtigen Zielzellen des SARS-CoV detektiert: Typ II Pneumozyten und ACE2-positiven Zellen im intestinalen Epithelium [Hamming *et al.*, 2004; Ding *et al.*, 2004; To and Lo, 2004; Chan *et al.*, 2006; Mossel *et al.*, 2008]. Eine Studie von Kuba und Kollegen demonstrierte schließlich, dass sich das SARS-CoV in ACE2-*knockout* Mäusen kaum noch ausbreiten kann [Kuba *et al.*, 2005].

Die Rezeptor-Bindungsdomäne (RBD) in der S1-Einheit (Abb. 6) ist für die Bindung vom SARS-S an ACE2 verantwortlich. Mutagenese-Studien und Strukturanalysen identifizierten die Aminosäuren 318-510 im S-Protein als eine unabhängig gefaltete RBD mit höherer Bindungsaffinität als das gesamte Spike-Protein [Xiao *et al.*, 2003; Wong *et al.*, 2004; Babcock *et al.*, 2004; Chakraborti *et al.*, 2005]. Darüber hinaus ist die RBD das Hauptangriffsziel neutralisierender Antikörper [He *et al.*, 2004a, 2004b, 2005]. Die Nutzung von Spezies-spezifischen Unterschieden im murinen und humanen ACE2 erlaubten die Kartierung von Aminosäureresten wie z.B. L353, die für die Rezeptorfunktion wichtig sind [Li *et al.*, 2004, 2005c]. Die Auflösung der RBD-Struktur in der Komplexbildung mit ACE2 zeigte, dass die Aminosäuren 424-494 [Li *et al.*, 2005a], auch Rezeptor-Bindungsmotiv (RBM) genannt, essentiell für die Interaktion vom SARS-S mit ACE2 sind [Wong *et al.*, 2004; Li *et al.*, 2005c].

SARS-S-getriebene Membranfusion

Eine wichtige Aufgabe des SARS-S-Proteins ist die Vermittlung der Fusion der viralen Membran mit der Wirtszellmembran [Liu *et al.*, 2004; Tripet *et al.*, 2004].

Der erste Schritt der durch Klasse I Fusionsproteine getriebenen Membranfusion ist die Einlagerung eines Fusionspeptids in die Zielzellmembran. Das Fusionspeptid ist häufig am N-Terminus der Transmembraneinheit des Fusionsproteins gelegen, der nach Spaltung des Fusionsproteins durch eine Wirtszellprotease freigesetzt wird (siehe unten). Alternativ kann das Fusionspeptid innerhalb des Transmembranproteins lokalisiert sein, typischerweise auf einer Loop-Struktur, an deren Basis eine Disulfidbrücke lokalisiert ist wie z.B. in der Transmembraneinheit des Ebola Virus Glykoproteins [Weissenhorn *et al.*, 1998, 1999, 2007]. Das Fusionspeptid im SARS-S wurde noch nicht identifiziert, es handelt sich jedoch wahrscheinlich um ein internes Fusionspeptid, das die Aminosäuren (AS) 770-788 umfasst [Sainz *et al.*,

2005]. Nach der Einlagerung des Fusionspeptides in die Wirtszellmembran ist die Transmembraneinheit sowohl mit der Wirtszellmembran (über das Fusionspeptid) als auch mit der viralen Membran (über die Transmembrandomäne) verbunden. Anschließend erfolgt eine Konformationsänderung im Transmembranprotein, die zur Bildung einer sogenannten 6-Helix-Bündelstruktur führt. Diese Struktur wird durch das Zurückfalten von HR2 (C-terminal) auf HR1 (N-terminal) gebildet und zeichnet sich durch die antiparallele Anordnung von HR1 und HR2 aus (Abb. 7) [Bosch *et al.*, 2003; Tripet *et al.*, 2004; Liu *et al.*, 2004; Ingallinella *et al.*, 2004; Xu *et al.*, 2004]. Durch die Bildung der 6-Helix-Bündelstruktur werden die virale und die zelluläre Membran in enge räumlich Nähe gebracht und ihre Verschmelzung induziert.

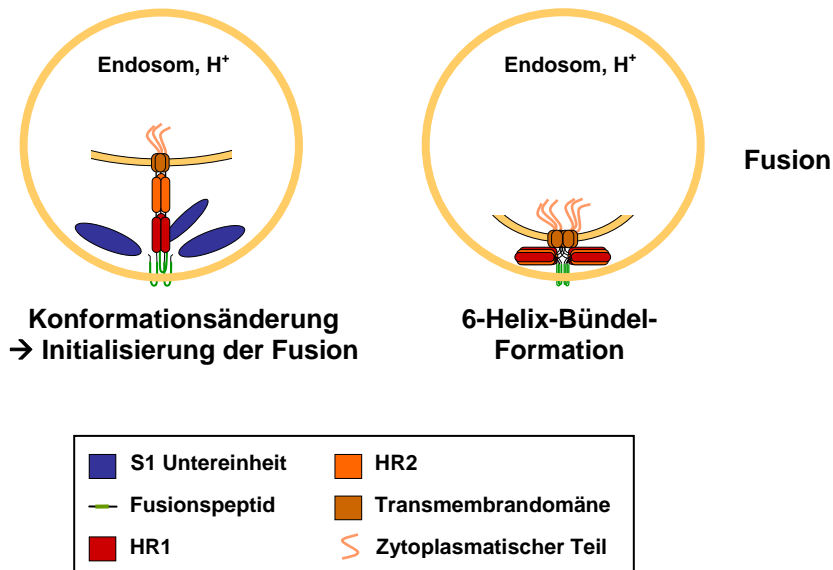


Abbildung 7: Die Ausbildung einer 6-Helix-Bündelstruktur im SARS-S-Protein. Nach der Initialisierung der Konformationsänderung kommt es, aufgrund des Umklappens und der antiparallelen Anlagerung von HR2 und HR1, zur Bildung der 6-Helix-Bündelstruktur.

1.3.4 Bedeutung von Wirtszellproteasen für den SARS-CoV-Eintritt

Ein typisches Merkmal viraler Klasse I Fusionsproteine ist die Aktivierung durch Wirtszellproteasen [Kielian and Rey, 2006]. Diese werden je nach ihrem katalytischen Zentrum in Aspartat-, Cystein-, Serin- oder Metalloproteasen eingeteilt [Barrett *et al.*, 1994]. Virale Glykoproteine werden posttranslational einer Proteolyse unterzogen, die zumeist an basischen Aminosäureresten stattfindet und für die Fusion mit der Wirtszellmembran von essentieller Bedeutung ist [Nagai und Klenk, 1977]. Die Spaltung kann dabei in verschiedenen zellulären Kompartimenten bzw. zu verschiedenen Stadien des viralen Vermehrungszyklus ablaufen. Das Hämagglutinin (HA) des Influenza Virus kann z.B. während der Biogenese im konstitutiven

sekretorischen Weg der infizierten Zelle [Klenk und Garten, 1994; Steinhauer, 1999; Garten und Klenk, 1999], im extrazellulären Raum [Kido *et al.*, 1992; Murakami *et al.*, 2001; Kido *et al.*, 2007] oder durch plasmamembranständige Proteasen während des Eintritts in Zielzellen aktiviert werden [Böttcher *et al.*, 2006; Chaipan *et al.*, 2009; Böttcher-Friebertshäuser *et al.*, 2010]. Im Gegensatz dazu erfolgt die proteolytische Aktivierung des Ebola Virus in endosomalen Kompartimenten, in die das Virus nach der Aufnahme in Wirtszellen transportiert wird [Chandran *et al.*, 2005]. Darüber hinaus wird das Ebola Virus Glykoprotein auch im sekretorischen Weg infizierter Zellen gespalten; die Spaltung führt jedoch nicht zur Aktivierung des Virus und ihre biologische Relevanz ist gegenwärtig unklar [Volchkov *et al.*, 1998; Wool-Lewis und Bates, 1999; Neumann *et al.*, 2007]. Die Spaltung vom SARS-S und deren funktionelle Relevanz sind dagegen nur unvollständig verstanden. Vereinzelte Hinweise auf eine proteolytische Spaltung vom SARS-S in infizierten Zellen wurden erbracht [Wu *et al.*, 2004]; ob die Spaltung für die S-Protein-getriebene Membranfusion wichtig ist, ist jedoch unklar. Die proteolytische Aktivierung vom SARS-S kann, analog zum Ebola Virus Glykoprotein, in Endosomen von Wirtszellen erfolgen [Simmons *et al.*, 2005]. Ob das SARS-CoV auch in wichtigen Wirtszellen wie Typ II Pneumozyten auf diesem Weg aktiviert wird, ist jedoch unklar. Weiterhin ist unbekannt, ob plasmamembranständige Proteasen das SARS-S aktivieren können.

Proteolytische Spaltung des SARS-Spike durch Cathepsin L

Cathepsine sind lysosomale bzw. endosomale Cysteinproteasen. Sie spielen eine wichtige Rolle in diversen physiologischen und pathologischen Prozessen. Einige Cathepsine wie B, C, F, H, L, O und Z werden ubiquitär im Gewebe exprimiert [Turk *et al.*, 2000; Stoka *et al.*, 2005]. Sie bestehen aus den zwei Domänen L (links) und R (rechts) und tragen in ihrem aktiven Zentrum (*cleft*) einen Cystein- und Histidin-Rest [Turk *et al.*, 2000]. Cathepsine werden als inaktive Präproenzyme synthetisiert. Im weiteren Verlauf der Biogenese erfolgt die Abspaltung des Propeptids im ER. Durch eine autokatalytische Prozessierung im sauren Milieu der späten Endosomen bzw. Lysosomen erlangt das Procathepsin seine aktive Form [Kominami *et al.*, 1988; Nishimura *et al.*, 1988].

Cathepsin L wurde 1976 von Kirschke *et al.* beschrieben [Kirschke *et al.*, 1976] und gehört zur Papainfamilie der Cysteinproteasen, die zumeist als Endopeptidasen fungieren. Die Rolle von Cathepsin L (CTSL) in viralen Prozessen wurde z.B. in der Reovirus-Infektion beim Abbau des Kapsidproteins [Baer *et al.*, 1999; Golden *et al.*, 2002] und im viralen Zelleintritt beschrieben [Simmons *et al.*, 2005; Huang *et al.*, 2006; Chandran *et al.*, 2005; Qiu *et al.*, 2006]. Dabei aktiviert CTS defense the viralen

Oberflächenglykoproteine, die für den Zelleintritt verantwortlich sind, im sauren Milieu der Endosomen von Wirtszellen für die Glykoprotein-getriebene Fusion der viralen mit der endosomalen Membran [Simmons *et al.*, 2005; Huang *et al.*, 2006; Chandran *et al.*, 2005, Qiu *et al.*, 2006]. So zeigten Simmons und Mitarbeiter, dass die SARS-CoV-Infektion durch CTSL-Inhibitoren, wie MDL 28170, blockiert werden kann und die Proteolyse durch CTSL das Spike-Fusionspotential aktiviert [Simmons *et al.*, 2005]. Auch Cathepsin B-Inhibitoren zeigten eine blockierende Wirkung; ihr Effekt war jedoch gering und es wird davon ausgegangen, dass Cathepsin B nur eine untergeordnete Rolle bei der SARS-S-Aktivierung spielt [Huang *et al.*, 2006]. Im Gegensatz dazu wurde demonstriert, dass das Cathepsin B für Aktivierung des Ebola Virus Glykoproteins von großer Bedeutung ist [Chandran *et al.*, 2005].

Somit ergibt sich ein neues Model des zellulären Eintritts des SARS-CoV: Der infektiöse Zelleintritt beginnt mit der Bindung vom SARS-S an ACE2. Die Rezeptorbindung induziert eine Konformationsänderung im SARS-S [Beniac *et al.*, 2007], die möglicherweise für die nachfolgende proteolytische Aktivierung vom SARS-S durch CTSL wichtig ist [Simmons *et al.*, 2005]. Die beschriebene pH-Wert-Abhängigkeit der SARS-S-getriebenen Membranfusion [Simmons *et al.*, 2004; Hofmann *et al.*, 2004b] ist daher nicht auf eine Aktivierung vom SARS-S durch Protonierung zurückzuführen, wie es z.B. für das Hämagglutinin des Influenza Virus beschrieben wurde, sondern auf eine essentielle Rolle des pH-Werts in der Cathepsin-Aktivität [Simmons *et al.*, 2004, 2005; Hofmann *et al.*, 2004b; Yang *et al.*, 2004]. Die Cathepsin Schnittstelle im SARS-S wurde in der gleichen Region kartiert (Tab. 1), in der die Spike-Proteine anderer Coronaviren durch Furin gespalten werden [Bosch *et al.*, 2008]. Jedoch gibt es bisher noch keine experimentellen Beweise dafür, dass die postulierte Spaltstelle für den SARS-S-getriebenen Eintritt wichtig ist.

Proteolytische Spaltung des SARS-Spike durch Typ II Transmembran-Serinproteasen

Das Hämagglutinin des Influenza Virus ist der Prototyp viraler Klasse I Fusionsproteine. Es wird als Vorläuferprotein synthetisiert [Skehel *et al.*, 2000; Harrison *et al.*, 2008] und kann durch Wirtszellproteasen in unterschiedlichen Stadien des viralen Vermehrungszyklus aktiviert werden (siehe oben).

Neue Arbeiten zeigen, dass die Typ II Transmembran-Serinproteasen (TTSPs) TMPRSS2/4 (*transmembrane protease/serine subfamily member 2 und 4*) und HAT (*human airway trypsin-like protease*) das Hämagglutinin von humanen Influenza Viren aktivieren [Böttcher *et al.*, 2006; Wang *et al.*, 2008; Chaipan *et al.*, 2009; Böttcher-Friebertshäuser *et al.*, 2010; Bertram *et al.*, 2010]. Serinproteasen sind eine der

größten Proteasefamilien und spielen eine Rolle in verschiedenen physiologischen Prozessen wie in der Regulation des Blutdrucks, der Verdauung und der Pathogen-Wirts-Interaktion. Die TTSPs zeigen eine charakteristische Domänenorganisation; sie bestehen aus einer N-terminalen intrazellulären Domäne, einer Transmembrandomäne und einer großen extrazellulären Domäne (Abb. 8). Letztere ist für die Einteilung der TTSPs in Unterfamilien von Bedeutung. Im Falle von TMPRSS2 und TMPRSS4 besteht die extrazelluläre Domäne aus einer *low-density lipoprotein receptor domain class A* (LDLA), einer *scavenger receptor cysteine-rich domain* (SR) und einer Serinprotease-Domäne. Anstelle der LDLA und SR Domäne besitzen HAT wie auch TMPRSS11a eine *single sea urchin sperm protein, enteropeptidase, agrin domain* (SEA) [Szabo *et al.*, 2003; Szabo und Bugge, 2008; Choi *et al.*, 2009].

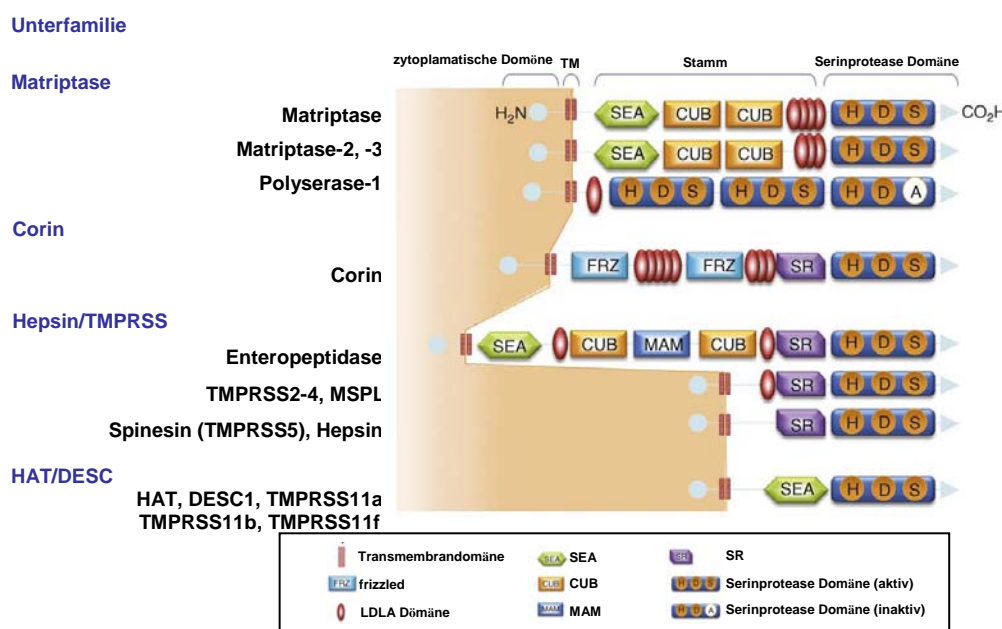


Abbildung 8: Schematische Darstellung der Familie der Typ II Transmembran-Serinproteasen (TTSPs). Aufgrund der phylogenetischen Verwandtschaftsverhältnisse wurden die TTSPs in vier Unterfamilien eingeteilt [Szabo und Bugge, 2008]. H (Histidin), D (Aspartat) und S (Serin) stehen für die katalytischen Reste in der Serinprotease-Domäne. Anstatt Serin befindet sich in der inaktiven Domäne von Polyserase-1 ein Alanin (A). DESC (*differentially expressed squamous cell carcinoma gene*); FRZ (*frizzled domain*); LDLA (*low-density lipoprotein receptor domain class A*); SEA (*single sea urchin sperm protein, enteropeptidase, agrin domain*); CUB (*Cls/Clr, urchin embryonic growth factor and bone morphogenic protein-1 domain*); MAM (*a meprin, A5 antigen and receptor protein phosphatase μ domain*); SR (*scavenger receptor cysteine-rich domain*); TM (Transmembrandomäne) [Abbildung modifiziert aus Choi *et al.*, 2009].

TMPRSS2 wurde im Juni 1997 identifiziert und auf dem Chromosom 21 kartiert [Paoloni-Giacobino *et al.*, 1997]. Es gehört der Hepsin/TMPRSS-Unterfamilie an und ist

mit Prostatakrebs assoziiert [Lin *et al.*, 1999]. Die Proteasedomäne von TMPRSS2 enthält N-terminal eine RIVGG Peptidsequenz [Rawlings und Barrett, 1994], welche eine typische Aktivierungsstelle von Zymogenen darstellt. TMPRSS2 wird in vielen Geweben wie Lunge, Herz und Leber exprimiert, wobei im Dünndarm die höchste mRNA-Expression dokumentiert wurde [Paoloni-Giacobino *et al.*, 1997; Donalsdon *et al.*, 2002]. TMPRSS2 spaltet sein Substrat nach einem Lysin- oder Argininrest [Paoloni-Giacobino *et al.*, 1997]. Somit stellt die bekannte Protease-sensitive Region im Hämagglutinin humaner Influenza Viren ein geeignetes Substrat dar. Die Replikation der Influenza Stämme H1N1, H2N9 und H3N2 in TMPRSS2-exprimierenden Zellen wurde 2006 dokumentiert [Böttcher *et al.*, 2006, Böttcher-Friebertshäuser *et al.*, 2010]. Zudem zeigten Chaipan und Mitarbeiter, dass das HA des 1918 Influenza Virus durch TMPRSS2 gespalten werden kann [Chaipan *et al.*, 2009].

TMPRSS11a, auch *airway trypsin-like protease-1* genannt, gehört der HAT/DESC-Unterfamilie der TTSPs an und wird im oberen respiratorischen Trakt, wie Pharynx und Trachea, exprimiert [Kam *et al.*, 2009; Choi *et al.*, 2009]. Es konnte gezeigt werden, dass rekombinantes, lösliches TMPRSS11a das SARS-S-Protein spaltet und die Infektiosität von rekombinanten SARS-S-Viren steigert. Die Protease-Schnittstellen auf dem S-Protein wurden als R667 und R797 identifiziert. Dabei handelt es sich um monobasische Spaltmotive (einzelnes Arginin, in einigen Fällen Lysin) [Kam *et al.*, 2009]. Jedoch ist unklar, ob das SARS-S durch membranständige TTSPs aktiviert wird.

Proteolytische Spaltung des SARS-Spike durch Furin

Das Gen für Furin wurde als *fur (fes/fps upstream region)* identifiziert [Roebroek *et al.*, 1986a, 1986b] und das Genprodukt 1990 als Endoprotease beschrieben [van den Ven *et al.*, 1990; Wise *et al.*, 1990]. Furin ist ein Mitglied der Proproteinkonvertase-Familie, welche zur Subtilisin-Superfamilie der Serinendopeptidasen gehört [Barr, 1991; Rawlings und Barrett, 1993, 1994]. Es spielt eine große Rolle in der Embryogenese und ist für die Spaltung vieler verschiedener humaner Proproteine (Proalbumin, Insulin-Prorezeptor) und für die proteolytischen Aktivierung verschiedener viraler Fusionsproteine verantwortlich [Nakayama, 1997; Thomas, 2002].

Furin ist 794 Aminosäuren groß und besteht aus einer zellulären bzw. extrazellulären globulären Struktur, die homolog zu anderen Proproteinkonvertasen ist [Wise *et al.*, 1990; van den Ven *et al.*, 1990; Roebroek *et al.*, 1994]. Furin wird ubiquitär im menschlichen wie auch im tierischen Gewebe exprimiert [Nakayama, 1997]. Die aktive Form des Enzyms ist subzellulär im Transgolginetzwerk und den Endosomen oder an der Zelloberfläche lokalisiert, wobei die Lokalisation unter der Kontrolle der

zytoplasmatischen Domäne erfolgt [Molloy *et al.*, 1994, 1999]. Furin spaltet sein Substrat am Erkennungsmotiv R-X-K/R-R und hat ein Aktivitätsoptimum bei pH 7,0 bis 7,5 [Molloy *et al.*, 1992].

Das HA hochpathogener aviärer Influenza Viren trägt eine multibasische Spaltstelle (R-X-R/K-R), die für die Aktivierung der Viren essentiell ist [Vey *et al.*, 1992] und die bei Influenza Viren ein Kennzeichen für hohe Pathogenität darstellt [Bosch *et al.*, 1981; Neumann *et al.*, 2009]. Im Jahr 1992 wurde gezeigt, dass diese Spaltstelle durch Furin erkannt wird und, dass Furin für die Aktivierung von hochpathogenen aviären Influenza Viren essentiell ist [Stieneke-Gröber *et al.*, 1992].

Das Spike-Vorläuferprotein des S-Proteins bestimmter Stämme des Maus-Hepatitis-Virus (MHV) wird im konstitutiven sekretorischen Weg infizierter Zellen durch Furin gespalten [Stieneke-Gröber *et al.*, 1992] und die Spaltung ist für die virale Infektiosität wichtig [de Haan *et al.*, 2004]. Jedoch werden nicht alle MHV-Stämme über diesen Weg aktiviert [Nash und Buchmeier, 1997]. Die S-Proteine bestimmter MHV-Stämme durchlaufen den sekretorischen Weg ohne durch Furin gespalten zu werden und die S-Protein-Aktivierung erfolgt in Wirtszellendosomen durch Cathepsin L, analog zur Aktivierung vom SARS-S [Qiu *et al.*, 2006].

Bergeron und Kollegen erbrachten erste Hinweise, dass Furin bei der SARS-S-Aktivierung eine Rolle spielen könnte. Sie zeigten, dass Furin das SARS-S spaltet, allerdings mit geringer Effizienz, und dass die Furinüberexpression den zytopathischen Effekt und den Virustiter des SARS-CoV in Vero E6-Zellen steigert. Im Einklang dazu konnte gezeigt werden, dass der Furininhitor dec-RVKR-cmk die SARS-S-Spaltung und den viralen Titer reduziert [Bergeron *et al.*, 2005]. Darüber hinaus ermöglichte die Einführung eines Furinmotives im Spike-Protein an Position R667 (Tab. 1) eine effiziente Spaltung des mutierten Glykoproteins und erhöht die Zell-Zell Fusionsaktivität, jedoch nicht die Infektiosität [Follis und Nunberg, 2006]. Zurzeit ist es fraglich, ob dieses Spaltmotiv für die SARS-S-Aktivierung nötig ist. Zudem beinhaltet das SARS-S ein minimales Furinmotiv 758-761 (RNTR), welches in Peptidform durch Furin erkannt wird [Bergeron *et al.*, 2005], jedoch ist unbekannt, ob dieses Motiv als Spaltstelle für die Aktivierung des SARS-S bedeutend ist.

Belouzard und Kollegen identifizierten eine weitere proteolytische Spaltstelle an Position R797 (Tab.1) in der S2-Domäne des SARS-S und lieferten Hinweise darauf, dass diese Spaltstelle für die Aktivierung des S-Proteins wichtig ist [Belouzard *et al.*, 2009]. Zudem postulierten sie, dass die proteolytische Spaltung an Position R797 mit der Spaltung am Aminosäurerest R667 einhergeht und somit die SARS-S-Aktivierung über eine sequentielle Proteolyse erfolgt [Belouzard *et al.*, 2009].

Spaltstelle	Mutation	Protease	Quelle
R667		Trypsin	Kam et al., 2009 ; Bosch et al., 2008; Follis et al., 2006
K672			Follis et al., 2006
K672	K672A		Bergeron et al., 2005
664SLLRSTSQSI671	664SLLRRSRRSI671	Furin/Trypsin	Belouzard et al., 2009
792LKPTKRSF799	792LKRTKRSF799	Furin/Trypsin	Belouzard et al., 2009
758RNTR761		Furin	Bergeron et al. 2005
797KPTKR801	797KRRKR801	Furin/Trypsin/Cathepsin	Watanabe et al., 2008
R667	R667→R667S	Furin	Follis et al., 2006
T678		Cathepsin L	Bosch et al., 2008
R667/R797		TMPRSS11a	Kam et al., 2009

Tabelle 1: Zusammenfassende Tabelle der potentiellen Spaltstellen im SARS-S-Protein. Die aufgelisteten Mutationen zeigen die Optimierung der Spaltstellen für die jeweiligen Proteasen.

Proteolyse von ACE2

Im November 2003 identifizierten Li und Mitarbeiter *angiotensin-converting enzyme 2* (ACE2) als zellulären Rezeptor für das SARS-CoV [Li et al., 2003]. ACE2 wurde im Jahre 2000 als Homolog von *angiotensin-converting enzyme* (ACE) identifiziert und kloniert [Tipnis et al., 2000]. Dieses Oberflächenprotein ist auf den zilientragenden Zellen des humanen nasalen Epithels als auch tracheobronchialen Luftröhrenepithels lokalisiert, die durch das SARS-CoV infizierbar sind [Sims et al., 2005]. Zudem wird ACE2 in Herz, Niere und Testes exprimiert [Tipnis et al., 2000; Donoghue et al., 2000], obwohl niedrige Konzentrationen auch in anderen Organen detektiert wurden [Hamming et al., 2004].

ACE2 ist ein Typ I Transmembranprotein bestehend aus 805 Aminosäuren mit einem N-terminalen Signalpeptid, einem C-terminalen Membrananker und einer extrazellulären katalytischen Domäne mit einer Zink-Metallopeptidase-aktiven Seite.

In dem kaskadenartigen Verlauf des Renin-Angiotensin-Aldosteron-System (RAAS) spaltet ACE Angiotensin I (ANG1) zu Angiotensin II (ANG2) [Skeggs et al., 1980; Corvol et al., 1995], wohingegen ACE2 einen Aminosäurerest vom ANG2 abspaltet, um es in ANG-(1-7) umzuwandeln [Douglas et al., 2004] und somit der Aktivierung des Angiotensin II Typ 1 Rezeptors entgegenwirkt (Abb. 9) [Santos et al., 2005]. ACE2 ist nicht nur ein Schlüsselenzym des RAAS, es schützt zudem vor der Entstehung des *acute respiratory distress syndrome* (ARDS) [Imai et al., 2005] und Lungenversagen [Imai et al., 2008; Penninger et al., 2008]. Die Infektion mit dem SARS-CoV unterdrückt die Expression von ACE2 *in vitro* und *in vivo* [Kuba et al., 2005; Haga et al., 2008, 2010] und die Interferenz mit der Rezeptorexpression ist möglicherweise wesentlich für die Progression von SARS verantwortlich (Abb. 10) [Kuba et al., 2005]. Interessanterweise war die Bindung vom SARS-S an ACE2 ausreichend um die ACE2-Expression zu reduzieren, was darauf hindeutet, dass die SARS-S-Interaktion mit

ACE2 nicht nur für den viralen Zelleintritt wichtig ist, sondern auch direkt die SARS-Pathogenese fördert.

Lambert und Kollegen entdeckten, dass ACE2 durch die Metalloprotease TACE gespalten werden kann [Lambert *et al.*, 2005]. TACE (*tumor necrosis factor- α converting enzyme*) oder auch ADAM17 (*ADAM metallopeptidase domain 17*) genannt, gehört der ADAM-Familie der Disintegrine und Metalloproteasen an. Es ist ein Typ I Transmembranprotein mit einer extrazellulären Zink-abhängigen Proteasedomäne und einer Disintegrin-cysteinreichen Sequenz [Black, 2002]. TACE wurde als Tumornekrosefaktor-spaltendes Enzym entdeckt, welches Transmembranproteine abspaltet, wobei eine lösliche und funktionelle Form des Substrates mit einer aktiven extrazellulären Domäne entsteht [Black *et al.*, 1997]. *In vitro* konnte gezeigt werden, dass das SARS-S-Protein eine TACE-abhängige Abspaltung von ACE2 bewirkt [Haga *et al.*, 2008, 2010]. Dieser Mechanismus ist auf die zytoplasmatische Domäne von ACE2 angewiesen, da ACE2-Deletionsmutanten ohne die C-terminale Region nicht gespalten werden [Haga *et al.*, 2008]. Außerdem wurde die SARS-CoV-Infektion in Zielzellen durch einen TACE-Inhibitor vermindert [Haga *et al.*, 2010]. Somit könnte die durch Kuba *et al.* gemachte Beobachtung, dass das SARS-S die ACE2-Expression verhindert, mit der Aktivität von TACE in Verbindung stehen (Abb. 9).

Das humane Coronavirus-NL63 (HCoV-NL63) wurde 2004 identifiziert [van der Hoek *et al.*, 2004; Fouchier *et al.*, 2004] und der Coronavirus-Gruppe I zugeordnet [van der Hoek *et al.*, 2006]. Es ist ubiquitär verbreitet und verursacht Erkrankungen der oberen Atemwege. Außerdem ist die HCoV-NL63-Infektion mit Pseudokrupp assoziiert [Chiu *et al.*, 2005; van der Hoek *et al.*, 2005, 2006]. Trotz hoher Sequenzhomologie mit dem humanen Coronavirus 229E, das CD13 als Rezeptor für den Zelleintritt verwendet, benutzt das HCoV-NL63 den SARS-CoV-Rezeptor ACE2 für den Zelleintritt. Es gibt Hinweise darauf, dass sich die S-Proteine des HCoV-NL63 (NL63-S) und SARS-CoV in der Interaktion mit ACE2 unterscheiden. Es ist daher denkbar, dass eine im Vergleich zum SARS-S reduzierte ACE2-Bindung vom NL63-S zu einem weniger effizienten Zelleintritt und zu einer geringeren Herabregulierung der ACE2-Expression führt, und damit wesentlich für die geringere Pathogenität des HCoV-NL63 im Vergleich zum SARS-CoV verantwortlich ist.

Zusammenfassung

Der Wirtszelleintritt des SARS-CoV ist ein mehrstufiger Prozess, an dem verschiedene zelluläre Faktoren beteiligt sind. Zuerst erfolgt die Bindung des SARS-S-Proteins an den Rezeptor ACE2. Diese Interaktion könnte möglicherweise mit Hilfe von TACE/ADAM17 eine Abspaltung von ACE2 bewirken, die die Entstehung von SARS

fördern könnte. Ob TACE/ADAM17 für die im Kontext der SARS-CoV-Infektion beschriebene ACE2-Herabregulierung verantwortlich ist, ist jedoch nicht geklärt. Die Rezeptorbindung geht mit einer Konformationsänderung des SARS-S-Proteins einher, die wahrscheinlich dazu beiträgt, dass das SARS-S durch CTSL in Wirtszellendosomen aktiviert werden kann. Ob andere Proteasen wie TMPRSS2/11a oder Furin das Spike-Protein aktivieren können und damit möglicherweise CTSL-unabhängigen Zelleintritt ermöglichen, ist jedoch unklar (Abb.9).

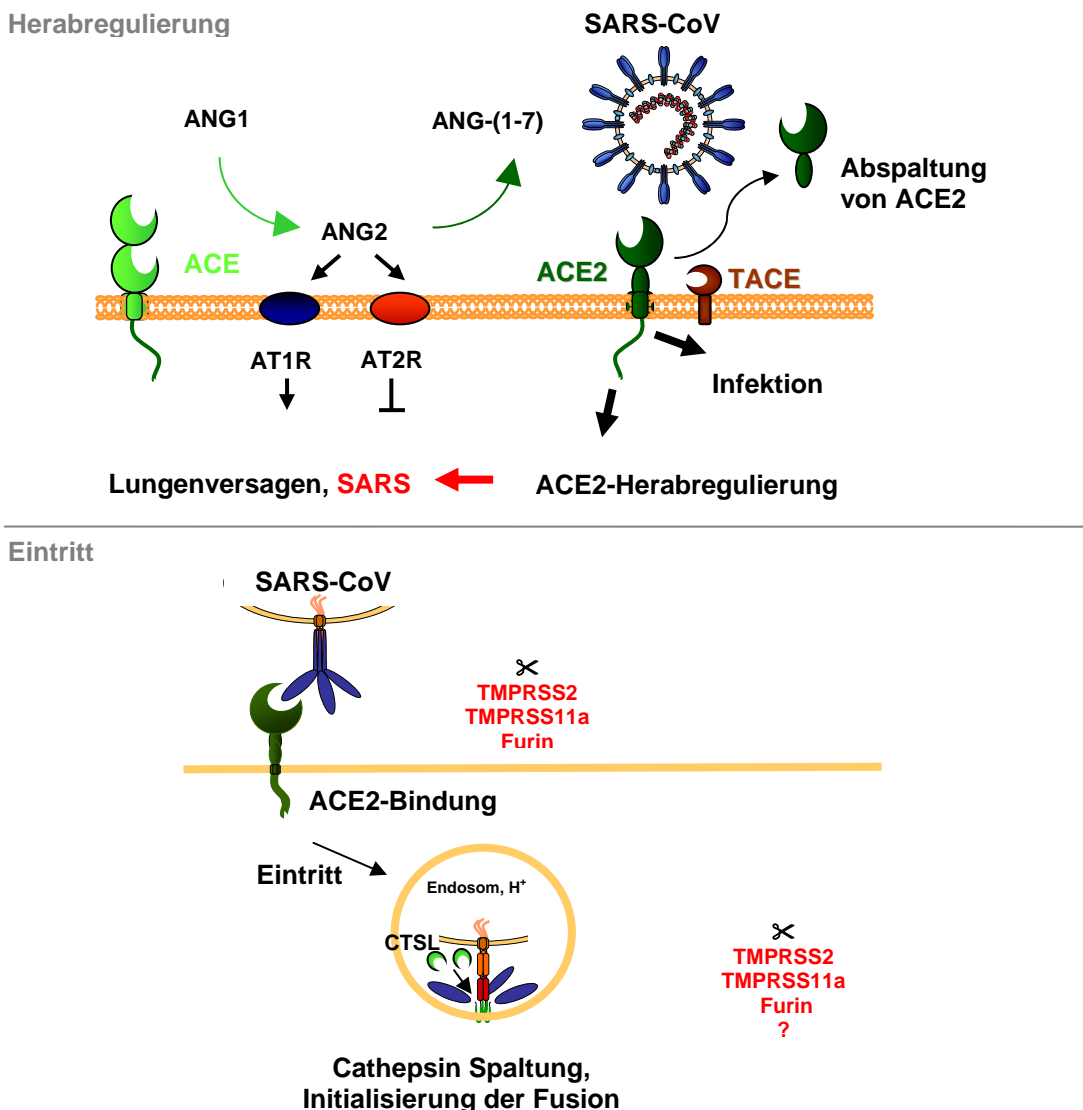


Abbildung 9: Eintritt des SARS-CoV und ACE2-Herabregulierung. ACE spaltet Angiotensin I (ANG1) zu Angiotensin II (ANG2), wohingegen ACE2 ANG2 in ANG-(1-7) umwandelt und somit der Funktion des Angiotensin II Typ 1 Rezeptors entgegen wirkt. ACE2 ist nicht nur ein Schlüsselenzym des Renin-Angiotensin Systems, es schützt somit vor der Entstehung des *acute respiratory distress syndrome* (ARDS) und vor Lungenversagen. Der SARS-S-getriebene Eintritt induziert die Herabregulierung von ACE2 unter möglicher Mithilfe von TACE. Dieser Prozess könnte zur SARS-Entstehung beitragen. Nach der Aufnahme des Viruspartikels folgt die Cathepsin L-vermittelte Spaltung des Spike-Proteins und somit die Initialisierung der SARS-S-getriebene Fusion von viraler mit endosomaler Membran. Welche Rolle TMPRSS2 und Furin

spielen ist noch ungeklärt. ACE (*angiotensin-converting enzyme*); ANG1 (Angiotensin I); ANG2 (Angiotensin II); AT1R (Angiotensin II Typ 1 Rezeptor); AT2R (Angiotensin II Typ 2 Rezeptor); Ang-(1-7) (Angiotensin 1-7); TACE (*TNF- α converting enzyme*), CTSL (Cathepsin L). [Abbildung modifiziert aus Kuba *et al.*, 2006].

2. Zielsetzung

Das hochpathogene SARS-CoV-1 verwendet ACE2 als Rezeptor für den Eintritt in Wirtszellen. Die Expression von ACE2 schützt im Mausmodell vor Lungenschädigung und wird im Kontext der SARS-CoV-Infektion negativ reguliert, was die Entwicklung von SARS fördern könnte. Die Wirtszellprotease TACE/ADAM17 spaltet ACE2, ihr Beitrag zur ACE2-Herabregulierung ist jedoch unklar. Das gering pathogene humane Coronavirus-NL63 verwendet ebenfalls ACE2 für den Zelleintritt und es ist denkbar, dass eine im Vergleich zum SARS-CoV weniger effiziente Interaktion mit ACE2 für die geringere Pathogenität des HCoV-NL63 mitverantwortlich ist.

Das erste Ziel dieser Arbeit war es zu klären, ob das SARS-S und NL63-S mit unterschiedlicher Effizienz an ACE2 binden und die ACE2-Expression reduzieren. Im Kontext der ACE2-Herabregulierung sollte insbesondere eine mögliche Rolle der Wirtszellprotease TACE/ADAM17 geklärt werden. Dazu sollten die jeweiligen S-Proteine rekombinant hergestellt und die Effizienz der Bindung an ACE2 in unterschiedlichen experimentellen Systemen gemessen werden, wie BIACore, ELISA und FACS. Durch Nutzung eines TACE-Inhibitors (TAPI-0) sollte untersucht werden, ob die TACE-vermittelte ACE2-Abspaltung zur Herabregulation der ACE2-Expression durch das SARS-CoV beiträgt. Schließlich sollte die Bedeutung der TACE-abhängigen ACE2-Spaltung für die Vermehrung vom SARS-CoV untersucht werden.

Zahlreiche virale Glykoproteine werden als inaktive Vorläuferproteine synthetisiert und anschließlich durch Wirtszellproteasen proteolytisch aktiviert [Kielian and Rey, 2006]. Das SARS-S wird durch eine Protease in Wirtszellendosomen, Cathepsin L, während des Eintritts in Zielzellen aktiviert [Simmons *et al.*, 2005]. Ob das SARS-S auch durch Proteasen in bereits infizierten Zellen gespalten wird, war jedoch unklar und sollte untersucht werden. Insbesondere sollte geklärt werden, ob Typ II Transmembran-Serinproteasen, die für die Aktivierung des Influenza Virus Hämagglutinin verantwortlich sind [Böttcher *et al.*, 2006; Chaipan *et al.*, 2009; Bertram *et al.*, 2010], auch das SARS-S aktivieren können.

Dazu sollte untersucht werden, ob die Expression von TTSPs in Virus-produzierenden Zellen oder in Zielzellen das SARS-S proteolytisch aktivieren kann. Von besonderem Interesse war dabei die Frage, ob eine mögliche Aktivierung vom SARS-S durch TTSPs die Aktivierung durch Cathepsin L ersetzen kann. Schließlich sollte gefragt werden, welche Bereiche im SARS-S für die proteolytische Aktivierung wichtig sind und ob aktivierende Proteasen in Zielzellen der SARS-CoV-Infektion exprimiert werden.

3. Manuskripte

Publikationsstadium

Titel

Differential Downregulation of ACE2 by the Spike Proteins of Severe Acute Respiratory Syndrome Coronavirus and Human Coronavirus NL63

Zeitschrift

Journal of Virology 2010 Jan; 84(2):1198-205.

Titel

Different host cell proteases activate the SARS-coronavirus spike-protein for cell-cell and virus-cell fusion

Zeitschrift

Virology, zur Publikation angenommen am 16. Februar 2011

Titel

Evidence that TMPRSS2 activates the SARS-coronavirus spike-protein for membrane fusion and reduces viral control by the humoral immune response

Zeitschrift

Journal of Virology, zur Publikation angenommen am 28. Januar 2011

Differential Downregulation of ACE2 by the Spike Proteins of Severe Acute Respiratory Syndrome Coronavirus and Human Coronavirus NL63^V

Ilona Glowacka,^{1†} Stephanie Bertram,^{1†} Petra Herzog,^{2,3} Susanne Pfefferle,² Imke Steffen,¹ Marcus O. Muench,⁴ Graham Simmons,⁴ Heike Hofmann,⁵ Thomas Kuri,⁶ Friedemann Weber,⁶ Jutta Eichler,⁷ Christian Drosten,⁸ and Stefan Pöhlmann^{1*}

Institute of Virology, Hannover Medical School, 30625 Hannover, Germany¹; Bernhard Nocht Institute for Tropical Medicine, Bernhard-Nocht-Str. 74, 20359 Hamburg, Germany²; Qiagen Hamburg GmbH, Königstr. 4a, 22767 Hamburg, Germany³; Blood Systems Research Institute and Department of Laboratory Medicine, University of California, San Francisco, California⁴; Department of Medical Microbiology and Virology, University of Kiel, 24105 Kiel, Germany⁵; Department of Virology, University of Freiburg, 79008 Freiburg, Germany⁶; Department of Medicinal Chemistry, University of Erlangen-Nürnberg, Schuhstrasse 19, 91052 Erlangen, Germany⁷; and Institute of Virology, University of Bonn Medical Centre, Sigmund-Freud-Str. 25, 53127 Bonn, Germany⁸

Received 16 June 2009/Accepted 16 October 2009

The human coronaviruses (CoVs) severe acute respiratory syndrome (SARS)-CoV and NL63 employ angiotensin-converting enzyme 2 (ACE2) for cell entry. It was shown that recombinant SARS-CoV spike protein (SARS-S) downregulates ACE2 expression and thereby promotes lung injury. Whether NL63-S exerts a similar activity is yet unknown. We found that recombinant SARS-S bound to ACE2 and induced ACE2 shedding with higher efficiency than NL63-S. Shedding most likely accounted for the previously observed ACE2 downregulation but was dispensable for viral replication. Finally, SARS-CoV but not NL63 replicated efficiently in ACE2-positive Vero cells and reduced ACE2 expression, indicating robust receptor interference in the context of SARS-CoV but not NL63 infection.

Severe acute respiratory syndrome coronavirus (SARS-CoV) emerged in 2002 in Guangdong province, China, and its subsequent spread to 26 countries was associated with 8,096 infections and 774 deaths (29). The human coronavirus NL63 was discovered in 2004 in the Netherlands (7, 33) and was shown to be globally distributed (2, 3, 6, 23, 31). NL63 infection seems to be acquired during childhood (2, 3, 6, 11, 23, 31) and is usually not associated with severe disease (2, 3, 6, 23, 31–33). Both SARS-CoV and NL63 employ angiotensin-converting enzyme 2 (ACE2) as receptor for infectious entry into target cells (11, 19, 34). Several lines of evidence suggest that ACE2 plays a key role in SARS-CoV spread: (i) ACE2 is expressed on the major SARS-CoV target cells, type II pneumocytes (4, 9, 25, 30), as well as on ciliated airway epithelial cells (28), (ii) ACE2 expression in cell lines correlates with susceptibility to SARS-CoV spike protein (SARS-S)-driven entry (11, 26), and (iii) knockout of ACE2 in mice abrogates permissiveness to SARS-CoV infection (16). For NL63, ACE2 expression was also shown to correlate with susceptibility to infection (11), and the virus has been found to infect ciliated bronchial epithelial cells in culture (1, 5), but the NL63 target cells in infected patients have not been defined, and an animal model for NL63 replication has not been established.

ACE2 is a component of the renin-angiotensin system, which regulates blood pressure (14, 17). In addition, Kuba and colleagues and Imai and colleagues showed that pulmonary ACE2 expression protects against experimentally induced lung injury (13, 16). Treatment of mice with soluble SARS-S reduced cell surface expression of ACE2 and thereby exacerbated experimentally induced lung disease (16), suggesting that interactions of SARS-S with its cellular receptor could promote acute lung injury in infected patients. Notably, it has recently been proposed that binding of SARS-CoV but not NL63 to ACE2 induces ACE2 shedding from the cell surface, and evidence has been presented that this process is required for cellular uptake of SARS-CoV (8). Whether ACE2 shedding is indeed a prerequisite to infectious entry and contributes to the previously observed ACE2 downregulation by SARS-S (16) remains to be determined. In addition, it is unclear if SARS-S and NL63-S differentially interfere with ACE2 expression, which might contribute to the differential pathogenicity of these viruses.

To address the questions raised above, we first investigated if SARS-S and NL63-S bind to ACE2 with different efficiencies, which could result in differential ACE2 downregulation. For this, the S1 units of the viral S proteins (SARS-S, amino acids 13 to 714; NL63-S, amino acids 16 to 741), fused to the Fc portion of human immunoglobulin, were transiently expressed in 293T cells and purified from the culture supernatants by chromatography with protein A columns (Fig. 1A). Purified SARS-S bound to ACE2-expressing cells with much higher efficiency than equal amounts of NL63-S (Fig. 1B). Similarly,

* Corresponding author. Mailing address: Institute of Virology, OE 5230, Hannover Medical School, Carl-Neuberg-Str. 1, 30625 Hannover, Germany. Phone: 49 511 532 4382. Fax: 49 511 532 8736. E-mail: Poehlmann.Stefan@MH-Hannover.DE.

† I.G. and S.B. contributed equally to this work.

Published ahead of print on 28 October 2009.

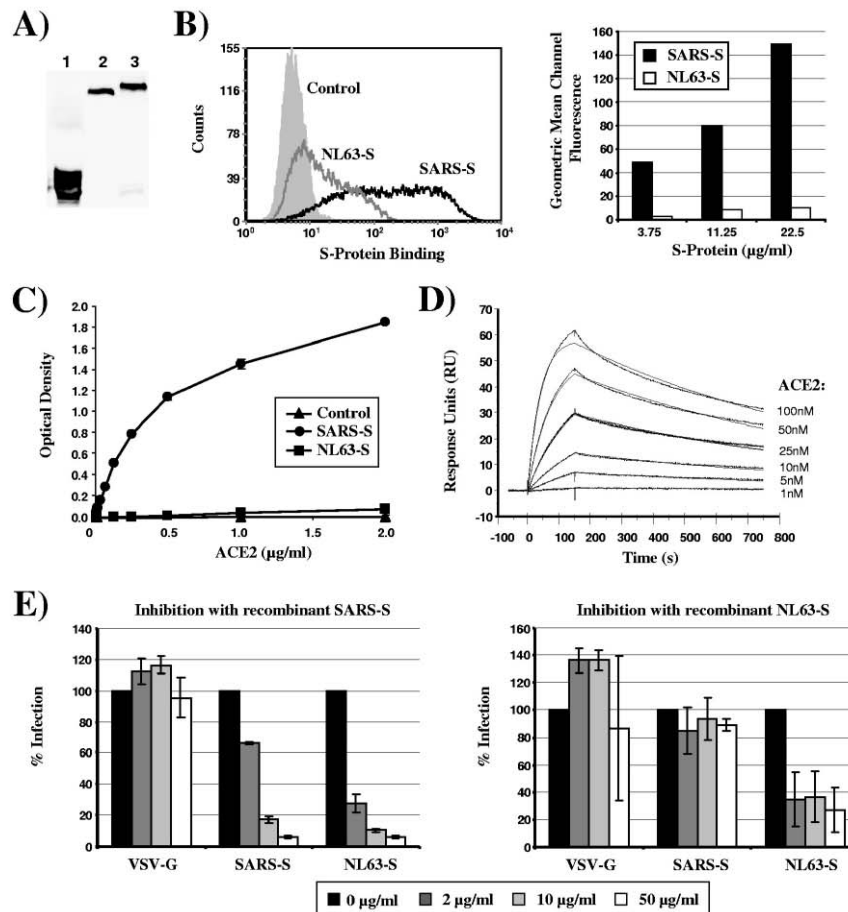


FIG. 1. SARS-S binds to ACE2 with higher efficiency than NL63-S. (A) For production of recombinant SARS-S and NL63-S proteins, the S1 unit of the respective proteins was fused to the Fc portion of human immunoglobulin, and the soluble S proteins and the Fc control protein were transiently expressed in 293T cells. The S proteins and the Fc control protein were purified from the culture supernatants by protein A chromatography, and protein content was analyzed by Western blot analysis using an anti-human Fc antibody. Lane 1, Fc control; lane 2, SARS-S; lane 3, NL63-S. (B) 293T cells stably expressing ACE2 were incubated with SARS-S, NL63-S, and Fc control protein at a concentration of 22.5 $\mu\text{g/ml}$, and protein binding was analyzed by a fluorescence-activated cell sorter (FACS). Results from a representative experiment are shown in the left panel, and the geometric mean channel fluorescence measured upon analysis of duplicate samples is shown in the right panel. (C) Binding of SARS-S and NL63-S to ACE2 was assessed by employing a sandwich ELISA. The ELISA plate was coated with anti-human Fc antibody to capture the soluble spike Fc proteins or a Fc control protein (2 $\mu\text{g/ml}$), followed by addition of different concentrations of recombinant ACE2 labeled with a FLAG tag, which was detected using an anti-FLAG antibody-horseradish peroxidase (HRP) conjugate. (D) An anti-human Fc antibody was immobilized onto a BIACore chip surface, and SARS-S Fc protein was added. Subsequently, unbound protein was removed, and binding of different concentrations of recombinant ACE2 was assessed. The binding of the receptor was measured by a decreased angle of the surface plasma resonance (SPR), which is illustrated in response units (RU) over time. (E) 293T cells overexpressing ACE2 were incubated with the indicated concentrations of recombinant SARS-S (left) or NL63-S (right) for 1 h at 37°C and infected with lentiviruses pseudotyped with SARS-S, NL63-S, or vesicular stomatitis virus G protein (VSV-G). At 72 h postinfection, the luciferase activity in the cell lysates was determined using a commercially available kit. The results of a representative experiment are shown and are graphed as relative infection efficiency. Upon infection in the absence of recombinant spike protein, the following luciferase counts per second (c.p.s.) were measured: VSV-G, 3,612,752 \pm 2,523,541 c.p.s.; SARS-S, 2,290,442 \pm 347,006 c.p.s.; NL63-S, 168,575 \pm 20,581 c.p.s.

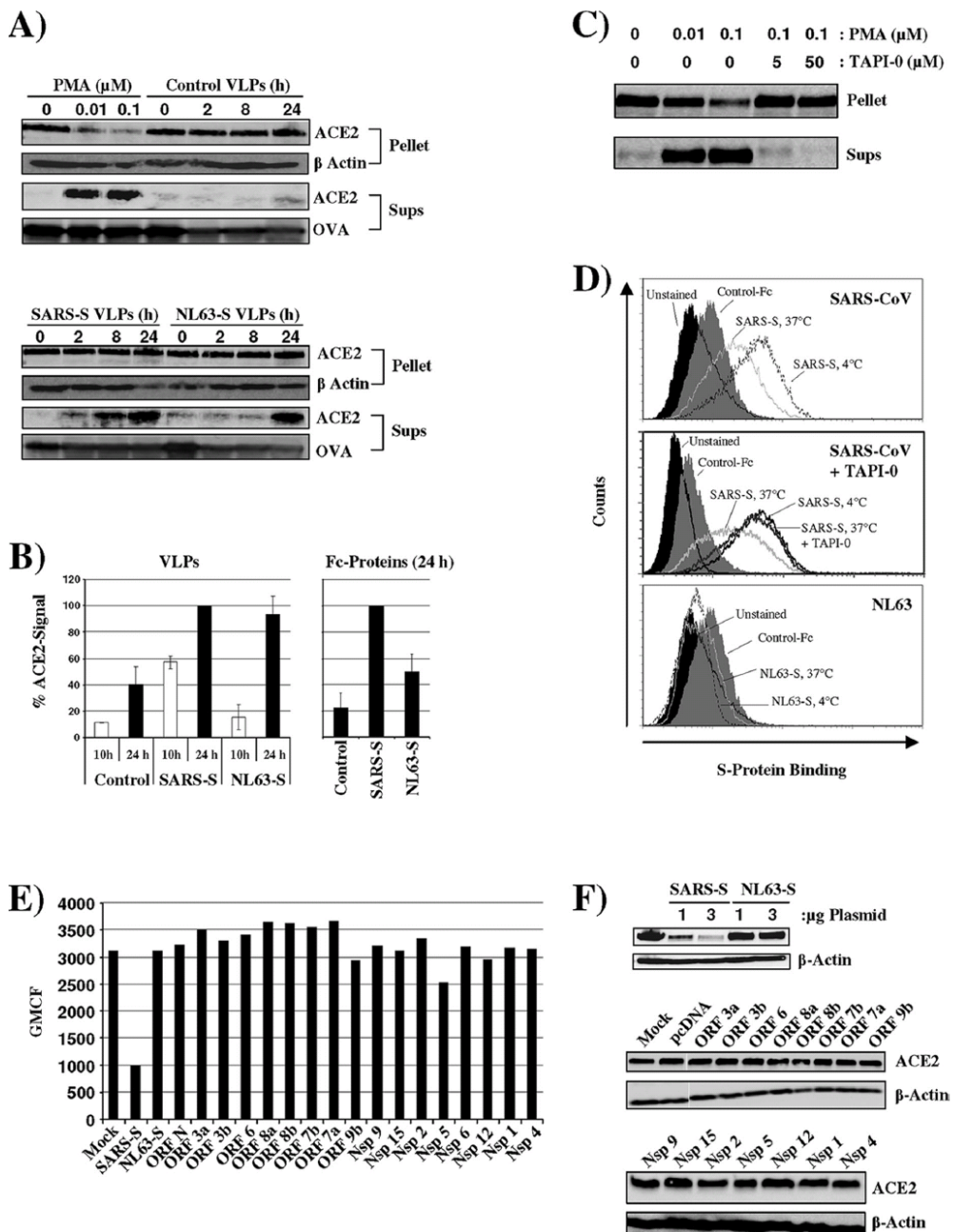


FIG. 2. SARS-S but not NL63-S induces efficient ACE2 shedding. (A) Vero E6 cells were incubated for 0, 2, 8, and 24 h with VLPs harboring SARS-S, NL63-S, or control particles containing no viral glycoprotein. As a positive control for ACE2 shedding, cells were treated with the indicated concentrations of PMA for 1 h. Thereafter, the supernatants were harvested, OVA was added, and the samples were precipitated with TCA. In parallel, the cells were lysed, pellets were obtained upon TCA precipitation, and cell lysates were analyzed for ACE2 expression by Western blot analysis. As precipitation and loading control, respectively, OVA content (supernatants) and β-actin expression (cell lysates) were also determined by Western blot analysis. (B) The signals obtained for ACE2 in the culture supernatants examined in panel A (left) or in the supernatants of cells treated with Fc control protein, SARS-S Fc, or NL63-S Fc protein (right) were quantified employing ImageJ software. The

binding studies in an enzyme-linked immunosorbent assay (ELISA) format revealed highly efficient capture of recombinant ACE2 by SARS-S, while binding of ACE2 to NL63-S was barely detectable (Fig. 1C). In addition, SARS-S binding to ACE2 was readily observed in a BiACore system-based analysis (Fig. 1D), while NL63-S did not specifically bind to ACE2 (data not shown). Finally, preincubation of ACE2-transfected cells with recombinant SARS-S blocked subsequent infection with lentiviruses pseudotyped with SARS-S and NL63-S, while inhibition with recombinant NL63-S was much less pronounced (Fig. 1E). In summary, our results and those of previous studies (20, 22) indicate that SARS-S binds to ACE2 with higher efficiency than NL63-S.

We next asked if ACE2 expression is differentially downregulated by the viral S proteins. Recent work by Haga and colleagues demonstrated that binding of recombinant and virion-associated SARS-S to ACE2 induces ACE2 shedding in a disintegrin and metalloproteinase domain 17 (ADAM17)/tumor necrosis factor alpha (TNF- α)-converting enzyme (TACE)-dependent manner (8, 18). These observations indicate that ACE2 shedding might reduce ACE2 surface expression. We therefore investigated ACE2 shedding from Vero E6 cells, which express endogenous ACE2. ACE2 expression in cell lysates and the presence of ACE2 in trichloroacetic acid (TCA)-precipitated cell culture supernatants was detected by Western blot analysis (Fig. 2A). Detection of β -actin served as a loading control for the analysis of cell lysates. For control of comparable precipitation efficiency, ovalbumin (OVA) was added to supernatants and also detected by Western blot analysis. Phorbol myristate acetate (PMA) treatment induced shedding of ACE2 into the cellular supernatants and reduced the amount of cell-associated ACE2, in agreement with previous results (Fig. 2A, top) (8, 18). Incubation of cells with control virus-like particles (VLPs) bearing no viral glycoprotein did not induce ACE2 shedding. In contrast, VLPs bearing SARS-S triggered ACE2 shedding over time (Fig. 2A). The levels of cell-associated ACE2 remained constant, suggesting that ACE2 release was less efficient than release from PMA-treated cells. Notably, ACE2 shedding was also observed upon incubation of cells with VLPs bearing NL63-S, albeit the kinetics were delayed compared to cells exposed to SARS-S-bearing VLPs (Fig. 2A, bottom, and 2B). Similarly, ACE2 shedding was induced by soluble NL63-S but with lower efficiency than virion-associated protein (Fig. 2B). Collectively, SARS-S and to a lesser extent NL63-S can induce ACE2 shedding.

We then assessed if shedding contributes to ACE2 downregulation. For this, we employed TAPI-0, a TACE inhibitor (24). Incubation of PMA-treated cells with TAPI-0 abrogated

ACE2 release (Fig. 2C), as expected (8, 18), confirming that the compound was active at the concentrations used. If ACE2 shedding contributes to ACE2 downregulation, as previously observed by Kuba and colleagues (16), we reasoned that this process should be sensitive to inhibition by TAPI-0. Following the previously established FACS-based protocol, binding of S proteins to Vero E6 cells was analyzed at 37°C (to allow shedding) in the presence and absence of TAPI-0. In addition, binding of S proteins to Vero E6 cells at 4°C (to prevent shedding) was determined as a control. SARS-S but not a control Fc protein bound efficiently to Vero E6 cells maintained at 4°C (Fig. 2D, top). Binding of SARS-S was markedly diminished when cells were incubated at 37°C (Fig. 2D, top), in agreement with published results (16). Notably, this effect could be completely reversed by incubation of cells with TAPI-0 (Fig. 2D, middle). Thus, ACE2 shedding accounted for the reduced SARS-S binding and was most likely responsible for the diminished ACE2 surface expression previously observed under these conditions (an antibody for detection of ACE2 on Vero cells by FACS was not available for the present study) (16). In contrast, appreciable binding of NL63-S to Vero E6 cells was not observed (Fig. 2D, bottom), in agreement with the less-efficient ACE2 binding (Fig. 1) and less-efficient ACE2 shedding (Fig. 2A) by NL63-S compared to SARS-S.

We next determined if coexpression of SARS-S or NL63-S with ACE2 can also reduce ACE2 expression. One rationale behind this approach is the observation that interactions of viral glycoproteins with their cognate cellular receptors within the secretory pathways of infected cells can lead to formation of receptor-glycoprotein complexes and subsequent receptor degradation (12). In addition, ligation of ACE2 on neighboring cells by surface-expressed S protein could contribute to ACE2 downregulation under these conditions. To investigate if coexpression of SARS-S and NL63-S interferes with ACE2 expression levels, we coexpressed these proteins in 293T cells stably expressing ACE2. Expression of SARS-S but not expression of NL63-S or other SARS-CoV proteins reduced ACE2 levels in transiently transfected 293T cells (Fig. 2E and F), at least under optimal transfection conditions, indicating that expression of SARS-S but not other SARS-CoV proteins in infected cells could interfere with ACE2 expression.

Haga and colleagues suggested that ACE2 shedding upon binding to SARS-S is required for uptake of SARS-CoV particles into 293T cells (8). We therefore assessed if ACE2 shedding is required for productive SARS-CoV and NL63 infection. To this end, we investigated if TAPI-0, which prevented ACE2 shedding in the experimental settings described above (Fig. 2C and D), could inhibit transduction of cells by a lentiviral vector pseudotyped with SARS-S and NL63-S. Preincu-

average of two independent experiments is shown in the left panel. The right panel depicts the average of three independent experiments. (C) To confirm the importance of TACE for ACE2 shedding, Vero E6 cells were incubated with 0.1 μ M PMA in the presence of the indicated concentrations of TAPI-0, a TACE inhibitor. ACE2 shedding was analyzed as described for panel A. (D) Vero E6 cells were incubated with SARS-S for 3 h at 4°C or 37°C in the absence (top) and presence (middle) of TAPI-0. Alternatively, cells were incubated with NL63-S protein for 3 h at 4°C or 37°C (bottom). Thereafter, unbound protein was removed by washing, and protein binding was determined by FACS analysis. (E) 293T cells engineered to express high levels of ACE2 were transiently transfected with 3 μ g of plasmids encoding SARS-S, NL63-S, or the indicated SARS-CoV proteins, and ACE2 surface expression was determined by FACS analysis. (F) The experiment was carried out as described in panel E. However, the cells were harvested at 48 h posttransfection, and ACE2 expression in cell lysates was analyzed by Western blot analysis. Expression of β -actin was determined as a loading control.

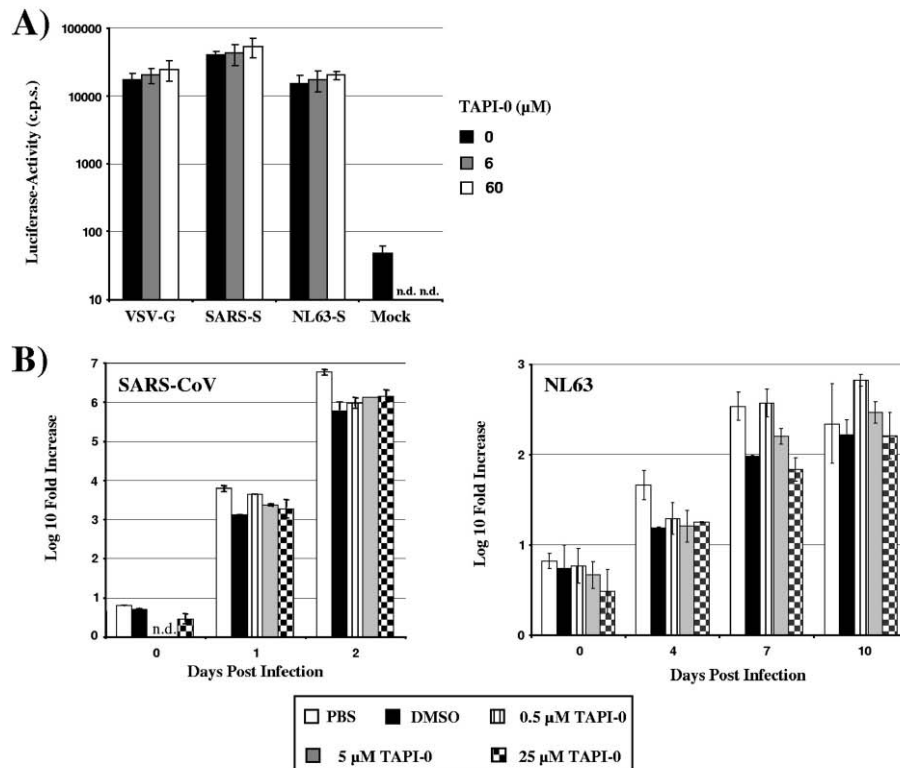


FIG. 3. Shedding of ACE2 is dispensable for SARS-CoV and NL63 spread. (A) In order to determine the importance of TACE activity for SARS-S- and NL63-driven infectious entry, ACE2-transfected 293T cells were incubated with the indicated concentrations of TAPI-0 and infected with infectivity-normalized lentiviral pseudotypes bearing the indicated glycoproteins. At 72 h postinfection, the cells were lysed and the luciferase activities in cell lysates were determined by employing a commercially available kit. (B) To assess the importance of ACE2 shedding to SARS-CoV and NL63 spread, Vero E6 cells were pretreated with the indicated concentrations of TAPI-0 or pretreated with dimethyl sulfoxide (DMSO) as a control and then infected with SARS-CoV (Frankfurt strain) or NL63 at an MOI of 0.001. Supernatants of the infected and noninfected cells were taken at the indicated time points postinfection, and the number of viral genome copies was determined by real-time reverse transcription-PCR (RT-PCR). The following primers and probes were used for detection of the SARS-CoV genome: BNITMSARS1 (5'-TTAT CACCCCGGAAGAACGCT-3') (forward primer), BNITMSARAS2 (5'-CTCTAGTTGCATGACAGCCCTC-3') (reverse primer), BNITMSARP (5'-FAM-TCGTGCGTGGATTGGCTTGATGT-TAMRA-3') (probe). For detection of the NL63 genome, the following primers and probes were used: 63RF2 (5'-CTTCTGGTGACGGCTAGTACAGCTTAT-3') (forward primer), 63RR2 (5'-AGACGTCGTTGATCCCTAACAT-3') (reverse primer), and 63RP (5'-FAM-CAGGTTGCTTAAGTGTCCCATCAGATTAC-3'-TAMRA) (probe). The SARS-CoV and NL63-specific primers both recognize ORF1B sequences. The result of a representative experiment carried out in duplicates is shown.

bation of target cells with TAPI-0 did not inhibit transduction of ACE2-transfected 293T cells by SARS-S- and NL63-S-bearing pseudotypes (Fig. 3A). More importantly, TAPI-0 did not inhibit replication of SARS-CoV and NL63 in Vero E6 cells (Fig. 3B), indicating that S protein-induced ACE2 shedding is dispensable for replication of SARS-CoV and NL63.

Our results indicated that SARS-S binds to ACE2 with higher efficiency than NL63-S and that this correlates with more efficient ACE2 shedding. We then examined how these findings related to ACE2 expression in SARS-CoV- and NL63-infected cells. Vero E6 cells were infected with SARS-CoV (Frankfurt strain) and NL63 at an equal multiplicity of infection (MOI), and ACE2 expression in cell lysates (Fig. 4A and B) and viral copy numbers in the cellular supernatants (Fig. 4C) were analyzed. SARS-CoV replicated with higher efficiency than NL63, with RNA levels in supernatants of SARS-CoV-infected cells at day 1 postinfection being comparable to those in NL63 cultures at 6 days postinfection (Fig. 4C). Replication of SARS-CoV was associated with efficient downregulation of ACE2 expression (Fig. 4A and B), which correlated inversely with viral RNA levels and expression of Nsp8 in cell lysates. In contrast, no appreciable ACE2 downregulation was observed in NL63-infected cell cultures, despite an increase in RNA levels and expression of NL63 proteins (Fig. 4A to C).

tion (MOI), and ACE2 expression in cell lysates (Fig. 4A and B) and viral copy numbers in the cellular supernatants (Fig. 4C) were analyzed. SARS-CoV replicated with higher efficiency than NL63, with RNA levels in supernatants of SARS-CoV-infected cells at day 1 postinfection being comparable to those in NL63 cultures at 6 days postinfection (Fig. 4C). Replication of SARS-CoV was associated with efficient downregulation of ACE2 expression (Fig. 4A and B), which correlated inversely with viral RNA levels and expression of Nsp8 in cell lysates. In contrast, no appreciable ACE2 downregulation was observed in NL63-infected cell cultures, despite an increase in RNA levels and expression of NL63 proteins (Fig. 4A to C).

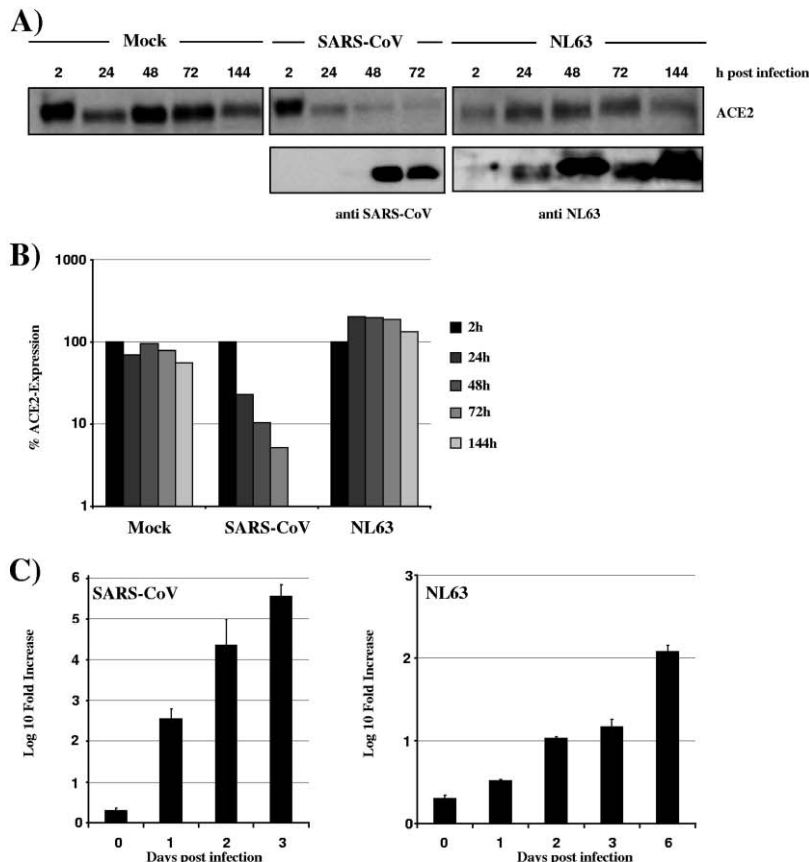


FIG. 4. Downmodulation of ACE2 expression in SARS-CoV-infected cells. (A) Vero E6 cells were infected with SARS-CoV (Frankfurt strain) or NL63 at an MOI of 0.001 in duplicates. At the indicated times postinfection, cells were washed with phosphate-buffered saline (PBS), lysed with sodium dodecyl sulfate (SDS) lysis buffer, and analyzed for expression of ACE2 or viral proteins by Western blot analysis. For detection of viral proteins, an antibody directed against SARS-CoV Nsp8 and a serum reactive against NL63-infected cells were used. (B) The signals for ACE2 in the cellular lysates shown in panel A were quantified using ImageJ software and are shown relative to the signals measured at 2 h postinfection. (C) The supernatants of the infected cells described above were analyzed for viral genome copies by real-time RT-PCR.

Thus, SARS-CoV downregulates its receptor, and the S protein might be instrumental to receptor interference. A direct comparison of ACE2 downregulation in SARS-CoV- and NL63-infected cultures was not possible due to the differential replication efficiencies. However, it can be speculated that relatively inefficient ACE2 engagement by NL63 might contribute to the reduced replication and ACE2 downmodulation compared to SARS-CoV.

Collectively, our data indicate that SARS-S engages ACE2 more efficiently than NL63-S and that this capacity correlates with more efficient induction of ACE2 shedding. Shedding of soluble ACE2 into the cellular supernatants upon binding of the viral S protein might be mainly responsible for the mark-

edly reduced ACE2 expression in the context of SARS-CoV infection (Fig. 2 and 4) (8, 16), albeit trapping and subsequent degradation of ACE2 in the constitutive secretory pathway of infected cells might contribute (Fig. 2E and F), a possibility that deserves further investigation. Previous studies demonstrated that soluble ACE2 can be released in the supernatants of cells exposed to SARS-S or PMA (8, 18) and that release is facilitated by ADAM10 (PMA) and/or ADAM17/TACE (PMA, SARS-S), which are believed to cleave ACE2 between amino acids 716 and 741 (15). Notably, it was suggested that TACE-dependent ACE2 release is induced by SARS-S but not NL63-S binding to ACE2 and that this process is required for infectious SARS-CoV entry (8). However, the latter conclu-

sion was supported only by virus uptake experiments (8), and it was not determined if uptake indeed resulted in infection. For instance, human immunodeficiency virus type 1 (HIV-1) is readily taken up by HeLa cells, but uptake does not result in productive infection (21), indicating that measuring uptake might not be appropriate to determine the efficiency of infectious entry. Our results confirm that SARS-S promotes ACE2 shedding, albeit this effect was not exclusive to SARS-S and was also observed with NL63-S. More efficient induction of ACE2 shedding by virion-associated, trimeric NL63-S compared to soluble, dimeric NL63-S (Fig. 2) was not unexpected, since the former binds to ACE2 with higher avidity. Notably, inhibition experiments with TAPI-0, an ADAM17/TACE inhibitor (24) previously shown to abrogate PMA- and SARS-S-induced ACE2 shedding (8, 18), demonstrated that shedding is dispensable for efficient viral spread (Fig. 3). These observations suggest that ACE2 shedding is a mere byproduct of SARS-CoV and NL63 infection and is not required for infectious entry. Whether shedding of ACE2 promotes the release of infectious particles by preventing interactions between SARS-S on progeny virions and cellular ACE2 remains to be determined (since genome copies and not infectivity in cellular supernatants were quantified in Fig. 3B). Anyway, soluble ACE2 might impact viral spread, since binding to soluble receptor has been shown to block SARS-S-dependent infectious entry (10). It also remains to be clarified if S protein-induced ACE2 release promotes lung injury. While soluble ACE2 can be used to combat lung injury (13, 16), the reduction of local concentrations of membrane-associated ACE2 might indeed promote SARS development.

Replication of SARS-CoV in Vero E6 cells was robust and resulted in efficient ACE2 downregulation (Fig. 4). In contrast, NL63 replicated in Vero E6 cells with relatively low efficiency and did not induce ACE2 downregulation, at least under the conditions tested. In conjunction with the results obtained for recombinant S proteins (Fig. 1), these observations suggest that relatively inefficient ACE2 binding of NL63 relative to SARS-CoV could result in both reduced viral replication and ACE2 downregulation. Conversely, acquisition of increased ACE2 binding capacity might cause emergence of pathogenic NL63 variants. Ultimately, these questions can be addressed only by generation of chimeric viruses and their analysis in animal models for SARS. The recent establishment of a reverse genetic system for NL63 (5) and an aged mouse model for SARS pathogenesis (27) will be instrumental to these research endeavors.

We thank T. F. Schulz for support and BMBF (01 KI 0705 to F.W.; 01KI 0703 to I.G., S.B., and S.P.) and the Center for Infection Biology (I.S.) at Hannover Medical School for funding. G.S. was supported by grant R01AI074986 from the National Institute of Allergy and Infectious Diseases.

REFERENCES

- Banach, S., J. M. Orenstein, L. M. Fox, S. H. Randell, A. H. Rowley, and S. C. Baker. 2009. Human airway epithelial cell culture to identify new respiratory viruses: coronavirus NL63 as a model. *J. Virol. Methods* **156**: 19–26.
- Bastien, N., K. Anderson, L. Hart, P. Van Caeseele, K. Brandt, D. Milley, T. Hatchette, E. C. Weiss, and Y. Li. 2005. Human coronavirus NL63 infection in Canada. *J. Infect. Dis.* **191**:503–506.
- Chiu, S. S., K. H. Chan, K. W. Chu, S. W. Kwan, Y. Guan, L. L. Poon, and J. S. Peiris. 2005. Human coronavirus NL63 infection and other coronavirus infections in children hospitalized with acute respiratory disease in Hong Kong, China. *Clin. Infect. Dis.* **40**:1721–1729.
- Ding, Y., L. He, Q. Zhang, Z. Huang, X. Che, J. Hou, H. Wang, H. Shen, L. Qin, Z. Li, J. Geng, J. Cai, H. Han, X. Li, W. Kang, D. Weng, P. Liang, and S. Jiang. 2004. Organ distribution of severe acute respiratory syndrome (SARS)-associated coronavirus (SARS-CoV) in SARS patients: implications for pathogenesis and virus transmission pathways. *J. Pathol.* **203**:622–630.
- Donaldson, E. F., B. Yount, A. C. Sims, S. Burkett, R. J. Pickles, and R. S. Baric. 2008. Systematic assembly of a full-length infectious clone of human coronavirus NL63. *J. Virol.* **82**:11948–11957.
- Ebihara, T., R. Endo, X. Ma, N. Ishiguro, and H. Kitakuta. 2005. Detection of human coronavirus NL63 in young children with bronchiolitis. *J. Med. Virol.* **75**:463–465.
- Fouchier, R. A., N. G. Hartwig, T. M. Bestebroer, B. Niemeyer, J. C. de Jong, J. H. Simon, and A. D. Osterhaus. 2004. A previously undescribed coronavirus associated with respiratory disease in humans. *Proc. Natl. Acad. Sci. USA* **101**:6212–6216.
- Haga, S., N. Yamamoto, C. Nakai-Murakami, Y. Osawa, K. Tokunaga, T. Sata, N. Yamamoto, T. Sasazaki, and Y. Ishizaka. 2008. Modulation of TNF-alpha-converting enzyme by the spike protein of SARS-CoV and ACE2 induces TNF-alpha production and facilitates viral entry. *Proc. Natl. Acad. Sci. USA* **105**:7809–7814.
- Hamming, I., W. Timens, M. L. Bulthuis, A. T. Lely, G. J. Navis, and H. van Goor. 2004. Tissue distribution of ACE2 protein, the functional receptor for SARS coronavirus. A first step in understanding SARS pathogenesis. *J. Pathol.* **203**:631–637.
- Hofmann, H., M. Geier, A. Marzl, M. Krumbiegel, M. Peipp, G. H. Fey, T. Gramberg, and S. Pöhlmann. 2004. Susceptibility to SARS coronavirus S protein-driven infection correlates with expression of angiotensin converting enzyme 2 and infection can be blocked by soluble receptor. *Biochem. Biophys. Res. Commun.* **319**:1216–1221.
- Hofmann, H., K. Pyrc, L. van der Hoek, M. Geier, B. Berkhouit, and S. Pöhlmann. 2005. Human coronavirus NL63 employs the severe acute respiratory syndrome coronavirus receptor for cellular entry. *Proc. Natl. Acad. Sci. USA* **102**:7988–7993.
- Hoxie, J. A., J. D. Alpers, J. L. Rackowski, K. Huebner, B. S. Haggarty, A. J. Cedarcbaum, and J. C. Reed. 1986. Alterations in T4 (CD4) protein and mRNA synthesis in cells infected with HIV. *Science* **234**:1123–1127.
- Imai, Y., K. Kubo, S. Rao, Y. Huan, F. Guo, B. Guan, P. Yang, R. Sarao, T. Wada, H. Leong-Poi, M. A. Crackower, A. Fukamizu, C. C. Hui, L. Hein, S. Uhlig, A. S. Slutsky, C. Jiang, and J. M. Penninger. 2005. Angiotensin-converting enzyme 2 protects from severe acute lung failure. *Nature* **436**: 112–116.
- Iwai, M., and M. Horinuchi. 2009. Devil and angel in the renin-angiotensin system: ACE-angiotensin II-AT(1) receptor axis vs. ACE2-angiotensin-(1-7)-Mas receptor axis. *Hypertens. Res.* **32**:533–536.
- Jia, H. P., D. C. Look, P. Tan, L. Shi, M. Hickey, L. Gakhar, M. C. Chappell, C. Wohlford-Lenane, and P. B. McCray, Jr. 2009. Ectodomain shedding of angiotensin converting enzyme 2 in human airway epithelia. *Am. J. Physiol. Lung Cell. Mol. Physiol.* **297**:L84–L96.
- Kuba, K., Y. Imai, S. Rao, H. Gao, F. Guo, B. Guan, Y. Huan, P. Yang, Y. Zhang, W. Deng, L. Bao, B. Zhang, G. Liu, Z. Wang, M. Chappell, Y. Liu, D. Zheng, A. Leibbrandt, T. Wada, A. S. Slutsky, D. Liu, C. Qin, C. Jiang, and J. M. Penninger. 2005. A crucial role of angiotensin converting enzyme 2 (ACE2) in SARS coronavirus-induced lung injury. *Nat. Med.* **11**:875–879.
- Lambert, D. W., N. M. Hooper, and A. J. Turner. 2008. Angiotensin-converting enzyme 2 and new insights into the renin-angiotensin system. *Biochem. Pharmacol.* **75**:781–786.
- Lambert, D. W., M. Yarski, F. J. Warner, P. Thornhill, E. T. Parkin, A. I. Smith, N. M. Hooper, and A. J. Turner. 2005. Tumor necrosis factor-alpha convertase (ADAM17) mediates regulated ectodomain shedding of the severe acute respiratory syndrome-coronavirus (SARS-CoV) receptor, angiotensin-converting enzyme-2 (ACE2). *J. Biol. Chem.* **280**:30113–30119.
- Li, W., M. J. Moore, N. Vasileva, J. Sul, S. K. Wong, M. A. Berne, M. Somasundaran, J. L. Sullivan, K. Luzuriaga, T. C. Greenough, H. Choe, and M. Farzan. 2003. Angiotensin-converting enzyme 2 is a functional receptor for the SARS coronavirus. *Nature* **426**:450–454.
- Li, W., J. Sui, I. C. Huang, J. H. Kuhn, S. R. Radoshitzky, W. A. Marasco, H. Choe, and M. Farzan. 2007. The S proteins of human coronavirus NL63 and severe acute respiratory syndrome coronavirus bind overlapping regions of ACE2. *Virology* **367**:567–574.
- Maréchal, V., F. Clavel, J. M. Heard, and O. Schwartz. 1998. Cytosolic Gag p24 as an index of productive entry of human immunodeficiency virus type 1. *J. Virol.* **72**:2208–2212.
- Mathewson, A. C., A. Bishop, Y. Yao, F. Kemp, J. Ren, H. Chen, X. Xu, B. Berkhouit, L. van der Hoek, and I. M. Jones. 2008. Interaction of severe acute respiratory syndrome-coronavirus and NL63 coronavirus spike proteins with angiotensin converting enzyme-2. *J. Gen. Virol.* **89**:2741–2745.
- Moës, E., L. Vigen, E. Keyaerts, K. Zlateva, S. Li, P. Maes, K. Pyrc, B. Berkhouit, L. van der Hoek, and M. Van Ranst. 2005. A novel pan-coronavirus RT-PCR assay: frequent detection of human coronavirus NL63 in children

- hospitalized with respiratory tract infections in Belgium. *BMC Infect. Dis.* 5:6.
24. Mohler, K. M., P. R. Sleath, J. N. Fitzner, D. P. Cerretti, M. Alderson, S. S. Kerwar, D. S. Torrance, C. Otten-Evans, T. Greenstreet, K. Weerawarna, et al. 1994. Protection against a lethal dose of endotoxin by an inhibitor of tumour necrosis factor processing. *Nature* 370:218–220.
 25. Mossel, E. C., J. Wang, S. Jeffers, K. E. Edeen, S. Wang, G. P. Cosgrove, C. J. Funk, R. Manzer, T. A. Miura, L. D. Pearson, K. V. Holmes, and R. J. Mason. 2008. SARS-CoV replicates in primary human alveolar type II cell cultures but not in type I-like cells. *Virology* 372:127–135.
 26. Nie, Y., P. Wang, X. Shi, G. Wang, J. Chen, A. Zheng, W. Wang, Z. Wang, X. Qu, M. Luo, L. Tan, X. Song, X. Yin, J. Chen, M. Ding, and H. Deng. 2004. Highly infectious SARS-CoV pseudotyped virus reveals the cell tropism and its correlation with receptor expression. *Biochem. Biophys. Res. Commun.* 321:994–1000.
 27. Roberts, A., C. Paddock, L. Vogel, E. Butler, S. Zaki, and K. Subbarao. 2005. Aged BALB/c mice as a model for increased severity of severe acute respiratory syndrome in elderly humans. *J. Virol.* 79:5833–5838.
 28. Sims, A. C., R. S. Baric, B. Yount, S. E. Burkett, P. L. Collins, and R. J. Pickles. 2005. Severe acute respiratory syndrome coronavirus infection of human ciliated airway epithelia: role of ciliated cells in viral spread in the conducting airways of the lungs. *J. Virol.* 79:15511–15524.
 29. Skowronski, D. M., C. Astell, R. C. Brunham, D. E. Low, M. Petric, R. L. Roper, P. J. Talbot, T. Tam, and L. Babiuk. 2005. Severe acute respiratory syndrome (SARS): a year in review. *Annu. Rev. Med.* 56:357–381.
 30. To, K. F., and A. W. Lo. 2004. Exploring the pathogenesis of severe acute respiratory syndrome (SARS): the tissue distribution of the coronavirus (SARS-CoV) and its putative receptor, angiotensin-converting enzyme 2 (ACE2). *J. Pathol.* 203:740–743.
 31. Vabret, A., T. Mourez, J. Dina, L. van der Hoek, S. Gouarin, J. Petitjean, J. Brouard, and F. Freymuth. 2005. Human coronavirus NL63, France. *Emerg. Infect. Dis.* 11:1225–1229.
 32. van der Hoek, L. 2007. Human coronaviruses: what do they cause? *Antivir. Ther.* 12:651–658.
 33. van der Hoek, L., K. Sure, G. Ihorst, A. Stang, K. Pyrc, M. F. Jebbink, G. Petersen, J. Forster, B. Berkhouit, and K. Uberla. 2005. Croup is associated with the novel coronavirus NL63. *PLoS Med.* 2:e240.
 34. Wang, P., J. Chen, A. Zheng, Y. Nie, X. Shi, W. Wang, G. Wang, M. Luo, H. Liu, L. Tan, X. Song, Z. Wang, X. Yin, X. Qu, X. Wang, T. Qing, M. Ding, and H. Deng. 2004. Expression cloning of functional receptor used by SARS coronavirus. *Biochem. Biophys. Res. Commun.* 315:439–444.

Different host cell proteases activate the SARS-coronavirus spike-protein for cell-cell and virus-cell fusion

Graham Simmons ^{a,*}, Stephanie Bertram ^b, Ilona Glowacka ^b, Imke Steffen ^b,
Chawaree Chaipan ^{c,d}, Juliet Agudelo ^a, Kai Lu ^a, Andrew J. Rennekamp ^e,
Heike Hofmann ^{c,d,f}, Paul Bates ^e, Stefan Pöhlmann ^{b,g,*}

^a *Blood Systems Research Institute and Department of Laboratory Medicine, University of California, San Francisco, California*

^b *Institute of Virology, Hannover Medical School, 30625 Hannover, Germany*

^c *Institute for Virology University Hospital Erlangen, 91054 Erlangen, Germany*

^d *Nikolaus-Fiebiger-Center, University Hospital Erlangen, 91054 Erlangen, Germany*

^e *Department Microbiology, University of Pennsylvania, PA 19104-6076, USA*

^f *Department of Medical Microbiology and Virology, University of Kiel, 24105 Kiel, Germany*

^g *German Primate Center, Infection Biology Unit, 37077 Göttingen, Germany*

G.S., S.B. and I.G. contributed equally to this work

* Corresponding author (S.P.): German Primate Research Center, Kellnerweg 4, 37077 Göttingen, Germany. Phone: ++49 551 3851 150, Fax: ++49 551 3851 184 E-mail: s.poehlmann@dpz.eu

* Corresponding author (G.S.): Blood Systems Research Institute, 270 Masonic Ave, San Francisco, CA,. USA. Phone: 001 94118 415 901 0748, Fax: 001 415 567-5899, E-mail: gsimmons@bloodsystems.org

Keywords: SARS coronavirus, spike protein, proteolytic cleavage, cathepsin L, furin

Abstract

Severe acute respiratory syndrome coronavirus (SARS-CoV) poses a considerable threat to human health. Activation of the viral spike (S)-protein by host cell proteases is essential for viral infectivity. However, the cleavage sites in SARS-S and the protease(s) activating SARS-S are incompletely defined. We found that R667 was dispensable for SARS-S-driven virus-cell fusion and for SARS-S-activation by trypsin and cathepsin L in a virus-virus fusion assay. Mutation T760R, which optimizes the minimal furin consensus motif 758-RXXR-762, and furin overexpression augmented SARS-S-activity, but did not result in detectable SARS-S cleavage. Finally, SARS-S-driven cell-cell fusion was independent of cathepsin L, a protease essential for virus-cell fusion. Instead, a so far unknown leupeptin-sensitive host cell protease activated cellular SARS-S for fusion with target cells expressing high levels of ACE2. Thus, different host cell proteases activate SARS-S for virus-cell and cell-cell fusion and SARS-S cleavage at R667 and 758-RXXR-762 can be dispensable for SARS-S activation.

Introduction

A novel coronavirus (CoV) has been identified as the causative agent of severe acute respiratory syndrome (SARS), which claimed almost 800 lives in 2002-03 (Drosten et al., 2003; Ksiazek et al., 2003; Peiris et al., 2004). Coronaviruses, including SARS-CoV, harbour three envelope proteins, spike (S), membrane (M), and envelope (E), which are required for virion assembly, release and infectious entry into target cells (Masters, 2006). The SARS-CoV-S-protein (SARS-S) mediates infectious cellular entry (Hofmann et al., 2004b; Simmons et al., 2003; Yang et al., 2004) and constitutes the major target of the neutralizing antibody response (Hofmann and Pöhlmann, 2004; Nie et al., 2004b; Nie et al., 2004a). The carboxypeptidase angiotensin-converting enzyme 2 (ACE2) is used by SARS-CoV as receptor for cell entry (Li et al., 2003; Wang et al., 2004) and is expressed on type II pneumocytes, the major viral target cells (Hamming et al., 2004; Mossel et al., 2008; To et al., 2004). Several cellular C-type lectins augment or facilitate SARS-S-driven entry (Gramberg et al., 2005; Jeffers et al., 2004; Marzi et al., 2004; Yang et al., 2004). However, ACE2 but not C-type lectin expression correlates with susceptibility to SARS-S-driven infection (Hofmann et al., 2004a; Nie et al., 2004b) and is essential for SARS-CoV spread in experimentally infected mice (Kuba et al., 2005), indicating that ACE2 is a major and likely the only receptor used by SARS-CoV in the infected host. Collectively, SARS-S interacts with host cell factors to

mediate the first essential step in the viral life cycle, virus entry into target cells, and constitutes an attractive target for preventive and therapeutic approaches.

The SARS-S-protein is synthesized in the constitutive secretory pathway of infected cells. Amino acid motifs in its cytoplasmic tail slow down transit through the Golgi compartment (McBride et al., 2007) where interactions with the M-protein facilitate virion incorporation (McBride and Machamer, 2010; Voss et al., 2009). The structural organization of SARS-S is similar to that of several other viral envelope proteins, termed class I fusion proteins: The extracellular S1 domain facilitates binding to the receptor, ACE2, while the membrane-anchored S2 domain harbours the functional elements required for fusion of the viral with a target cell membrane (Hofmann and Pöhlmann, 2004). Viral class I fusion proteins are usually synthesized in an inactive form, and require activation by host cell proteases to transit into a fusion-active state (Eckert and Kim, 2001; Harrison, 2008). However, viral strategies to accomplish proteolytic activation can vary. For instance, the majority of strains of the murine coronavirus mouse hepatitis virus (MHV) contain S-proteins that are cleaved by furin in infected cells, and these viruses are believed to enter target cells by receptor-dependent, pH-independent fusion with the plasma membrane (de Haan et al., 2004; Nash and Buchmeier, 1997; Qiu et al., 2006), although some of these findings are controversial (Eifart et al., 2007; Simmons et al., 2005). In contrast, the S-protein of the MHV type 2 strain is not cleaved by furin and the spike protein on incoming virions is activated in target cell vesicles by endosomal proteases of the cathepsin family (Qiu et al., 2006).

Similar to MHV-2, proteolytic activation of SARS-S is mediated by cathepsins in target cells, most importantly by cathepsin L (Simmons et al., 2005). Cleavage-activation by cathepsin L is thought to require previous binding of SARS-S to ACE2, which is believed to induce a conformational change in the S-protein (Simmons et al., 2005), and seems to involve at least two consecutive proteolytic processing steps (Belouzard et al., 2009; Simmons et al., 2005). However, the cleavage sites in SARS-S have been incompletely defined. Arginine 667 was shown to be required for the robust augmentation of SARS-S-driven cell-cell (Belouzard et al., 2009; Follis et al., 2006) and virus-cell fusion (Kam et al., 2009) by trypsin and for the trypsin-dependent circumvention of the entry blockade imposed by lysosomotropic agents (Belouzard et al., 2009). In spite of these results, it is at present unknown if R667 is required for SARS-S activation by cathepsin L. Recent evidence suggests that R797 is a component of a second cleavage site (Belouzard et al., 2009; Watanabe et al., 2008). Thus, similar as for R667, residue R797 was demonstrated to be required for trypsin-dependent augmentation of SARS-S-dependent membrane fusion and for trypsin-

dependent resistance to lysosomotropic agents (Belouzard et al., 2009). Nevertheless, efficient proteolytic processing of wild type SARS-S at this site, or at any other site, has so far not been demonstrated in cells (Hofmann et al., 2004b; Simmons et al., 2004; Xiao et al., 2003; Yang et al., 2004; Yao et al., 2004), with one exception (Wu et al., 2004). Notably, the SARS-S-protein contains a minimal furin cleavage site at position 758 – 761 (RNTR), and a peptide comprising this sequence is efficiently cleaved by furin (Bergeron et al., 2005). However, the contribution of the RNTR motif to proteolytic activation of SARS-S is unknown.

In order to explore the role of the minimal furin cleavage site at position 758-761 and to further investigate the importance of the protease sensitive site at position R667, we analyzed the SARS-S mutants R667A and T760R. Our analysis revealed the R667 was required for responsiveness to trypsin-treatment in some experimental systems but had no effect on SARS-S activation by trypsin and cathepsin L in a virus-virus fusion assay, which adequately mimics, in isolation, the conditions required for SARS-S-driven membrane fusion, suggesting that R667 might not play a major role in SARS-S activation in target cells. Mutation T760R, which optimized an existing minimal furin cleavage motif, increased SARS-S activity but no evidence for cleavage of mutant T760R was obtained. Finally, our results demonstrate the cathepsin L activates SARS-S for virus-cell but not cell-cell fusion, which was dependent on the activity of a so far uncharacterized serine protease (for fusion with targets expressing high amounts of ACE2) or addition of exogenous trypsin (for fusion with targets expressing low amounts of ACE2).

Results

Residue R667 but not K672 determines sensitivity of SARS-S to inactivation by trypsin

Based on alignments with other coronaviruses, it has been suggested that residues R667 and K672 define a potential cleavage site for host cell proteases (Bergeron et al., 2005; Follis et al., 2006). To determine the importance of these residues for SARS-S sensitivity to proteolysis, we introduced mutations R667A or K672L into wt SARS-S (Fig. 1). Analysis of the SARS-S mutants by lentiviral pseudotyping, an experimental approach which adequately models SARS-S-driven entry into target cells (Hofmann et al., 2004b; Moore et al., 2004; Simmons et al., 2004), showed that the mutations R667A and K672L were both compatible with robust SARS-S-driven virion incorporation and entry (Fig. 2A,B), albeit the entry efficiency of viruses harbouring the mutant S-proteins was somewhat reduced compared to

pseudotypes bearing wt SARS-S (Fig. 2A). Similar results were seen with a R667A and K672L double mutant (wt SARS-S: $44,390 \pm 3286$ counts per second (c.p.s.), R667A/K672DL: $39,953 \pm 1329$ c.p.s.), demonstrating that these particular basic residues are not required for infectious entry in tissue culture.

We next assessed if the exchanges R667A and K672L altered sensitivity of SARS-S-bearing pseudotypes to trypsin treatment, which was previously shown to inactivate cell-free virions (Simmons et al., 2004; Simmons et al., 2005). Indeed, pre-treatment of pseudotypes bearing wt SARS-S and SARS-S mutant K672L reduced viral infectivity in a dose-dependent manner (Fig. 2C). In contrast, SARS-S mutant R667A was resistant to inactivation by trypsin (Fig. 2B,C), indicating that R667 defines a trypsin-sensitive site and that cleavage at this site abrogates infectivity of free virions. To further characterize the importance of R667 for SARS-S sensitivity to proteolysis, we compared pseudotypes bearing wt SARS-S and SARS-S mutant R667A for their sensitivities to inactivation by a panel of proteases. Treatment with trypsin, plasmin factor Xa and, to a lesser extent, thrombin reduced infectivity of viruses harbouring wt SARS-S but not SARS-S mutant R667A (Fig. 2D), further underlining that R667 defines a protease sensitive site. Thermolysin and chymotrypsin treatment also diminished viral infectivity, but wt SARS-S and SARS-S mutant R667A were equally sensitive to inactivation by these proteases (Fig. 2D), indicating that they cleave SARS-S at a site distinct from R667. Collectively, R667 but not K672 defines a protease-sensitive site and proteolysis of cell-free virions at this site abrogates viral infectivity.

Residue R667 is indispensable for trypsin-induced infection of target cells treated with ammonium chloride

Lysosomotropic agents, such as ammonium chloride, interfere with endosomal acidification and block infectious entry of SARS-CoV (Hofmann et al., 2004b; Simmons et al., 2004; Yang et al., 2004), presumably by inhibiting cathepsins, which require low pH for optimal activity. Treatment of cell-bound virus with trypsin was shown to allow infectious SARS-S-driven entry into ammonium chloride-treated cells (Simmons et al., 2005), indicating that trypsin can functionally replace cathepsin L as a SARS-S-activating protease under these conditions (“trypsin bypass”). We asked if R667 is required for a trypsin bypass of endosomal acidification. Treatment of target cells with ammonium chloride markedly inhibited infectious entry driven by wt SARS-S and SARS-S mutant R667A, and infectivity of wt SARS-S bearing viruses could be fully restored by treatment of cell-bound virions with trypsin (Fig. 3). In contrast, infectivity of R667A bearing virions was not rescued by trypsin treatment (Fig. 3), indicating that R667 is required for activation of cell-bound virions by trypsin.

Residue R667 is dispensable for activation of SARS-S by trypsin and cathepsin L in a virus-virus fusion assay

We next assessed the impact of R667A on SARS-S proteolytic activation in a virus-virus membrane-fusion assay. In this assay, SARS-S bearing viruses (which also contain the Avian Sarcoma Leukosis Virus-A envelope protein, EnvA, in their membrane) are allowed to fuse with ACE2 harbouring viruses. The fusion efficiency is then quantified by addition of virions to leupeptin-treated (to exclude an impact of host cell proteases on SARS-S activation) HeLa cells, which express the EnvA receptor TvA, and which are not susceptible to SARS-S-driven infection (Simmons et al., 2005). Thus, the virus-virus fusion assay is a reductionistic model system, which allows the proteolytic activation of SARS-S to proceed under cell free conditions. Efficient fusion of virions bearing wt SARS-S with virions bearing ACE2 was only observed upon treatment of particles with trypsin and recombinant activated cathepsin L (Fig. 4), in agreement with previously reported results (Simmons et al., 2005). Strikingly, trypsin and cathepsin L treatment activated virions bearing wt SARS-S and SARS-S mutant R667A with similar efficiency (Fig. 4), demonstrating that R667 was dispensable for SARS-S activation under these conditions. In summary, R667 defines a trypsin cleavage site, which is responsible for trypsin-dependent activation of cell-bound and inactivation of cell-free virions, respectively. However, R667 is dispensable in tissue culture infection and for SARS-S activation by trypsin and cathepsin L in a virion-virion fusion assay, and might thus be dispensable for proteolytic activation of SARS-CoV in target cells.

Substitution T760R augments SARS-S-driven infection and cell-cell fusion

We hypothesized that the minimal furin cleavage site (RXXR) at position 758 - 761 might contribute to SARS-S-dependent membrane fusion by allowing SARS-S cleavage, albeit with low efficiency. To investigate the role of this motif in SARS-S-driven entry, we assessed if optimization of the minimal furin cleavage site by exchange of T760R (resulting in the sequence RXRR, Fig. 1) affects SARS-S function. Fluorescence-activated cell sorting analysis revealed that SARS-S mutant T760R and wt SARS-S were expressed to comparable levels at the surface of transfected 293T cells, and could thus be directly compared in functional studies (supplementary figure 1). We first determined if substitution T760R affected S-protein-driven infectious entry. In order to assess infectious entry facilitated by the S-protein variant, pseudotypes were used for infection of control or ACE2-transfected 293T cells (Fig. 5, left panel). The 293T cell line expresses endogenous ACE2 and is therefore susceptible to SARS-

S-driven infection (Hofmann et al., 2004b; Hofmann et al., 2004a; Li et al., 2003; Simmons et al., 2004; Yang et al., 2004). Accordingly, infectious entry of SARS-S-bearing pseudovirions into control transfected cells was detectable (Fig. 5, left panel). Notably, entry driven by the T760R variant was about 2-fold more efficient than infection driven by SARS-S wt, and a similar observation (4-fold increase) was made when infection of ACE2-transfected cells was examined (Fig. 5, left panel), suggesting that T760R augments S-protein activity. Indeed, when SARS-S-driven membrane fusion was assessed in a previously reported cell-cell fusion assay (Hofmann et al., 2006), which measures fusion of effector 293T cells expressing S-proteins with 293T target cells expressing ACE2 or pcDNA3, again the S-protein mutant was more active than SARS-S wt (Fig. 5, right panel). Thus, the introduction of an arginine residue at position 760 increases the membrane fusion activity of SARS-S.

Overexpression of furin enhances cell-cell and virus-cell fusion driven by SARS-S wt and mutant T760R

Exchange T760R optimizes a minimal furin cleavage site in SARS-S and might increase SARS-S activity by facilitating cleavage by furin or related proteases. We investigated whether furin can augment SARS-S activity by determining the infectivity of p24-normalized SARS-S pseudotypes produced in the absence and presence of overexpressed furin (Fig. 6, left panel). Overexpression of furin moderately increased infectivity of pseudotypes bearing wt SARS-S or mutant T760R. The most notable effect was observed for SARS-S wt pseudotypes, which showed a ~7-fold augmented infectivity (Fig. 6, left panel), albeit this increase was not statistically significant. Comparable observations were made when S-driven cell-cell fusion was examined, and the increase in activity of wt SARS-S and mutant T760R observed upon furin overexpression was statistically significant (Fig. 6, right panel). However, fusion driven by SARS-S wt and T760R were augmented to similar degrees (about 2-3 fold) by furin overexpression. Thus, high levels of furin enhance SARS-S-protein driven cell-cell and virus-cell fusion.

Furin overexpression does not facilitate detectable cleavage of wt SARS-S and mutant T760R

Our functional data showed that mutation of T760R and overexpression of furin augmented SARS-S activity, presumably by facilitating proteolytic processing of the S-protein. To assess SARS-S cleavage, we conducted Western blot analyses of lysates of S-protein transfected 293T cells, using a serum specific for the S2-portion of SARS-S. Expression of β-actin served as loading control. Our results revealed a prominent

band of approximately 160 kDa for both wt SARS-S and mutant T760R (Fig. 7), which is expected for uncleaved SARS-S (Hofmann et al., 2004b). Treatment of cells with trypsin before lysis reduced the signal obtained for uncleaved SARS-S, and a band of approximately 90 kDa appeared, in accordance with the previously reported size of the S2-fragment of SARS-S (Bergeron et al., 2005; Follis et al., 2006). Coexpression of furin with SARS-S wt or the S-protein variant T760R did not result in the appearance of a S2-band, indicating that furin-mediated cleavage was inefficient or absent.

Virus-cell fusion but not cell-cell fusion by SARS wt and T760R depends on cathepsin activity

We next investigated whether exchange T760R altered the sensitivity of SARS-S-dependent membrane fusion to inhibition by the cathepsin L and B inhibitor MDL 28170. In agreement with published data (Simmons et al., 2005), MDL 28170 efficiently reduced infection by SARS-S-bearing pseudotypes (Fig. 8, left panel). Similar inhibition was observed with the SARS-S mutant T760R, indicating that this change did not modulate cathepsin-dependence of viral entry. In stark contrast, MDL 28170 had no inhibitory effect on wt SARS-S and T760R dependent cell-cell fusion (Fig. 8, right panel), indicating the SARS-S-protein-driven fusion of cellular membranes does not depend on cathepsin activity.

SARS-S-dependent cell-cell fusion is inhibited by leupeptin

Since SARS-S-driven cell-cell fusion was not dependent on cathepsin-activity, we asked if the activity of other proteases might be required. For this, we first sought to clarify to which extend SARS-S-driven cell-cell fusion depends on the presence of exogenous trypsin, since previous studies reported that efficient SARS-S-driven cell-cell fusion occurred only upon treatment of SARS-S expressing cells with trypsin (Howard et al., 2008; Simmons et al., 2004), while in our experiments trypsin was dispensable for robust cell-cell fusion (Figs. 5, 6 and 8). When we examined fusion of SARS-S or VSV-G transfected 293T cells with control transfected 293T cells (which express low levels of endogenous ACE2 (Hofmann et al., 2004a; Li et al., 2003; Simmons et al., 2004)), we found that trypsin treatment was required for SARS-S- but not VSV-G-driven cell-cell fusion, and that fusion driven by VSV-G but not SARS-S was induced by low pH (Fig. 9A). However, when cell-cell fusion with ACE2 transfected 293T cells was examined, robust SARS-S-driven fusion was already observed in the absence of trypsin treatment, and the fusion activity was further augmented in the presence of trypsin (Fig. 9A). Thus, SARS-S-driven cell-cell fusion depends on trypsin-activation of SARS-S only if receptor levels are limiting. If ACE2 is expressed at high

levels, robust fusion occurs in the absence of trypsin and is most likely due to SARS-S activation by a host cell protease other than cathepsins.

In order to investigate the need for a host cell protease for trypsin-independent SARS-S-driven cell-cell fusion, we inhibited the wt SARS-S-driven cell-cell fusion reaction by leupeptin, an inhibitor of cysteine and serine protease, AEBSF, a serine protease inhibitor, and the cathepsin inhibitors E64c and MDL28170. All inhibitors were used at non-cytotoxic concentrations, as determined by a commercially available cytotoxicity assay (Promega, Madison, USA) and by the lack of inhibition of luciferase expression in cells cotransfected with the reporter plasmids employed to quantify cell-cell fusion (supplementary figure 2). Of all inhibitors tested, only leupeptin inhibited SARS-S-driven cell-cell fusion, and inhibition was dose-dependent (Fig. 9B). Finally, leupeptin, E64c and MDL28170 inhibited SARS-S-driven virus-cell fusion (Fig. 9C), as expected from the results shown in Fig. 8 and from previous work (Simmons et al., 2005). Thus, SARS-S-driven cell-cell fusion depends on the activity of a so far uncharacterized cysteine or serine protease, while virus-cell fusion requires cathepsin activity.

Discussion

The processing of SARS-S by cellular proteases might determine route and efficiency of viral entry into target cells and might have important consequences for development of preventive and therapeutic strategies (Belouzard et al., 2009; Simmons et al., 2005; Watanabe et al., 2008). However, the sites in SARS-S, which are recognized by host cell proteases, are incompletely defined. We show that R667 defines a trypsin sensitive site, which is required for inactivation of cell-free virus by trypsin and for trypsin-dependent infectious entry of cell-bound virus into targets pretreated with ammonium chloride. In contrast, the integrity of R667 was dispensable for infectious entry in cell culture and activation of SARS-S-driven virus-virus fusion by trypsin and cathepsin L. Optimization of an existing minimal furin cleavage site, 758-RNTR-761, by mutation T760R augmented SARS-S-driven cell-cell and virus-cell fusion. However, no evidence for cleavage of SARS-S at this motif was obtained. Finally, differential blockade of SARS-S-driven virus-cell and cell-cell fusion by protease inhibitors showed that these processes depend on different activating proteases, with a so far poorly characterized serine or cysteine protease being responsible for SARS-S-driven cell-cell fusion.

The spike protein of SARS-CoV contains several potentially protease sensitive sites, which have been implicated in proteolytic processing of SARS-S (Belouzard et al., 2009; Bergeron et al., 2005; Follis et al., 2006). The most N-terminal motif, amino acids 657 to 676, shows some similarity to cleavage sites of other coronavirus S-proteins but does not comprise an RXXR motif recognized by proprotein convertases in the context of cleavable coronavirus S-proteins (Follis et al., 2006). Nevertheless, mutation of R667 was reported to block the increase in SARS-S membrane fusion activity observed for wt SARS-S upon furin overexpression, and introduction of a furin consensus sequence at this site was shown to increase SARS-S-driven cell-cell fusion (Belouzard et al., 2009; Follis et al., 2006). Our results demonstrate that this site is important for SARS-S cleavage by trypsin, and that trypsin cleavage depends on the presence of R667 but not K672. Thus, cell-free virions bearing wt SARS-S but not SARS-S mutant R667A were inactivated by trypsin, while cell-bound virions bearing wt SARS-S but not mutant R667A were activated by trypsin for infection of ammonium chloride pretreated target cells (trypsin bypass). These findings are in agreement with published work (Belouzard et al., 2009; Follis et al., 2006), and highlight that R667 defines a protease sensitive site in SARS-S. Unexpectedly, however, mutation of R667 was compatible with robust SARS-S activation by trypsin and cathepsin L in a virion-virion fusion assay. The reasons for the differential requirement for R667 in the trypsin bypass and virion-virion fusion assays are at present unclear, but might relate to different properties of target cell membrane relative to virion membrane, in terms of receptor concentration and presence of cellular proteases. Regardless of the underlying mechanism, the present data suggest that R667 might be dispensable for activation of SARS-CoV by trypsin and by cathepsin L. Such a scenario would be in agreement with results by Bosch and colleagues, who mapped the cathepsin L cleavage site in SARS-S to amino acid T678 (Bosch et al., 2008).

Belouzard and colleagues suggested that proteolytic activation of SARS-S might be a two-step process and might involve cleavage at R667 and at R797 (Belouzard et al., 2009). Evidence for an important role of R797 in proteolytic activation of SARS-S was obtained in cell-cell fusion and trypsin bypass experiments, in which the SARS-S mutant R797N was found to be refractory to activation by trypsin (Belouzard et al., 2009). In addition, the insertion of a furin consensus motif at this site increased SARS-S activity in a cell-cell fusion assay (Belouzard et al., 2009) and, as documented by an independent study, allowed cathepsin-independent infectious entry into target cells (Watanabe et al., 2008). Notably, a minimal furin cleavage site, RXXR, is present in SARS-S at amino acids 758 to 761, and a peptide spanning this motif was previously shown to be cleaved by furin, while peptides spanning R667 and R797 were

not recognized by the protease (Bergeron et al., 2005). We found that optimizing the minimal furin site at position 758 (mutant T760R) significantly increased SARS-S activity in cell-cell and virus-cell fusion assays, and we noted that the virus-cell fusion activity of wt SARS-S but not mutant T760R was augmented by overexpression of furin in virus-producer cells, although this effect was not statistically significant. These results suggest that amino acids 758 to 761 might constitute an alternative processing site, which might be recognized by proprotein convertases or related enzymes. However, proteolytic processing of wt SARS-S or variant T760R upon furin overexpression could not be demonstrated, indicating that cleavage was inefficient or absent. Therefore, alternative scenarios for the role of amino acids 758 to 761 in SARS-S activation must be considered. Thus, it is possible that augmentation of SARS-S activity upon furin overexpression and mutation T760R were separate effects, with T760R potentially modulating protease sensitivity of other sites in SARS-S.

Cell to cell fusion assays are commonly used to functionally analyze SARS-S, including the characterization of potential proteolytic processing sites in SARS-S (Belouzard et al., 2009; Follis et al., 2006; Hofmann et al., 2006; Simmons et al., 2003). In most studies, SARS-S-driven cell-cell fusion was examined upon activation of SARS-S by exogenous trypsin. However, it has so far not been determined if SARS-S-driven cell-cell fusion can also be activated by a host cell protease. For instance, it is unknown if the proteases responsible for proteolytic activation of virus-associated SARS-S, cathepsins B and L, can also activate cell-associated SARS-S. We found that trypsin-activation of SARS-S was only required for fusion with cells expressing low amounts of ACE2, while fusion with target cells expressing high levels of ACE2 proceeded efficiently in the absence of trypsin, in agreement with a recent study (Glowacka et al., 2011). Under the latter conditions, cell-cell fusion driven by SARS-S was inhibited by leupeptin but not cathepsin inhibitors, indicating that a serine protease, or a cysteine protease other than cathepsins B and L, can activate SARS-S for cell-cell fusion. The identity of the responsible protease(s) is at present unclear. A role for factor Xa, a serine protease, has been suggested but the results await confirmation (Du et al., 2007). The type II transmembrane serine proteases (TTSPs) TMPRSS2 and TMPRSS4 can activate the influenza virus hemagglutinin by cleavage (Bottcher et al., 2006; Chaipan et al., 2009) and these proteases were recently shown to also activate SARS-S for membrane fusion (Glowacka et al., 2011; Matsuyama et al., 2010; Shulla et al., 2011). However, appreciable expression of TMPRSS2 or TMPRSS4 was not detected in 293T cells in a previous study (Bertram et al., 2010), and SARS-S-driven cell-cell fusion was not inhibited by the serine protease inhibitor AEBSF (present study), which was shown to be active against other TTSPs (Beliveau et al., 2009).

Therefore, TTSPs and related serine proteases are unlikely to account for SARS-S activation under the conditions tested here, and future studies should focus on the role of cysteine proteases.

Materials and Methods

Plasmid construction and in vitro-mutagenesis

Expression plasmids pCAGGS-SARS-S, encoding the spike proteins of SARS-CoV strain Frankfurt (Hofmann et al., 2004b) or Urbani (Simmons et al., 2003), and pcDNA3-hACE2, encoding the human ACE2 receptor, have been described previously (Hofmann et al., 2004b; Hofmann et al., 2004a). Site-directed mutagenesis of the SARS-S-protein was performed by overlap-extension PCR. For generation of mutation T760L the following overlapping primers were used: p5 SARS-S T760R (5'-CCGACGTGAAGTGGTCGCTCAAGTC-3') and p3 SARS-S T760R (5'-GACTTGAGCGAA CACTTCACGTCGGTTGCGATCCTGTTCAAGCAATACC-3'). To facilitate generation of PCR fragments bearing the desired mutations, only the 3' prime portion of the S-sequence was amplified using overlapping PCR. Subsequently, the PCR-amplified fragments were introduced into a pCAGGS variant harbouring the corresponding 5' portion of the SARS-S sequence. Variants R667A, K672L and KPTKR to EPTED were generated using Quikchange site directed mutagenesis (Stratagene), with SARS-S in pcDNA as template, and then transferred to pCAGGS. All PCR amplified sequences were confirmed by automated sequence analysis.

Cell culture

293T cells were propagated in Dulbecco's modified Eagle's medium (DMEM) supplemented with 10% fetal bovine serum (FBS), penicillin and streptomycin, and grown in a humified atmosphere of 5% CO₂. 293T cells stably expressing ACE2 (293T-hACE2) were generated by transfection of plasmid pcDNA3.1zeo-hACE2 (Hofmann et al., 2004a) into 293T cells followed by selection of resistant cells with zeocin (Invitrogen) at 50µg/ml. Surface expression of ACE2 on clonal cells was confirmed by FACS analysis.

Cell-cell fusion assays

For analysis of cell-cell fusion, 293T effector cells seeded in 6-well plates at 3x10⁵/well were CaPO₄-cotransfected with plasmid pGAL4-VP16, encoding the Herpes

Simplex VP16 transactivator fused to the DNA binding domain of the yeast transcription factor GAL4 (Stamminger et al., 2002), and plasmids encoding SARS-S-variants (or empty plasmid) and furin (or empty plasmid). In parallel, 293T target cells were seeded in 48-well plates at 3x10⁴/well and transfected with pcDNA3 or the hACE2 expression plasmid together with plasmid pGal5-luc, in which luciferase reporter gene expression is controlled by five GAL4 binding sites (Stamminger et al., 2002). The day after transfection, effector cells were diluted in fresh medium and added to the target cells. Cell-cell fusion was quantified by determination of luciferase activities in cell lysates 48 h after cocultivation using a commercially available kit (Promega, Madison, USA). Results generated in the experimental system described above are shown in figures 5, 6, 8 and 9B. Alternatively, cell-cell fusion was assayed using α -complementation of β -galactosidase fragments, as previously described for HIV (Holland et al., 2004). For this, effector 293T cells were co-transfected with plasmids encoding SARS-S or VSV-G and a plasmid encoding an N-terminal fragment of β -galactosidase (amino-acids 1-80; termed α peptide), while target 293T cells were co-transfected with a plasmid encoding ACE2 or with the corresponding empty plasmid and a plasmid encoding the remaining C-terminal portion of β -galactosidase (amino-acids 80-1023; termed ω fragment). The day after transfection, effector cells were diluted in fresh medium and added to the target cells at a ratio of 1:1. After one hour incubation for attachment and binding, cells were washed in serum-free medium and pulsed with medium adjusted to pH5.0, pH7.0, pH8.0 or containing TPCK-trypsin at 15 μ g/ml for 10 minutes at 37°C. pH or trypsin were neutralized by the addition of excess medium containing serum and trypsin inhibitor. Cells were then incubated for a further five hours. Upon viral envelope-driven membrane fusion the α peptides and ω fragments of β -galactosidase trans-complement each other to give functional β -galactosidase enzymatic activity, which was detected in cell lysates employing a commercially available kit (Galacton Plus substrate, Applied Biosystems). Results generated in this experimental system are shown in figure 9A.

Production of lentiviral pseudotypes and infection experiments

For generation of lentiviral pseudoparticles, CaPO₄ transfections were performed as described (Hofmann et al., 2004b; Simmons et al., 2003). In brief, 293T cells were transiently cotransfected with pNL4-3 E-R- Luc (Connor et al., 1995) and expression plasmids for SARS-S-variants or VSV-G. For some experiments, human furin was co-expressed during production of pseudoparticles. The culture medium was replaced at 16 h and harvested at 48 h post transfection. The supernatants were passed through 0.45 μ m filters, aliquotted and stored at -80°C. Capsid contents (p24) in harvested supernatants were determined using a commercially available kit (Murex,

Wiesbaden, Germany). For infection, 293T cells or 293T cells transiently transfected with pcDNA3 or hACE2 or 293T cells stably expressing hACE2 were incubated with pseudotypes, normalized for infectivity or p24-capsid protein content, for three days before cells were lysed and luciferase-activities determined using a commercially available kit (Promega, Madison, USA).

Blockade of pseudotype infection by cathepsin inhibitors

293T cells in 96-wells were pre-incubated with the cathepsin L and B inhibitor MDL 28170 (Calbiochem, Darmstadt, Germany) for 30 min. Thereafter, pseudotypes of comparable infectivity were added for 12-16 h, the culture medium was replaced and luciferase activities in cell extracts were determined after 72 h as described above.

Protease inactivation of pseudotyped viruses

Infectivity normalized pseudovirions bearing wild-type or mutant SARS-S protein were incubated with varying amounts of protease for 30 minutes at room temperature. Proteolysis was halted by the addition of an equal volume of medium containing 10%FBS, 100 µg/ml soy bean trypsin inhibitor (STI) and 100 µg/ml aprotinin. Virus was then plated on 293T-ACE2 cells, spin infected for 90 minutes at 2500 rpm and incubated at 37°C. After 4 hours, medium was replaced with fresh medium, and cells were incubated for 48 hours before measurement of luciferase activity. All proteases were obtained from Sigma, and final concentrations used in the assay were determined by preliminary experiments, or the maximal practical level achievable based on the stock solutions of 1mg/ml. Proteases were diluted in PBS. Trypsin and chymotrypsin were used at a final concentration of 25 µg/ml, elastase and factor Xa at 50 µg/ml, thermolysin and thrombin at 125 µg/ml and plasmin at 250 µg/ml.

Trypsin bypass

Trypsin bypass experiments were performed as described (Simmons et al., 2005). Briefly, 293T-ACE2 cells were pretreated for 1 h with cold medium containing ammonium chloride (40 mM). An equal volume of diluted cold pseudovirion mixture (virus was ultracentrifuge-concentrated and resuspended in PBS to remove FBS) was added, and the cells were spin-infected at 4°C to allow virus-binding to cells. The medium was replaced with warm serum-free medium containing ammonium chloride (20 mM) and incubated at 37°C for 15 min. Subsequently, the medium was removed, and fresh medium containing TPCK-trypsin (10 µg/ml) was added for 10 minutes at 25°C. The trypsin-containing medium was then removed and medium supplemented with STI (75 µg/ml) and ammonium chloride (20 mM) was added. After a 12 h

incubation period, medium was replaced with fresh medium without ammonium chloride, and cells were incubated for a further 36 hours before luciferase activity was measured.

Virus-virus fusion assay

Virus to virus fusion was assayed as described (Simmons et al., 2005). Briefly, equal amounts of pseudovirions bearing either ACE2 and encoding luciferase as a reporter (HIV-luc(ACE2)) or both SARS-CoV Spike (or mutants) and Avian Sarcoma Leukosis Virus-A envelope and encoding GFP (HIV-gfp(S+E)) were mixed and incubated for 30 min on ice to allow binding. The temperature was then raised to 37°C for 15 min to allow induction of conformational rearrangements. Particles were then either treated with 10 µg/ml TPCK-trypsin (Sigma) or the pH was lowered to pH 6 by the addition of 0.1M citric acid, and preactivated recombinant cathepsin L was added to a final concentration of 2 µg/ml. Proteolysis was halted after 10 min at 25°C by addition of soybean trypsin inhibitor and leupeptin. Virus mixtures were then diluted and used to infect HeLa cells stably expressing Tva that had been pretreated with 20 µg/ml leupeptin for 1 h.

Analysis of SARS-S expression by Western blot

Cells transiently expressing SARS-S or VLPs harboring SARS-S were lysed in SDS-Laemmli buffer and boiled for 15-30 min at 95°C. Samples were separated via 12,5% SDS-PAGE and transferred onto nitrocellulose membranes (Schleicher & Schuell, Dassel, Germany). SARS-S proteins were detected by staining with SARS-S specific rabbit serum (Imgenex, San Diego, USA) at a 1:1000 dilution, followed by detection of bound antibodies by use of a peroxidase-conjugated anti-rabbit IgG (Dianova, Hamburg, Germany) at a dilution of 1:5000. For loading control, the stripped membranes were incubated with an anti-β-actin antibody (Sigma, Deisenhofen, Germany) at a 1:1000 dilution, followed by incubation with peroxidase-conjugated anti-mouse IgG (Dianova, Hamburg, Germany) at a dilution of 1:5000. Chemiluminescence detection was performed employing a commercially available kit, according to the manufacturer's protocol (ECL Western detection kit; Amersham Pharmacia Biotech Europe, Freiburg, Germany).

Statistics

Statistical significance was calculated employing a two-tailed student's t-test for dependent samples.

Acknowledgements

We thank B. Fleckenstein, K. von der Mark and T.F. Schulz for constant support and K. Korn for p24-ELISA.

References

- Beliveau, F., Desilets, A., Leduc, R., 2009. Probing the substrate specificities of matriptase, matriptase-2, hepsin and DESC1 with internally quenched fluorescent peptides. *FEBS J.* 276, 2213-2226.
- Belouzard, S., Chu, V. C., Whittaker, G. R., 2009. Activation of the SARS coronavirus spike protein via sequential proteolytic cleavage at two distinct sites. *Proc.Natl.Acad.Sci.U.S.A* 106, 5871-5876.
- Bergeron, E., Vincent, M. J., Wickham, L., Hamelin, J., Basak, A., Nichol, S. T., Chretien, M., Seidah, N. G., 2005. Implication of proprotein convertases in the processing and spread of severe acute respiratory syndrome coronavirus. *Biochem.Biophys.Res.Commun.* 326, 554-563.
- Bertram, S., Glowacka, I., Blazejewska, P., Soilleux, E., Allen, P., Danisch, S., Steffen, I., Choi, S. Y., Park, Y., Schneider, H., Schughart, K., Pöhlmann, S., 2010. TMPRSS2 and TMPRSS4 facilitate trypsin-independent spread of influenza virus in Caco-2 cells. *J.Viro.* 84, 10016-10025.
- Bosch, B. J., Bartelink, W., Rottier, P. J., 2008. Cathepsin L functionally cleaves the severe acute respiratory syndrome coronavirus class I fusion protein upstream of rather than adjacent to the fusion peptide. *J.Viro.* 82, 8887-8890.
- Böttcher, E., Matrosovich, T., Beyerle, M., Klenk, H. D., Garten, W., Matrosovich, M., 2006. Proteolytic activation of influenza viruses by serine proteases TMPRSS2 and HAT from human airway epithelium. *J.Viro.* 80, 9896-9898.
- Chaipan, C., Kobasa, D., Bertram, S., Glowacka, I., Steffen, I., Tsegaye, T. S., Takeda, M., Bugge, T. H., Kim, S., Park, Y., Marzi, A., Pöhlmann, S., 2009. Proteolytic activation of the 1918 influenza virus hemagglutinin. *J Virol.* 83, 3200-3211.
- Connor, R. I., Chen, B. K., Choe, S., Landau, N. R., 1995. Vpr is required for efficient replication of human immunodeficiency virus type-1 in mononuclear phagocytes. *Virology* 206, 935-944.

- de Haan, C. A., Stadler, K., Godeke, G. J., Bosch, B. J., Rottier, P. J., 2004. Cleavage inhibition of the murine coronavirus spike protein by a furin-like enzyme affects cell-cell but not virus-cell fusion. *J.Virol.* 78, 6048-6054.
- Drosten, C., Gunther, S., Preiser, W., van der, W. S., Brodt, H. R., Becker, S., Rabenau, H., Panning, M., Kolesnikova, L., Fouchier, R. A., Berger, A., Burguiere, A. M., Cinatl, J., Eickmann, M., Escriou, N., Grywna, K., Kramme, S., Manuguerra, J. C., Muller, S., Rickerts, V., Sturmer, M., Vieth, S., Klenk, H. D., Osterhaus, A. D., Schmitz, H., Doerr, H. W., 2003. Identification of a novel coronavirus in patients with severe acute respiratory syndrome. *N Engl J Med.* 348, 1967-1976.
- Du, L., Kao, R. Y., Zhou, Y., He, Y., Zhao, G., Wong, C., Jiang, S., Yuen, K. Y., Jin, D. Y., Zheng, B. J., 2007. Cleavage of spike protein of SARS coronavirus by protease factor Xa is associated with viral infectivity. *Biochem.Biophys.Res.Commun.* 359, 174-179.
- Eckert, D. M., Kim, P. S., 2001. Mechanisms of viral membrane fusion and its inhibition. *Annu.Rev.Biochem.* 70, 777-810.
- Eifart, P., Ludwig, K., Bottcher, C., de Haan, C. A., Rottier, P. J., Korte, T., Herrmann, A., 2007. Role of endocytosis and low pH in murine hepatitis virus strain A59 cell entry. *J.Virol.* 81, 10758-10768.
- Follis, K. E., York, J., Nunberg, J. H., 2006. Furin cleavage of the SARS coronavirus spike glycoprotein enhances cell-cell fusion but does not affect virion entry. *Virology* 350, 358-369.
- Glowacka, I., Bertram, S., Muller, M. A., Allen, P., Soilleux, E., Pfefferle, S., Steffen, I., Tsegaye, T. S., He, Y., Gnirss, K., Niemeyer, D., Schneider, H., Drosten, C., Pöhlmann, S., 2011. Evidence that TMPRSS2 activates the SARS-coronavirus spike-protein for membrane fusion and reduces viral control by the humoral immune response. *J.Viro*.
- Gramberg, T., Hofmann, H., Moller, P., Lalor, P. F., Marzi, A., Geier, M., Krumbiegel, M., Winkler, T., Kirchhoff, F., Adams, D. H., Becker, S., Munch, J., Pöhlmann, S., 2005. LSECtin interacts with filovirus glycoproteins and the spike protein of SARS coronavirus. *Virology* 340, 224-236.
- Hamming, I., Timens, W., Bulthuis, M. L., Lely, A. T., Navis, G. J., van Goor, H., 2004. Tissue distribution of ACE2 protein, the functional receptor for SARS coronavirus. A first step in understanding SARS pathogenesis. *J Pathol.* 203, 631-637.
- Harrison, S. C., 2008. Viral membrane fusion. *Nat.Struct.Mol Biol.* 15, 690-698.
- Hofmann, H., Geier, M., Marzi, A., Krumbiegel, M., Peipp, M., Fey, G. H., Gramberg, T., Pöhlmann, S., 2004a. Susceptibility to SARS coronavirus S protein-driven infection

correlates with expression of angiotensin converting enzyme 2 and infection can be blocked by soluble receptor. *Biochem.Biophys.Res.Commun.* 319, 1216-1221.

Hofmann, H., Hattermann, K., Marzi, A., Gramberg, T., Geier, M., Krumbiegel, M., Kuate, S., Überla, K., Niedrig, M., Pöhlmann, S., 2004b. S protein of severe acute respiratory syndrome-associated coronavirus mediates entry into hepatoma cell lines and is targeted by neutralizing antibodies in infected patients. *J.Viro.* 78, 6134-6142.

Hofmann, H., Pöhlmann, S., 2004. Cellular entry of the SARS coronavirus. *Trends Microbiol.* 12, 466-472.

Hofmann, H., Simmons, G., Rennekamp, A. J., Chaipan, C., Gramberg, T., Heck, E., Geier, M., Wegele, A., Marzi, A., Bates, P., Pöhlmann, S., 2006. Highly conserved regions within the spike proteins of human coronaviruses 229E and NL63 determine recognition of their respective cellular receptors. *J.Viro.* 80, 8639-8652.

Holland, A. U., Munk, C., Lucero, G. R., Nguyen, L. D., Landau, N. R., 2004. Alpha-complementation assay for HIV envelope glycoprotein-mediated fusion. *Virology* 319, 343-352.

Howard, M. W., Travanty, E. A., Jeffers, S. A., Smith, M. K., Wennier, S. T., Thackray, L. B., Holmes, K. V., 2008. Aromatic amino acids in the juxtamembrane domain of severe acute respiratory syndrome coronavirus spike glycoprotein are important for receptor-dependent virus entry and cell-cell fusion. *J Virol.* 82, 2883-2894.

Jeffers, S. A., Tusell, S. M., Gillim-Ross, L., Hemmila, E. M., Achenbach, J. E., Babcock, G. J., Thomas, W. D., Jr., Thackray, L. B., Young, M. D., Mason, R. J., Ambrosino, D. M., Wentworth, D. E., Demartini, J. C., Holmes, K. V., 2004. CD209L (L-SIGN) is a receptor for severe acute respiratory syndrome coronavirus. *Proc Natl Acad Sci U.S A* 101, 15748-15753.

Kam, Y. W., Okumura, Y., Kido, H., Ng, L. F., Bruzzone, R., Altmeyer, R., 2009. Cleavage of the SARS coronavirus spike glycoprotein by airway proteases enhances virus entry into human bronchial epithelial cells in vitro. *PLoS.One.* 4, e7870.

Ksiazek, T. G., Erdman, D., Goldsmith, C. S., Zaki, S. R., Peret, T., Emery, S., Tong, S., Urbani, C., Comer, J. A., Lim, W., Rollin, P. E., Dowell, S. F., Ling, A. E., Humphrey, C. D., Shieh, W. J., Guarner, J., Paddock, C. D., Rota, P., Fields, B., DeRisi, J., Yang, J. Y., Cox, N., Hughes, J. M., LeDuc, J. W., Bellini, W. J., Anderson, L. J., 2003. A novel coronavirus associated with severe acute respiratory syndrome. *N Engl J Med.* 348, 1953-1966.

Kuba, K., Imai, Y., Rao, S., Gao, H., Guo, F., Guan, B., Huan, Y., Yang, P., Zhang, Y., Deng, W., Bao, L., Zhang, B., Liu, G., Wang, Z., Chappell, M., Liu, Y., Zheng, D., Leibbrandt, A., Wada, T., Slutsky, A. S., Liu, D., Qin, C., Jiang, C., Penninger, J. M., 2005. A crucial role of

- angiotensin converting enzyme 2 (ACE2) in SARS coronavirus-induced lung injury. *Nat Med* 11, 875-879.
- Li, W., Moore, M. J., Vasilieva, N., Sui, J., Wong, S. K., Berne, M. A., Somasundaran, M., Sullivan, J. L., Luzuriaga, K., Greenough, T. C., Choe, H., Farzan, M., 2003. Angiotensin-converting enzyme 2 is a functional receptor for the SARS coronavirus. *Nature* 426, 450-454.
- Marzi, A., Gramberg, T., Simmons, G., Moller, P., Rennekamp, A. J., Krumbiegel, M., Geier, M., Eisemann, J., Turza, N., Saunier, B., Steinkasserer, A., Becker, S., Bates, P., Hofmann, H., Pöhlmann, S., 2004. DC-SIGN and DC-SIGNR Interact with the Glycoprotein of Marburg Virus and the S Protein of Severe Acute Respiratory Syndrome Coronavirus. *J.Viro*. 78, 12090-12095.
- Masters, P. S., 2006. The molecular biology of coronaviruses. *Adv.Virus Res.* 66, 193-292.
- Matsuyama, S., Nagata, N., Shirato, K., Kawase, M., Takeda, M., Taguchi, F., 2010. Efficient activation of the severe acute respiratory syndrome coronavirus spike protein by the transmembrane protease TMPRSS2. *J.Viro*. 84, 12658-12664.
- McBride, C. E., Li, J., Machamer, C. E., 2007. The cytoplasmic tail of the severe acute respiratory syndrome coronavirus spike protein contains a novel endoplasmic reticulum retrieval signal that binds COPI and promotes interaction with membrane protein. *J Virol.* 81, 2418-2428.
- McBride, C. E., Machamer, C. E., 2010. A single tyrosine in the severe acute respiratory syndrome coronavirus membrane protein cytoplasmic tail is important for efficient interaction with spike protein. *J Virol.* 84, 1891-1901.
- Moore, M. J., Dorfman, T., Li, W., Wong, S. K., Li, Y., Kuhn, J. H., Coderre, J., Vasilieva, N., Han, Z., Greenough, T. C., Farzan, M., Choe, H., 2004. Retroviruses pseudotyped with the severe acute respiratory syndrome coronavirus spike protein efficiently infect cells expressing angiotensin-converting enzyme 2. *J.Viro*. 78, 10628-10635.
- Mossel, E. C., Wang, J., Jeffers, S., Edeen, K. E., Wang, S., Cosgrove, G. P., Funk, C. J., Manzer, R., Miura, T. A., Pearson, L. D., Holmes, K. V., Mason, R. J., 2008. SARS-CoV replicates in primary human alveolar type II cell cultures but not in type I-like cells. *Virology* 372, 127-135.
- Nash, T. C., Buchmeier, M. J., 1997. Entry of mouse hepatitis virus into cells by endosomal and nonendosomal pathways. *Virology* 233, 1-8.
- Nie, Y., Wang, G., Shi, X., Zhang, H., Qiu, Y., He, Z., Wang, W., Lian, G., Yin, X., Du, L., Ren, L., Wang, J., He, X., Li, T., Deng, H., Ding, M., 2004a. Neutralizing antibodies in patients

with severe acute respiratory syndrome-associated coronavirus infection. *J Infect Dis.* 190, 1119-1126.

Nie, Y., Wang, P., Shi, X., Wang, G., Chen, J., Zheng, A., Wang, W., Wang, Z., Qu, X., Luo, M., Tan, L., Song, X., Yin, X., Chen, J., Ding, M., Deng, H., 2004b. Highly infectious SARS-CoV pseudotyped virus reveals the cell tropism and its correlation with receptor expression. *Biochem.Biophys.Res.Commun.* 321, 994-1000.

Peiris, J. S., Guan, Y., Yuen, K. Y., 2004. Severe acute respiratory syndrome. *Nat Med* 10, S88-S97.

Qiu, Z., Hingley, S. T., Simmons, G., Yu, C., Das, S. J., Bates, P., Weiss, S. R., 2006. Endosomal proteolysis by cathepsins is necessary for murine coronavirus mouse hepatitis virus type 2 spike-mediated entry. *J.Viro.* 80, 5768-5776.

Shulla, A., Heald-Sargent, T., Subramanya, G., Zhao, J., Perlman, S., Gallagher, T., 2011. A transmembrane serine protease is linked to the severe acute respiratory syndrome coronavirus receptor and activates virus entry. *J.Viro.* 85, 873-882.

Simmons, G., Gosalia, D. N., Rennekamp, A. J., Reeves, J. D., Diamond, S. L., Bates, P., 2005. Inhibitors of cathepsin L prevent severe acute respiratory syndrome coronavirus entry. *Proc Natl Acad Sci U.S.A* 102, 11876-11881.

Simmons, G., Reeves, J. D., Grogan, C. C., Vandenberghe, L. H., Baribaud, F., Whitbeck, J. C., Burke, E., Buchmeier, M. J., Soilleux, E. J., Riley, J. L., Doms, R. W., Bates, P., Pöhlmann, S., 2003. DC-SIGN and DC-SIGNR bind ebola glycoproteins and enhance infection of macrophages and endothelial cells. *Virology* 305, 115-123.

Simmons, G., Reeves, J. D., Rennekamp, A. J., Amberg, S. M., Piefer, A. J., Bates, P., 2004. Characterization of severe acute respiratory syndrome-associated coronavirus (SARS-CoV) spike glycoprotein-mediated viral entry. *Proc.Natl.Acad.Sci.U.S.A* 101, 4240-4245.

Stamminger, T., Gstaiger, M., Weinzierl, K., Lorz, K., Winkler, M., Schaffner, W., 2002. Open reading frame UL26 of human cytomegalovirus encodes a novel tegument protein that contains a strong transcriptional activation domain. *J.Viro.* 76, 4836-4847.

To, K. F., Tong, J. H., Chan, P. K., Au, F. W., Chim, S. S., Chan, K. C., Cheung, J. L., Liu, E. Y., Tse, G. M., Lo, A. W., Lo, Y. M., Ng, H. K., 2004. Tissue and cellular tropism of the coronavirus associated with severe acute respiratory syndrome: an in-situ hybridization study of fatal cases. *J Pathol.* 202, 157-163.

Voss, D., Pfefferle, S., Drosten, C., Stevermann, L., Traggiai, E., Lanzavecchia, A., Becker, S., 2009. Studies on membrane topology, N-glycosylation and functionality of SARS-CoV membrane protein. *Virol.J* 6, 79.

- Wang, P., Chen, J., Zheng, A., Nie, Y., Shi, X., Wang, W., Wang, G., Luo, M., Liu, H., Tan, L., Song, X., Wang, Z., Yin, X., Qu, X., Wang, X., Qing, T., Ding, M., Deng, H., 2004. Expression cloning of functional receptor used by SARS coronavirus. *Biochem.Biophys.Res.Commun.* 315, 439-444.
- Watanabe, R., Matsuyama, S., Shirato, K., Maejima, M., Fukushi, S., Morikawa, S., Taguchi, F., 2008. Entry from the cell surface of severe acute respiratory syndrome coronavirus with cleaved s protein as revealed by pseudotype virus bearing cleaved s protein. *J.Viro.* 82, 11985-11991.
- Wu, X. D., Shang, B., Yang, R. F., Yu, H., Ma, Z. H., Shen, X., Ji, Y. Y., Lin, Y., Wu, Y. D., Lin, G. M., Tian, L., Gan, X. Q., Yang, S., Jiang, W. H., Dai, E. H., Wang, X. Y., Jiang, H. L., Xie, Y. H., Zhu, X. L., Pei, G., Li, L., Wu, J. R., Sun, B., 2004. The spike protein of severe acute respiratory syndrome (SARS) is cleaved in virus infected Vero-E6 cells. *Cell Res.* 14, 400-406.
- Xiao, X., Chakraborti, S., Dimitrov, A. S., Gramatikoff, K., Dimitrov, D. S., 2003. The SARS-CoV S glycoprotein: expression and functional characterization. *Biochem Biophys Res Commun.* 312, 1159-1164.
- Yang, Z. Y., Huang, Y., Ganesh, L., Leung, K., Kong, W. P., Schwartz, O., Subbarao, K., Nabel, G. J., 2004. pH-dependent entry of severe acute respiratory syndrome coronavirus is mediated by the spike glycoprotein and enhanced by dendritic cell transfer through DC-SIGN. *J.Viro.* 78, 5642-5650.
- Yao, Y. X., Ren, J., Heinen, P., Zambon, M., Jones, I. M., 2004. Cleavage and serum reactivity of the severe acute respiratory syndrome coronavirus spike protein. *J.Infect.Dis.* 190, 91-98.

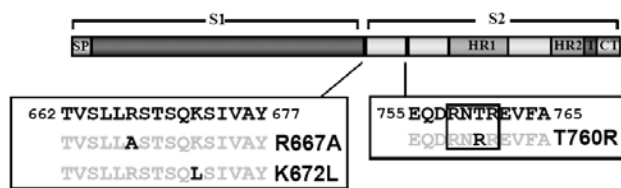


Figure 1. Domain organization of the SARS-CoV spike-protein, including potential cleavage sites. The mutations introduced into the SARS-S are depicted. The box indicates a potential furin cleavage motif. HR, heptad repeat; SP, signal peptide; T, transmembrane domain; CT, cytoplasmic domain.

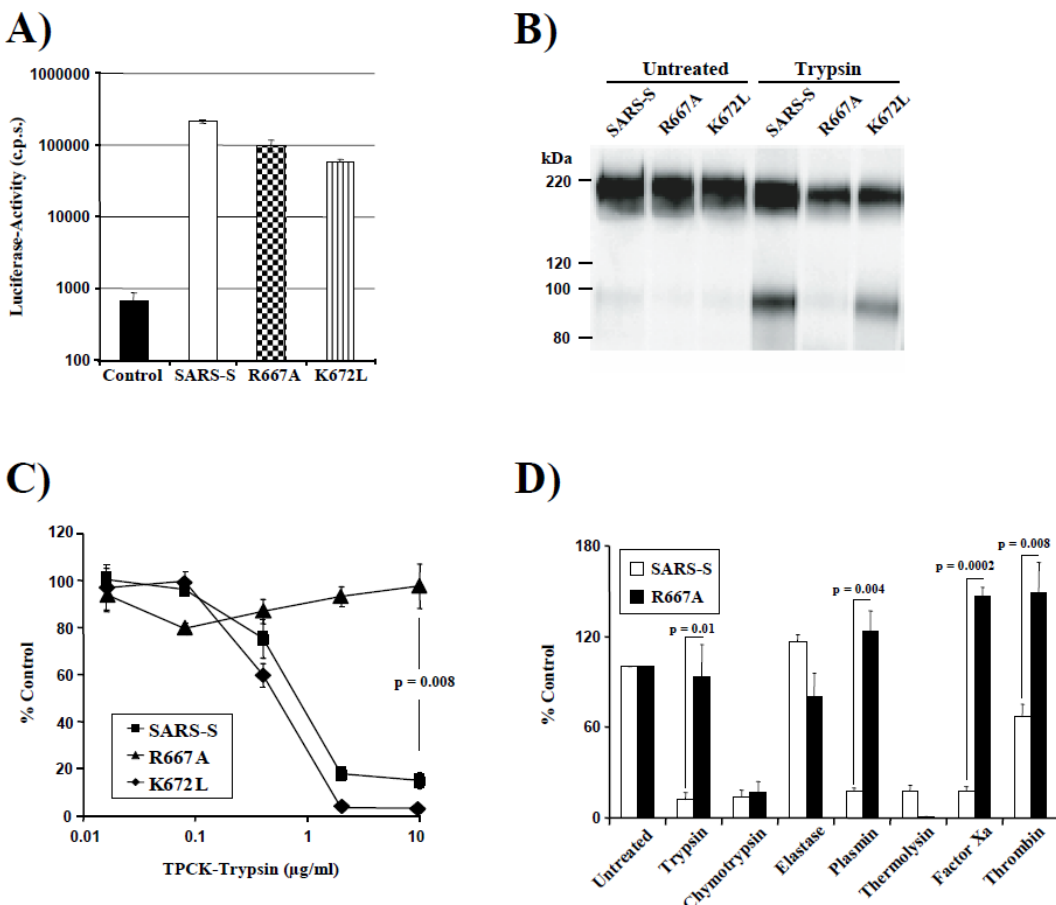


Figure 2. Role of R667 and K672 in SARS-CoV entry and inactivation. (A) Infectivity of pseudovirions bearing wild-type SARS-S and SARS-S variants R667A or K672L or no envelope protein (control) for VeroE6 cells. Results are presented as means and standard deviations of triplicate wells. Similar results were seen in 293T and 293T-ACE2 cells. (B) Expression of SARS-S and mutant SARS-S-proteins on pseudovirions. Equal volumes of virus stocks were concentrated by ultracentrifugation through a sucrose gradient, treated with PBS or trypsin and spike-proteins were detected using a monoclonal antibody directed against the N-terminal portion of SARS-S. (C) Trypsin inactivation of pseudotypes bearing SARS-S or mutant SARS-S proteins. Ultracentrifuge-concentrated virus was pretreated with varying concentrations of TPCK-trypsin for 10 min at 25°C, before trypsin inactivation and spin infection of 293T-ACE2 cells. Results are presented relative to infectivity measured for untreated virions and are means and standard deviations of triplicate wells. (D) Inactivation of SARS-S and SARS-S mutant R667A by various proteases prior to infection of 293T-ACE2 cells. Results are presented relative to the infectivity measured for untreated viruses and are means and standard deviations of triplicate wells. Similar results were seen in two additional experiments.

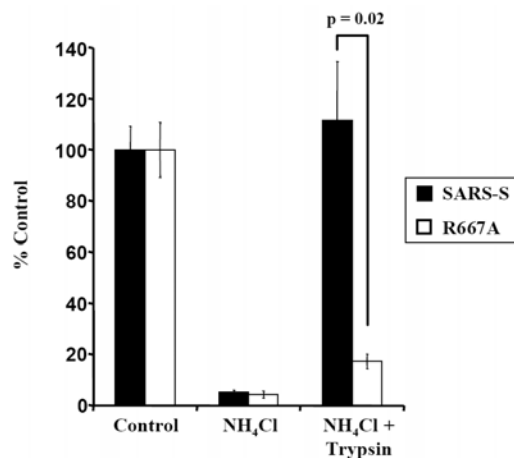


Figure 3. Trypsin bypass of wt SARS-S and SARS-S R667A infection of ammonium chloride treated VeroE6 cells. Virus was allowed to bind, but not internalize into VeroE6 cells pretreated with 20 mM ammonium chloride. Subsequently, the cells were treated with TPCK-trypsin (10 µg/ml) to activate SARS-S for membrane fusion. Results are presented as a percentage of no trypsin, no ammonium chloride control and are means and standard deviations of triplicate wells. Similar results were seen on 293T-ACE2 cells.

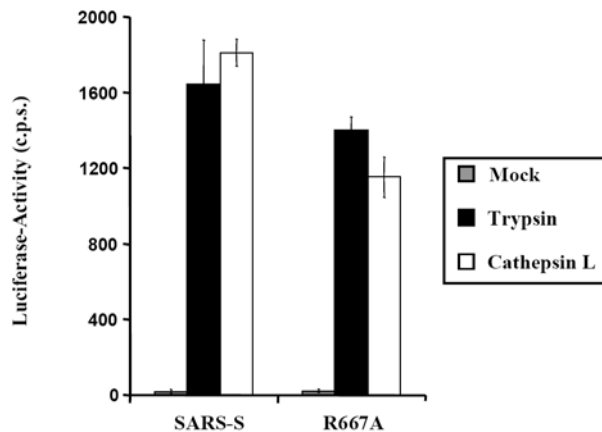


Figure 4. Protease activation of virus-virus fusion mediated by wt SARS-S and mutant R667A. Pseudovirions bearing SARS-S or ACE2 were mixed and virion-fusion activated by trypsin (10 µg/ml) or cathepsin L (2 µg/ml). Results are presented as means and standard deviations of replicates of four wells. Similar results were seen in 2 additional experiments.

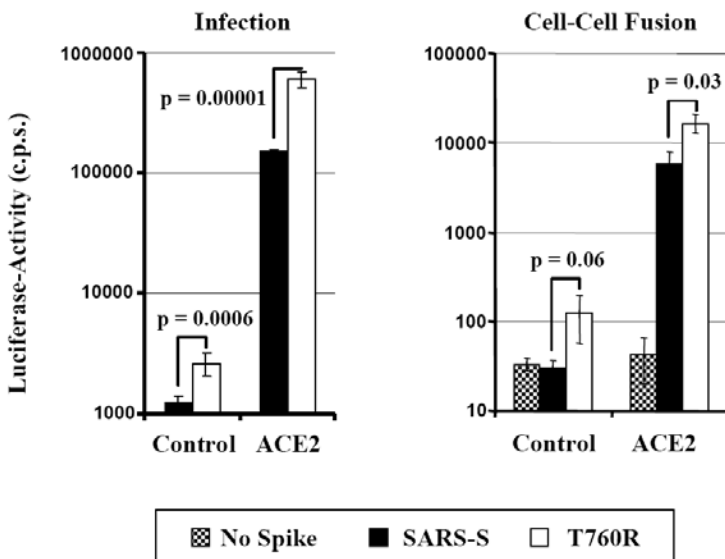


Figure 5. Activity of wt SARS-S and variant T760R in virus-cell (left panel) and cell-cell fusion (right panel) experiments. Activity of wt SARS-S and variant T760R in virus-cell (left panel) and cell-cell fusion (right panel) experiments. Left panel: Pseudoparticles harboring the indicated SARS-S proteins or no S-protein as a control were normalized for equal capsid content and used for infection of 293T cells expressing either pcDNA3 or ACE2 in quadruplicates. Luciferase-activities were determined after 72 h. A representative experiment is shown, comparable results were obtained in two independent experiments. Error bars indicate standard deviation (SD). Right panel: 293T effector cells cotransfected with expression vectors encoding the indicated S-proteins (or transfected with empty vector) in combination with a GAL-VP16 expression plasmid were co-cultivated with target cells transfected with either pcDNA3 or ACE2 plasmid together with a plasmid encoding a GAL-VP16-responsive luciferase reporter gene. Luciferase-activities were measured two days after cocultivation. The results of a representative experiment are shown and were confirmed in two separate experiments. Error bars indicate SD.

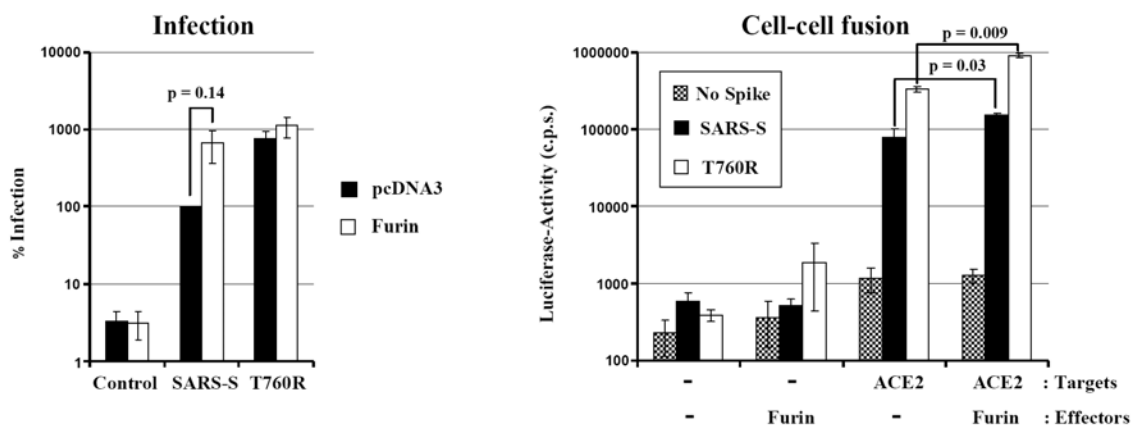


Figure 6. Impact of furin expression on virus-cell (left panel) and cell-cell fusion (right panel) driven by wt SARS-S and SARS-S variant T760R. Left panel: Pseudotypes harboring the indicated S-proteins were prepared in the presence (white bars) or absence (black bars) of co-expressed furin. After normalization for p24-content, the particles were used for infection of 293T cells in triplicates. Luciferase-activities in cell lysates were determined after 72 h and values measured for SARS-S pseudotypes prepared in the absence of overexpressed furin were set as 100%. The average of four independent experiments is shown, error bars indicate standard error of the mean (SEM). Right panel: 293T effector cells cotransfected with expression plasmids for the indicated S-variants (or transfected with empty vector as control), GAL-VP16 and furin (or transfected with empty vector as control), were co-cultivated with 293T target cells transfected with plasmids encoding a GAL-VP16-responsive luciferase gene and hACE2 (or transfected with empty vector as control) in triplicates. Luciferase-activities in cell lysates were measured two days after co-cultivation. The experiment shown is representative of three independent experiments, error bars indicate SD.

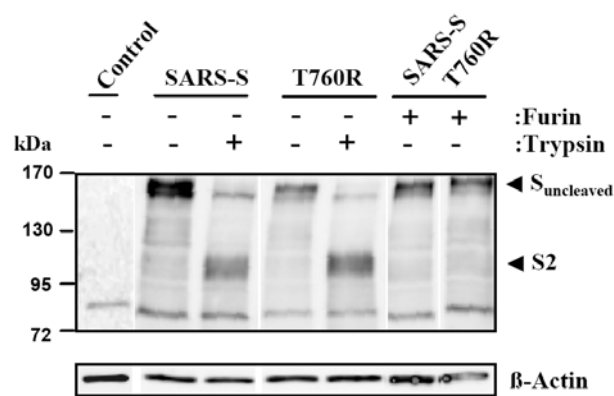


Figure 7. Proteolytic processing of wt SARS-S and SARS-S mutant T760R in the presence and absence of furin overexpression. The indicated S-proteins were transiently expressed in 293T cells in the absence and presence of furin (expression plasmids for SARS-S and furin were transfected at a 1:1 ratio), the cells treated with PBS or trypsin as indicated and cell lysates analyzed with S2-specific antiserum. As control, β-actin expression in cell lysates was assessed. The results of a single gel are shown from which irrelevant lanes were removed.

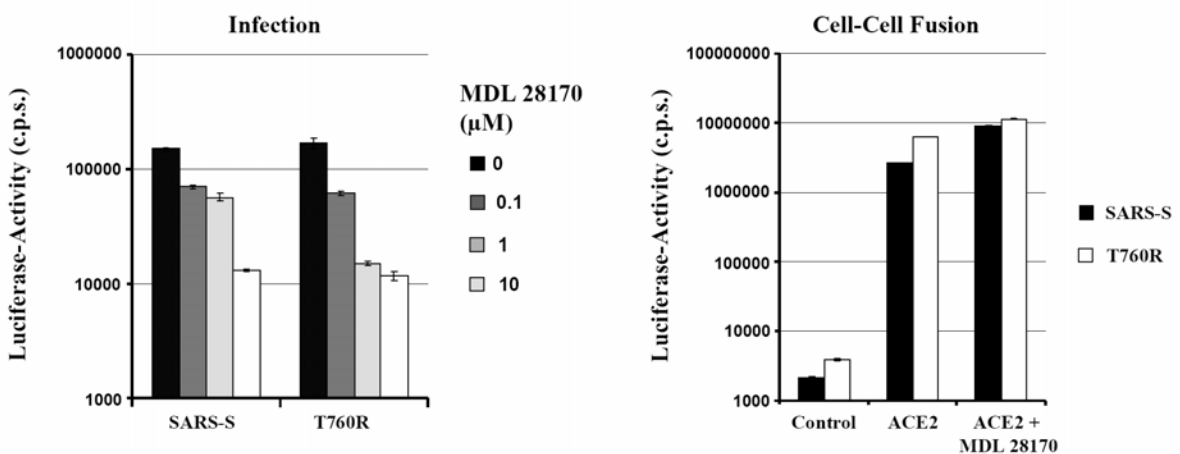


Figure 8. Impact of the cathepsin B/L inhibitor MDL 28170 on virus-cell (left panel) and cell-cell fusion (right panel) driven by wt SARS-S and SARS-S mutant T760R. Left panel: 293T target cells were pre-incubated with the indicated concentrations of MDL 28170 for 1 h and thereafter infected in quadruplicates with infectivity-normalized pseudotypes bearing the indicated S-proteins. Luciferase activities in cell lysates were determined at 72 h post infection. The results of a representative experiment carried out in triplicates are shown and were confirmed in two separate experiments. Right panel: 293T target cells transfected with gal5-luc and either pcDNA3 (control) or ACE2 were mixed with effector cells expressing GAL-VP16 in combination with the indicated S-proteins. After mixing, cells were either left untreated or treated with 1 μM MDL 28170. Luciferase-activities were determined two days after mixing. The results of a representative experiment are shown; comparable results were obtained in an independent experiment. Error bars indicate SD.

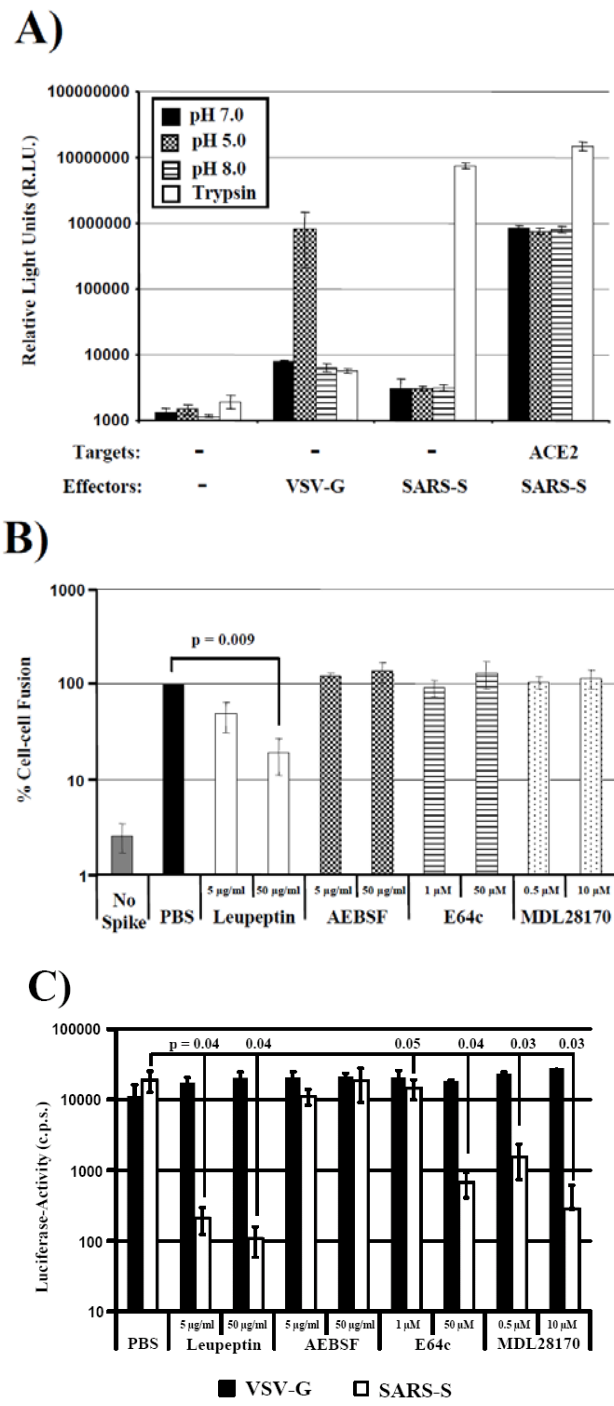


Figure 9. SARS-S-dependent cell-cell fusion depends on the activity of a cysteine or serine protease. (A) Target 293T cells cotransfected with a plasmid encoding β -galactosidase ω fragment and either pcDNA3 (control) or plasmid encoding ACE2 were mixed with 293T effector cells transiently expressing β -galactosidase α peptide in combination with either the SARS-S or VSV-G proteins. After one hour, cells were pulsed with different pH's or TPCK-trypsin. After a further five hours, β -galactosidase trans-complementation was assessed and expressed as relative light units. The results of a representative experiment carried out in triplicates are shown. Error bars indicate SD. Similar results were obtained in an independent experiment.

(B) Target 293T cells transfected with gal5-luc and ACE2 were mixed with 293T effector cells expressing GAL-VP16 in combination with the SARS-S-protein. Effector cells transfected with empty vector (no spike) served as negative controls. Target cells were pre-incubated with PBS or the indicated concentrations of protease inhibitors before mixing with effector cells. After mixing of cells, which involved detachment and washing of cells, the inhibitors were replenished and cocultures were maintained for 48 h. Thereafter, luciferase-activities in cell lysates were determined. The results of a representative experiment carried out in triplicates are shown, cell-cell fusion measured in the absence of inhibitor was set as 100%. Error bars indicate SD. Similar results were obtained in two independent experiments. (C) 293T-hACE2 cells were incubated with the indicated inhibitors of 1 h and subsequently infected with infectivity-normalized pseudotypes bearing VSV-G or SARS-S. Luciferase activities in cell lysates were determined at 72 h post infection. The results of a representative experiment performed in triplicates are shown; error bars indicate SD. Similar results were obtained in two independent experiments.

Evidence that TMPRSS2 activates the SARS-coronavirus spike-protein for membrane fusion and reduces viral control by the humoral immune response

Ilona Glowacka,¹ Stephanie Bertram,¹ Marcel A. Müller,² Paul Allen,³ Elizabeth Soilleux,³ Susanne Pfefferle,⁴ Imke Steffen,¹ Theodros Solomon Tsegaye,¹ Yuxian He,⁵ Kerstin Gnirss,¹ Daniela Niemeyer,² Heike Schneider,⁶ Christian Drosten,² and Stefan Pöhlmann,^{1,7*}

Institute of Virology, Hannover Medical School, 30625 Hannover, Germany¹; Institute of Virology, University of Bonn Medical Centre, 53127 Bonn, Germany²; Department of Cellular Pathology, John Radcliffe Hospital, Oxford OX3 9DU, England³; Bernhard Nocht Institute for Tropical Medicine, 20359 Hamburg, Germany³; Institute of Pathogen Biology, Chinese Academy of Medical Sciences and Peking Union Medical College, Beijing 1007302, China⁵; Institute for Physiological Chemistry, Hannover Medical School, 30625 Hannover, Germany⁶; German Primate Center, Kellnerweg 4, 37077 Göttingen, Germany⁷

I.G. and S.B. contributed equally to this work

* Corresponding author. Infection Biology Unit, German Primate Center, Kellnerweg 4, 37077 Göttingen, Germany. ++49 551 3851 150 (T), ++49 551 3851 184 (F), E-Mail: s.poehlmann@dpz.eu

Keywords: SARS coronavirus, spike protein, proteolytic cleavage, TMPRSS2

ABSTRACT

The spike (S) protein of the SARS-coronavirus can be proteolytically activated by cathepsins B and L upon viral uptake into target cell endosomes. In contrast, it is largely unknown whether host cell proteases located in the secretory pathway of infected cells and/or on the surface of target cells can cleave SARS-S. We and others could previously show that the type II transmembrane protease TMPRSS2 activates the influenza virus hemagglutinin and the human metapneumovirus F protein by cleavage. Here, we assessed whether SARS-S is proteolytically processed by TMPRSS2. Western blot analysis revealed that SARS-S was cleaved into several fragments upon coexpression of TMPRSS2 (cis-cleavage) and upon contact between SARS-S expressing cells and TMPRSS2 positive cells (trans-cleavage). Cis-cleavage resulted in release of SARS-S fragments into the cellular supernatant and in inhibition of antibody-mediated neutralization, most likely because SARS-S fragments function as antibody decoys. Trans-cleavage activated SARS-S on effector cells for fusion with target cells and allowed efficient SARS-S-driven viral entry into targets treated with a lysosomotropic agent or a cathepsin inhibitor. Finally, ACE2, the cellular receptor for SARS-CoV, and TMPRSS2 were found to be co-expressed by type II pneumocytes, which represent important viral target cells, suggesting that SARS-S is cleaved by TMPRSS2 in the lung of SARS-CoV-infected individuals. In summary, we show that TMPRSS2 might promote viral spread and pathogenesis by diminishing viral recognition by neutralizing antibodies and by activating SARS-S for cell-cell and virus-cell fusion.

INTRODUCTION

The severe acute respiratory syndrome coronavirus (SARS-CoV) is the causative agent of the lung disease SARS, which claimed ~800 lives in 2002/2003 (49). SARS-CoV-related viruses were identified in bats and palm civets (19, 33, 37) and it is believed that human contact with the latter animals, possibly within animal markets in Southern China, was responsible for the introduction of SARS-CoV into the human population. The viral spike (S)-protein mediates infectious entry into target cells by engaging the carboxypeptidase angiotensin-converting enzyme 2 (ACE2) (36, 60), and several changes in the spike sequence of SARS-CoV from humans relative to SARS-CoV from palm civets reflect the adaptation to efficient usage of the human receptor (35, 38, 39), most likely a prerequisite for high viral pathogenicity. Thus, the SARS-S-protein is an important determinant of viral cell and species tropism (27) and

exploration of its functions is essential to devise effective strategies for prevention and therapy.

The SARS-S-protein comprises 1255 amino acids and harbours 23 consensus sequences for N-linked glycosylation. The S-protein is synthesized in the secretory pathway of infected cells and S-protein trimers are incorporated into the viral envelope (derived from the endoplasmatic reticulum Golgi intermediate compartment, ERGIC) and the plasma membrane of the host cell (34). The S-protein exhibits the domain organisation of class I fusion proteins; it contains an N-terminal surface unit (S1), which engages the receptor, and a C-terminal transmembrane unit (S2), which contains the membrane fusion machinery (27). A prominent feature of many class I fusion proteins is the requirement for proteolytic activation by host cell enzymes (14). A seminal study by Simmons and colleagues showed that proteolytic activation of SARS-S is mediated by cathepsins in target cells, most importantly by cathepsin L (53). In contrast, the efficiency and biological relevance of SARS-S processing by proteases in infected cells is at present incompletely understood.

The type II transmembrane serine protease TMPRSS2 has recently been shown to proteolytically activate the fusion proteins of human influenza viruses (6, 8) and TMPRSS2 was found to activate human metapneumovirus (51). In addition, the related protein TMPRSS11a has been demonstrated to cleave SARS-S and to moderately increase viral infectivity (30). Here, we investigated whether SARS-S is a substrate of TMPRSS2 and if cleavage modulates biological properties of SARS-S-bearing viruses. We show that SARS-S is proteolytically processed by TMPRSS2. Cleavage resulted in shedding of SARS-S fragments and interference with antibody-mediated neutralization or in activation of SARS-S for cell-cell and virus-cell fusion, depending on the presence of TMPRSS2 on SARS-S expressing cells or on adjacent susceptible cells. These observations, in conjunction with our finding that ACE2 and TMPRSS2 are coexpressed in type II pneumocytes, important viral target cells, suggest that TMPRSS2 might impact SARS-CoV spread by at least two independent mechanisms.

MATERIAL AND METHODS

Plasmid construction and in vitro-mutagenesis. Expression plasmids pCAGGS-SARS-S, encoding the spike protein of SARS-CoV strain Frankfurt, and pcDNA3-hACE2, encoding human ACE2, have been described previously (25, 26).

The plasmids encoding human TMPRSS2 and TMPRSS4 and mouse matriptase-3 have also been described previously (29, 51, 57).

Cell culture. Vero E6 and 293T cells were propagated in Dulbecco's modified Eagle's medium (DMEM) supplemented with 10% fetal bovine serum (FBS), penicillin and streptomycin, and were grown in a humidified atmosphere containing 5% CO₂. 293T cells stably expressing ACE2 (293T-hACE2, (18)) were generated by transfection of plasmid pcDNA3.1zeo-hACE2 (25) into 293T cells followed by selection of resistant cells with zeocin (Invitrogen) at 50µg/ml. Homogenous surface expression of ACE2 on stably transfected cells was confirmed by FACS analysis.

Production of lentiviral pseudotypes and infection experiments. For generation of lentiviral pseudotypes, calcium phosphate transfections were performed as described (26, 54). In brief, 293T cells were transiently cotransfected with pNL4-3 E-R- Luc (11) and expression plasmids for SARS-S or the G-protein of vesicular stomatitis virus (VSV-G). For some experiments, human TMPRSS2 or TMPRSS4 or mouse matriptase-3 were co-expressed during production of pseudotypes. The culture medium was replaced at 16 h and harvested at 48 h post transfection. The supernatants were passed through 0.45 µm filters, aliquotted and stored at -80°C. For normalization of different virus stocks, capsid protein (p24) contents were determined using a commercially available kit (Murex, Wiesbaden, Germany). Alternatively, virus stocks were normalized for infectivity, which was assessed by infecting 293T-hACE2 cells with different dilutions of pseudotypes followed by determination of luciferase-activities in cell lysates employing a commercially available kit (Promega, Madison, USA). For infection experiments, 293T-hACE2 cells were incubated with equal volumes of p24- or infectivity-normalized pseudotypes for 16 h. Thereafter, medium was changed and luciferase-activities in cell lysates were determined at 72 h post infection. For inhibition experiments, cells were preincubated with cathepsin inhibitor MDL 28170 (Calbiochem, Nottingham, UK) for 30 min, or viruses were preincubated with antisera (obtained by immunization of mice with a S1-protein fragment comprising amino acids 12-327 (62)) for 60 min before addition to target cells. Culture supernatants were removed at 16 h post infection and replaced by fresh medium without inhibitor. For some inhibition studies, the pseudotypes were pelleted through a sucrose cushion by ultracentrifugation for 2 h at 25,000 rpm and 4°C to separate particles from SARS-S fragments not associated with virions and afterwards incubated with antisera in the presence and absence of shed SARS-S-protein.

Production of virus-like particles (VLPs). For production of VLPs, 293T cells were cotransfected with the HIV-1 Gag (p55) encoding plasmid p96ZM651gag-opt (16), SARS-S expression plasmid and expression plasmids for proteases or empty vector. The supernatants containing the VLPs were collected at 48 h post transfection and concentrated by ultrafiltration using vivaspin centrifugal concentrators (Sartorius, Aubagne Cedex, France). Alternatively or additionally, the VLPs were concentrated by ultracentrifugation through a 20% sucrose cushion for 2 h at 25,000 rpm and 4°C. Subsequently, the concentrated supernatants were treated with PBS or trypsin, followed by addition of soybean trypsin inhibitor (Sigma, Deisenhofen, Germany).

Production of shed SARS-S-protein. For production of shed SARS-S-protein, 293T cells were cotransfected with plasmids encoding for SARS-S and TMPRSS2 or empty vector. At 48 h post transfection the supernatants were harvested and concentrated employing vivaspin columns (Sartorius, Aubagne Cedex, France) followed by ultracentrifugation through a 20% sucrose cushion for 2 h at 25,000 rpm and 4°C to remove vesicles harboring SARS-S-protein. The SARS-S-protein remaining in the supernatants of ultracentrifuged material was then analyzed by immunoblotting to confirm size and purity.

Detection of SARS-S by immunoblot. For Western blot analysis, lysed VLP preparations were separated by SDS-PAGE and transferred onto nitrocellulose membranes. SARS-S-protein was detected by staining with rabbit sera specific for the S1-subunit (generated by immunization with a peptide comprising SARS-S amino acids 19-48 (24)) or the S2-subunit (Imgenex, San Diego, USA). For loading control, the stripped membranes were incubated with an anti-HIV p24 antibody.

PNGaseF digest of SARS-S. For the analysis of SARS-S glycosylation, VLPs were concentrated via vivaspin columns (samples taken for immunoblotting) and additionally ultracentrifuged through a 20% sucrose cushion at 25,000 rpm for 2 h at 4°C. The resulting pellets were harvested with TNE-buffer and digested by PNGaseF (New England Biolabs, Frankfurt, Germany). The digested samples were then analyzed by immunoblotting as described above.

Immunohistochemistry. Tissue samples, obtained with full ethical approval from the National Research and Ethics Service (Oxfordshire Research and Ethics Committee A: reference 04/Q1604/21), were haematoxylin and eosin stained using standard techniques and were immunostained for ACE2 (affinity purified goat

polyclonal serum, R&D Systems, Abingdon, UK), detected with biotinylated secondary donkey anti-goat polyclonal antiserum (Abcam, Cambridge, UK) and the Bond Intense R kit (Leica Microsystems Newcastle Ltd, Newcastle, UK), or for TMPRSS-2 (mouse monoclonal antibody P5H9, (41)) using the manufacturer's standard protocols and reagents for mouse primary antibodies. Immunostaining was performed using a Bond Max™ immunostaining machine (Leica Microsystems Newcastle Ltd, Newcastle, UK). As a negative control for ACE2 immunostaining, normal goat polyclonal serum was substituted for the primary antibody. As a negative control for TMPRSS-2 immunostaining, an irrelevant mouse monoclonal (anti-melan A antibody, clone A103, Leica Microsystems Newcastle Ltd, Newcastle, U.K.) was substituted for the primary antibody. Stained sections were photographed with a Nikon DS-Fi1 camera with a Nikon DS-L2 control unit (Nikon UK Limited, Kingston-upon-Thames, UK) and an Olympus BX40 microscope (Olympus UK Limited, Watford, UK).

Quantitative RT-PCR analysis of TMPRSS2 mRNA expression. For detection of tmrss2 transcripts by real-time PCR, the ABI7500 FAST real-time PCR system (Applied Biosystems, Carlsbad, USA) was used. The PCR reactions contained 0.5 µl of cDNA (Clontech, Saint-Germain-en-Laye, France) in a total volume of 10 µl. Specific amplification was assured with TaqMan gene expression assays (Applied Biosystems; #4331182), which were used according to the manufacturer's recommendations. The following specific assays were used: Hs00237175_m1 (TMPRSS2), Hs99999908_m1 (GUSB). The average cycle-threshold value (Ct) for each individual assay was calculated from triplicate measurements by means of the instrument's software in "auto Ct" mode (7500 FAST System Software v.1.3.0). Average Ct values calculated for TMPRSS2 were normalized by subtraction from the Ct values obtained for GUSB (housekeeping reference). Template-free cDNA-reactions were analyzed in parallel, using both TaqMan assays; no specific signal was detected in any of these experiments.

Trans-cleavage of SARS-S by TMPRSS2. In order to analyze if SARS-S on the cell surface can be cleaved by TMPRSS2 on neighbouring cells (trans-cleavage), 293T cells were transfected with plasmids encoding for SARS-S, TMPRSS2 or TMPRSS4 or empty vector. At 24 h post transfection the cells were resuspended in fresh FCS-free DMEM and cells expressing SARS-S were mixed with cells expressing empty vector or protease at a ratio of 1:1,7. The mixed cells were seeded again in new cell culture flasks for further incubation for 30 h at 37°C. Subsequently, the supernatants were harvested, centrifuged for 5 min at 4000 rpm, passed through a

0,45 µm filter and concentrated by ultrafiltration using vivaspin centrifugal concentrators (Sartorius, Aubagne Cedex, France). Additionally, the concentrated supernatants were loaded on a 20% sucrose cushion and ultracentrifuged for 2 h at 25.000 rpm and 4°C. After ultracentrifugation, the supernatants were harvested and the pellet was resuspended in TNE-buffer. To analyze SARS-S cleavage, lysates of transfected cells and samples of supernatants taken during the different processing steps were analyzed for the presence of SARS-S by Western blotting, employing sera specific for the S1 and S2 subunits of SARS-S.

SARS-S-driven cell-cell fusion. For analysis of SARS-S-driven cell-cell fusion, 293T effector cells seeded in 6-well plates at $1,2 \times 10^5$ /well were CaPO₄-transfected with either an empty pCAGGS plasmid or pCAGGS encoding SARS-S in combination with plasmid pGAL4-VP16, which encodes the Herpes Simplex VP16 transactivator fused to the DNA binding domain of the yeast transcription factor GAL4. In parallel, 293T target cells were seeded in 48-well plates at $0,8 \times 10^5$ /well and transfected with pcDNA3 or the hACE2 expression vector or with a protease expressing vector together with plasmid pGal5-luc, which encodes the luciferase reporter gene under control of a promoter containing five GAL4 binding sites. The day after transfection, effector cells were diluted in fresh medium and added to the target cells. For trypsin treatment, medium from target cells was completely removed and effector cells in medium supplemented with 100 ng/ml trypsin (Sigma, Deisenhofen, Germany) or PBS was added. After 6 h incubation time fresh medium was added to the trypsin- and PBS-treated samples. Cell-cell fusion was quantified by determination of luciferase activities in cell lysates 48 h after cocultivation using a commercially available kit (Promega, Madison, USA).

TMPRSS2-dependent syncytia formation. Vero E6 cells (seeded in a 6 well plate at 6×10^5 cells/well) were lipofectamine transfected with TMPRSS2 or TMPRSS4 expression plasmid or control transfected with empty vector. After 24 h cells were infected with SARS-CoV (strain Frankfurt 1) at an MOI of 0.1 for 1 h at 37°C. Subsequently, the cells were washed and fresh culture medium was added. At 29 h post infection, the cells were fixed with paraformaldehyde (8%) and analysed by microscopy. Pictures were taken with a Zeiss phase contrast inverted microscope (Televal 31) at a 200-fold magnification.

TMPRSS2-dependent, cathepsin-independent cellular entry of SARS-CoV. 293T-hACE2 cells (seeded in a 6 well plate at 6×10^5 cells/well) were transfected in triplicates with expression plasmids encoding TMPRSS2 or TMPRSS4 or control

transfected with empty vector. After 24 h transfected cells were either incubated with DMEM containing the cathepsin-inhibitor MDL 28170 (stock solution prepared in DMSO) at a final concentration of 9 µM or DMEM containing the same volume of DMSO (as negative control) for 60 min at 37°C. Subsequently, the cells were infected with SARS-CoV (Frankfurt strain 1) at an MOI of 0.1 for 30 min at 4°C, washed twice with PBS and incubated with fresh DMEM. At five hours post infection the cells were washed with PBS, lysed and total RNA was extracted by RNeasy Protect Mini kit (Qiagen, Hilden, Germany). SARS-CoV entry was determined by quantitative RT-PCR specific for the subgenomic (sg) mRNA of the N transcript. For this, the following oligonucleotides were used, SsgN-F AACCTCGATCTCTTAGATCTGT, SsgN-R TGAATCTGTGGTCCACCAA and SsgN-P FAM-CTCTAAACGAACAAATTAAAATGTCTGATAATGG-BHQ1, employing the SuperscriptIII One-Step RT-PCR kit (Invitrogen). The total reaction volume was 12.5 µl (quarter reaction) and contained 30 nmol MgSO₄, 5 pmol of each oligonucleotide and 2.5 pmol of the probe. The Ct values, measured in single experiments performed in triplicates, were normalized by subtracting the respective Ct values for Tata-box binding protein (housekeeping reference gene (50)). For clarity, values were subtracted by a fixed number [20]. A Ct difference of 3 correlated approximately with a 10-fold increase as determined by a dilution series of both targets.

RESULTS

The pulmonary protease TMPRSS2 cleaves SARS-S at multiple sites. Recent studies showed that TMPRSS2, TMPRSS4 and other type II transmembrane serine proteases (TTSPs) can activate human influenza viruses (6, 8, 10). Since the lung is also the major target organ of SARS-CoV, we asked whether TMPRSS2 and TMPRSS4 can cleave the SARS-S protein. We included murine matriptase-3 in these experiments, since we previously found that this protease was unable to process influenza hemagglutinin (HA) and would thus serve as a negative control (8). Employing an S2-specific antibody, Western blot analysis of virus-like particles (VLPs) released from transiently transfected cells revealed a prominent 160-170 kDa band representing full length SARS-S, and, upon trypsin treatment, a 90 kDa band representing S2 (Fig. 1, top panel), in agreement with published data (3, 67). When TMPRSS2 and S-protein were coexpressed, the largest band observed was approximately 150 kDa (instead of 160 kDa expected for full length SARS-S), with

additional bands of 45, 55 and 85 kDa (Fig. 1, top panel). In contrast, coexpression of TMPRSS4 or matriptase-3 did not facilitate SARS-S cleavage.

Efficient proteolytic processing of SARS-S by TMPRSS2 was confirmed when an S1-specific serum was used for S-protein detection (Fig. 1, bottom panel). Thus, SARS-S fragments of 100 and 150 kDa were observed upon coexpression of SARS-S with TMPRSS2 while only a single, 160 kDa band was detected when SARS-S was produced in cells cotransfected with empty vector instead of TMPRSS2 expression plasmid (Fig. 1, bottom panel). Cumulatively, TMPRSS2 cleaves SARS-S at multiple sites, generating fragments of 150, 110, 85 (weak signal), 55 and 45 kDa.

SARS-S cleavage by TMPRSS2 decreases viral sensitivity to inhibition by neutralizing antibodies. Considering that TMPRSS2 cleaves SARS-S at multiple sites, we first asked if processed S-protein was still active. For this, we employed lentiviral pseudotypes bearing SARS-S, which faithfully model host cell entry of SARS-CoV (26, 55, 65). Analysis of infectivity of viruses produced in control- and TMPRSS2-transfected cells and normalized for equal content of p24-capsid antigen did not reveal major differences (data not shown), suggesting that cleavage of SARS-S by TMPRSS2 was compatible with viral infectivity. We next investigated whether processing of SARS-S by TMPRSS2 alleviated the requirement for cathepsin activity during infectious SARS-S-dependent cell entry. Preincubation of 293T-hACE2 cells with a cathepsin L and B inhibitor, MDL 28170 (40, 53), had no effect on infectious entry of VSV-G bearing pseudotypes but efficiently reduced infection by SARS-S pseudotypes (Fig. 2A, see figure legend for raw data), in agreement with published results (28, 53). The pronounced reduction of infectivity of SARS-S pseudotypes by MDL 28170 was not rescued by SARS-S processing by TMPRSS2 (Fig. 2A), indicating that proteolysis of SARS-S by TMPRSS2 does not abrogate the requirement for cleavage by cathepsin L and/or B.

The humoral immune response critically contributes to vaccine-mediated protection against SARS-CoV infection in mice (66), and recovery from SARS is accompanied by the development of a neutralizing antibody response in human patients (9, 26, 47). To analyze the impact of SARS-S cleavage by TMPRSS2 on antibody-mediated neutralization, we employed sera from mice immunized with soluble S-protein. Preincubation of SARS-S wt pseudotypes with serum R1LI1, which was generated by immunization of mice with a baculovirus-expressed S protein (21), caused a profound and dose-dependent reduction in viral infectivity (Fig. 2B, see figure legend for raw data). Strikingly, the reduction was much less pronounced for pseudotypes generated in TMPRSS2 expressing cells, and similar results were

obtained with serum R1 (21), although the overall neutralizing activity of this serum was lower (Fig. 2B). These results, which were confirmed with two independently generated virus stocks (not shown), indicate that cleavage by TMPRSS2 reduces SARS-S susceptibility to inhibition by neutralizing antibodies.

TMPRSS2 induces SARS-S shedding. In order to understand how cleavage of SARS-S by TMPRSS2 reduces neutralization sensitivity, we characterized the nature of the cleavage fragments. We first asked if the decreased molecular mass of the 150 kDa cleavage product relative to uncleaved SARS-S was indeed due to removal of amino acids or was the result of altered S-protein glycosylation. The latter scenario required consideration, since coexpression of TMPRSS2 and influenza hemagglutinin (HA) not only facilitated HA cleavage but also altered HA glycosylation (4). However, the size difference between uncleaved SARS-S and the largest S-protein fragment obtained upon TMPRSS2 cleavage remained constant after PNGaseF digest (Fig. 3A), which removes all N-linked carbohydrates, indicating that changes in glycan composition did not account for the differential gel mobility of these proteins.

For characterization of S-protein-bearing VLPs, we had so far used VLP preparations concentrated by ultrafiltration, which selectively enriched material in cell culture medium with a molecular weight greater than 50 kDa. We next asked if similar results would be obtained with material concentrated by ultracentrifugation through a 20% sucrose cushion. Under these conditions, mainly particle-associated material is pelleted. Notably, when ultracentrifuge-concentrated VLPs were examined, SARS-S produced in TMPRSS2- and control-transfected cells showed identical gel mobility, independently of PNGaseF digest (Fig. 3B). In addition, a marked decrease in signal intensity for SARS-S from TMPRSS2 expressing cells compared to SARS-S from control cells was observed under these conditions (Fig. 3B).

The results described above were most compatible with the interpretation that at least the largest S-protein fragment generated by TMPRSS2 is not virion-associated but shed into the culture supernatants. To further investigate this hypothesis, we concentrated VLP preparations by ultrafiltration and subsequently by ultracentrifugation and determined the effects of these procedures on the presence of uncleaved and cleaved SARS-S. As observed before (Fig. 1), SARS-S signals of similar intensity were observed upon concentration of VLPs produced in TMPRSS2- and control-transfected cells, and the largest S-protein fragment detected in VLPs from TMPRSS2 expressing cells migrated faster than uncleaved SARS-S (Fig. 3C, top panel). The differential gel migration remained when VLPs were further subjected to ultracentrifugation and supernatants were analyzed by Western blot (Fig. 3C, top panel). However, the signal

measured for uncleaved SARS-S was markedly reduced compared to that detected for cleaved SARS-S (Fig. 3C, top panel), indicating that the former was selectively removed from the supernatants by ultracentrifugation, as expected for virion-associated S-protein. Indeed, analysis of pellets revealed a massive concentration of uncleaved SARS-S (Fig. 3C, top panel). In contrast, only a faint signal was obtained for VLPs from TMPRSS2 expressing cells, and the respective S-protein migrated identically to uncleaved SARS-S (Fig. 3C, top panel). In some experiments incomplete cleavage of SARS-S by TMPRSS2 was observed upon analysis of VLPs concentrated by ultrafiltration, with a band corresponding to full length SARS-S still being readily detectable (Fig. 3C, middle panel). When these VLPs were subjected to ultracentrifugation, a prominent signal for uncleaved SARS-S was detected in the pellets (Fig. 3C, middle panel), indicating that upon incomplete cleavage of SARS-S by TMPRSS2 full length S-protein was incorporated into VLPs. Finally, analysis of the HIV Gag contents of VLP preparations confirmed that VLPs were efficiently pelleted upon ultracentrifugation (Fig. 3C, bottom panel). Collectively, these results suggest that cleavage of SARS-S by TMPRSS2 induces SARS-S shedding. However, cleavage is incomplete and a fraction of SARS-S produced in TMPRSS2 expressing cells remains uncleaved and is incorporated into particles.

TMPRSS2-dependent SARS-S shedding confers resistance against antibody-mediated neutralization. Having demonstrated that TMPRSS2 induces SARS-S shedding, we investigated the role of shed SARS-S-protein in susceptibility of SARS-S pseudotypes to inhibition by neutralizing antibodies. For this, we first compared neutralization sensitivity of SARS-S pseudotypes generated in TMPRSS2- and control-transfected cells after purification of virions by ultracentrifugation through a 20% sucrose cushion. Under these conditions, virions produced in the presence and absence of TMPRSS2 exhibited comparable neutralization sensitivity (Fig. 4A), indicating that indeed a non-particle-associated factor present in virion preparations from TMPRSS2- but not from control-transfected cells was responsible for the previously observed neutralization resistance. Western blot analysis confirmed the absence of cleaved SARS-S in (ultracentrifuge-concentrated) virions generated in TMPRSS2 expressing cells (Fig. 4B), indicating that the presence of shed SARS-S predicts neutralization sensitivity. Finally, our Western blot analysis showed that virion incorporation of uncleaved SARS-S was markedly reduced in TMPRSS2- relative to control-transfected cells (Fig. 4B), confirming the hypothesis that a fraction of SARS-S remains uncleaved and is incorporated into virions in TMPRSS2 expressing cells.

To directly demonstrate that shed SARS-S confers neutralization resistance, we purified shed SARS-S. For this, we transiently expressed SARS-S in the presence and absence of TMPRSS2. Subsequently, the cellular supernatants were concentrated by ultrafiltration and then subjected to ultracentrifugation through a 20% sucrose cushion, to remove S-protein potentially associated with vesicles released from S-protein transfected cells. The supernatants of the ultracentrifuge samples were collected and analyzed for the presence of S-protein by Western blot (Fig. 4C). As expected, the SARS-S cleavage fragments previously observed upon coexpression of TMPRSS2 were concentrated under these conditions (Fig. 4C), confirming that they were shed into the cellular supernatants. In contrast, uncleaved SARS-S was absent in samples from TMPRSS2 expressing cells and barely detectable in samples from control transfected cells (Fig. 4C), demonstrating that uncleaved SARS-S is either virion- or cell-associated, as expected. The material purified under these conditions was then added to SARS-S pseudotypes purified by ultracentrifugation, and its effect on neutralization resistance was analyzed. Strikingly, the concentrated supernatants from TMPRSS2 expressing cells (containing shed SARS-S) conferred neutralization resistance to SARS-S-pseudotypes in a dose-dependent manner, while the supernatants from control-transfected cells did not (Fig. 4D), demonstrating that TMPRSS2-dependent shedding of SARS-S induces neutralization resistance.

TMPRSS2 cleaves and activates SARS-S in trans. The results obtained so far indicated that TMPRSS2 cleaves SARS-S when both proteins are coexpressed in the same cell. We next examined if TMPRSS2 was also able to cleave SARS-S when both proteins were expressed on different cells (trans-cleavage), a scenario that mimics contact of infected cells with TMPRSS2 positive cells in the infected host. When cells expressing SARS-S were mixed with TMPRSS4 expressing cells or with control transfected cells, SARS-S remained uncleaved (Fig. 5A). In contrast, mixing SARS-S and TMPRSS2 expressing cells resulted in SARS-S cleavage, and S-protein fragments of the previously observed sizes were detected in the culture supernatants (Fig. 5A). Thus, TMPRSS2 facilitates trans-cleavage of SARS-S.

In order to investigate potential consequences of trans-cleavage for SARS-S activity, we asked if expression of TMPRSS2 on target cells impacts the efficiency of SARS-S-driven cell to cell fusion. For this, we measured fusion of 293T effector cells transfected to express SARS-S with 293T target cells transfected to express ACE2 or TMPRSS2, employing a previously described cell-cell fusion assay (28). In addition, target cells expressing the TMPRSS2-related proteases TMPRSS4, TMPRSS3, TMPRSS6 and hepsin were tested; none of which was previously associated with

activation of viral glycoproteins. Effector and target cells transfected with empty vector served as controls. SARS-S-driven fusion with cells transfected with empty plasmid was inefficient (Fig. 5B), as expected, since 293T cells express only low amounts of endogenous ACE2, which are insufficient to support robust cell-cell fusion (36). Similarly, no appreciable membrane fusion activity was detected when effector cells were transfected with empty plasmid instead of plasmid encoding SARS-S (Fig. 5B). In contrast, trypsin treatment of effector and target cell mixtures or overexpression of ACE2 on target cells allowed efficient SARS-S-driven cell-cell fusion (Fig. 5B), indicating that proteolytic activation of SARS-S is required for SARS-S-driven cell-cell fusion only when receptor expression is limiting. Expression of TMPRSS2 on target cells also allowed efficient SARS-S-dependent cell-cell fusion, while expression of TMPRSS3, TMPRSS6 and hepsin did not (Fig. 5B), indicating that trans-cleavage by TMPRSS2 can activate SARS-S for cell-cell fusion. Unexpectedly, expression of TMPRSS4 on target cells also activated SARS-S for membrane fusion (Fig. 5B). TMPRSS4 failed to cleave SARS-S (Figs. 1 and 5A), and the molecular mechanism underlying SARS-S-activation by TMPRSS4 is at present unclear.

We then asked if the augmentation of SARS-S-driven cell-cell fusion by TMPRSS2 (Fig. 5B) is reflected by increased syncytia formation in TMPRSS2-positive cells infected with replication competent SARS-CoV. To this end, we examined the impact of protease expression on syncytia formation in Vero E6 cells, which are commonly used to analyze SARS-CoV spread. Large syncytia were frequently detected in TMPRSS2 expressing Vero E6 cells infected with SARS-CoV (Frankfurt strain 1), while syncytia in TMPRSS4 expressing cells and in control transfected cells were largely absent (Fig. 5C). These results suggest that TMPRSS2 but not TMPRSS4 is able to activate SARS-S in the context of surrogate systems and in the context of authentic SARS-CoV.

TMPRSS2 on target cells allows efficient SARS-S-driven virus-cell fusion in the presence of a lysosomotropic agent and a cathepsin inhibitor. The SARS-S-driven virus-cell fusion depends on endosomal low pH and the activity of the pH-dependent endosomal protease cathepsin L (53, 55). Consequently, infectious entry can be inhibited by lysosomotropic agents like ammonium chloride (NH_4Cl), which elevate the endosomal pH, and by cathepsin L inhibitors like MDL 28170 (53, 55). In the light of the efficient cleavage and activation of SARS-S by TMPRSS2 we asked if activation of virion-associated SARS-S by TMPRSS2 might allow SARS-S-driven infectious entry into cells treated with NH_4Cl or MDL 28170. Infectious entry of SARS-S pseudotypes into control transfected 293T-hACE2 cells was efficiently inhibited by both

NH₄Cl and MDL 28170, and inhibition was unaffected by expression of TMPRSS4 on target cells (Fig. 6A). In contrast, expression of TMPRSS2 on target cells markedly reduced inhibition of SARS-S-driven entry by NH₄Cl and MDL 28170 (Fig. 6A). Importantly, similar results were obtained when cellular entry of authentic SARS-CoV was examined: Expression of TMPRSS2 did not modulate entry into mock treated cells, as judged by the presence of N-gene mRNA in cell lysates, but allowed efficient viral entry into cells treated with MDL 28170 (Fig. 6B). In contrast, the expression of TMPRSS4 had no effect (Fig. 6B). These results indicate that activation of virion-associated SARS-S by TMPRSS2 can render low pH and cathepsin L activity dispensable for virus-cell fusion.

TMPRSS2 and ACE2 are coexpressed by type II pneumocytes. In order to address whether SARS-S could be cleaved by TMPRSS2 in the lung of SARS-CoV-infected patients, we first determined expression of messenger RNA for TMPRSS2 in human tissues. Messenger RNA was low or absent in brain and heart tissue but was readily detected in tissue samples obtained from pancreas, kidney and lung (Fig. 7A). We then determined if the presence of TMPRSS2 mRNA in human lung was reflected by expression of TMPRSS2 protein, and we analyzed if the protein expression patterns of TMPRSS2 and ACE2 were overlapping. For this, human lung epithelium was analyzed by immunohistochemistry, employing a monoclonal antibody against TMPRSS2 (41) and a polyclonal serum directed against ACE2. Immunostaining for TMPRSS2 and ACE2 demonstrated strong positive staining of type II pneumocytes and alveolar macrophages, while type I pneumocytes were negative (Fig. 7B). Incubation of tissues with control antibodies did not result in significant staining. Thus, TMPRSS2 and ACE2 are coexpressed by type II pneumocytes, which constitute major targets for SARS-CoV (20, 45, 58), indicating that SARS-S could be processed by TMPRSS2 in the lung of infected humans.

DISCUSSION

Processing of viral glycoproteins by host cell proteases can have several consequences: Cleavage can increase or can be essential for viral infectivity (3, 10, 15, 17, 30). In addition, cleavage can result in glycoprotein shedding (12), and the shed proteins can act as antibody decoys (12) or can modulate cellular functions by binding to host cell receptors. We show that the SARS-S protein is cleaved by TMPRSS2 and that cleavage has different consequences, depending on the location of TMPRSS2. If TMPRSS2 is coexpressed with SARS-S in the same cell, cleavage results in SARS-S shedding into the supernatants, where the S-protein fragments function as antibody

decoys. In case TMPRSS2 is expressed on viral target cells, it can activate SARS-S for virus-cell and cell-cell fusion. Finally, TMPRSS2 was found to be coexpressed with the SARS-CoV receptor ACE2 on type II pneumocytes, which are major viral target cells (20, 45, 58), indicating that SARS-S cleavage by TMPRSS2 could modulate viral spread in the infected host.

Simmons and colleagues demonstrated that inhibition of cathepsin activity blocks infectious cellular entry of SARS-CoV (53), indicating that cathepsins proteolytically activate SARS-S upon viral uptake into target cell endosomes. In contrast, the efficiency and functional relevance of SARS-S processing in productively infected cells are less clear (3, 15, 55, 63, 64, 67). In the majority of studies one or two prominent bands (due to differential glycosylation) representative of full length SARS-S have been detected upon analysis of SARS-S expression in transiently transfected or infected cells. Exceptions are the findings by Wu and colleagues, who reported efficient cleavage of SARS-S in infected Vero E6 cells (63), and Du and colleagues, who provided evidence of SARS-S cleavage by factor Xa (13). It has also been suggested that furin cleaves SARS-S and thereby moderately augments viral infectivity (3, 15). However, the cleavage-efficiency seems to be low. Similarly, a recent study reported cleavage of recombinant trimeric SARS-S by trypsin, plasmin and TMPRSS11a, but cleavage was not demonstrated in the context of cellular or virion-associated SARS-S, and cleavage was associated with only a minor increase in infectivity of SARS-S pseudotypes (30). Collectively, there is little evidence that SARS-S is efficiently processed by proteases in productively infected cells. However, SARS-S processing by pulmonary proteases has rarely been examined.

We and others could previously show that type II transmembrane serine proteases TMPRSS2 and TMPRSS4 proteolytically activate human influenza viruses (6, 8), and it is conceivable that these proteases might support viral spread in and between infected individuals (5). When we assessed the impact of TMPRSS2 and TMPRSS4 expression on the proteolytic processing of SARS-S, cleavage of SARS-S into several fragments was observed upon coexpression of TMPRSS2 but not TMPRSS4. Thus, SARS-S, like influenza virus HA (6, 8) and human metapneumovirus fusion protein (51), is cleaved by TMPRSS2. However, in contrast to the latter proteins, which are processed by TMPRSS2 at a single site, SARS-S is cleaved at multiple motifs, indicating that the functional consequences of cleavage might be different.

A previous study indicated that the introduction of an artificial cleavage site into SARS-S can allow cathepsin-independent infection (61). Similar results were not observed with viruses produced in TMPRSS2 expressing cells, with minor differences in sensitivity to high doses of cathepsin inhibitors reflecting variability inherent to the

experimental system rather than biologically meaningful differences. However, pseudotypes produced in the presence of TMPRSS2 were largely resistant to neutralization by two different mouse sera, obtained by immunization of animals with recombinant SARS-S (21). Although differences in the neutralization efficiency of SARS-S pseudotypes and SARS-CoV might exist, this finding could have important implications for SARS-CoV spread in the infected host. Thus, the humoral immune response critically contributes to immune control of SARS-CoV infection (9, 26, 47, 66) and a delayed or diminished control of SARS-CoV by antibodies due to TMPRSS2 might contribute to disease progression. Such a scenario raises the question of how cleavage by TMPRSS2 modulates SARS-S neutralization sensitivity.

To understand the mechanisms underlying neutralization-resistance of SARS-S pseudotypes generated in TMPRSS2 expressing cells, we characterized the SARS-S cleavage products. Analysis by PNGaseF digest showed that size differences between uncleaved and TMPRSS2 cleaved SARS-S were not due to differential glycosylation, which has been observed for influenza virus HA generated in TMPRSS2- relative to TMPRSS4- and control-transfected cells (4). In addition, analysis of cleavage products by ultracentrifugation revealed that SARS-S fragments produced by TMPRSS2 did not pellet in a 20% sucrose cushion, indicating that they were not virion-associated. It must be noted, however, that cleavage of SARS-S by TMPRSS2 was frequently incomplete, with some uncleaved SARS-S or potential cleavage intermediates still being detectable by Western blot. As a consequence, pseudotypes generated in the presence of TMPRSS2 retained substantial infectivity and were largely protected against antibody-mediated neutralization, due to the presence of shed SARS-S in the virion preparations – as demonstrated by the findings that removal of shed SARS-S from virus preparations ablated neutralization resistance, while addition of shed SARS-S conferred neutralization resistance.

The SARS-S sequence motifs cleaved by TMPRSS2 are at present unknown. Trypsin treatment of SARS-S produced a single S1 and S2 fragment, as expected from published data (2, 43), and similar fragments were not, or only inefficiently, produced by TMPRSS2, indicating that TMPRSS2 and trypsin recognize different motifs in SARS-S. Analysis of SARS-S cleavage products with antisera directed against defined portions of SARS-S revealed that the largest cleavage fragment (150 kDa), was most likely produced by a cleavage event occurring between amino acids 1152 and 1200 (not shown). If so, the 150 kDa fragment contained the conserved receptor binding domain (RBD) in SARS-S, amino acids 318 to 510 (1, 35, 62, 64), which is a major target for neutralizing antibodies (22-24), and an antibody decoy function of this fragment would thus be conceivable.

There is evidence that type II transmembrane serine proteases can activate the influenza virus hemagglutinin in productively infected cells and upon binding and uptake of virions into uninfected cells (7). The latter finding triggered us to examine if expression of TMPRSS2 on target cells allowed SARS-S cleavage. SARS-S cleavage products in cell lysates and cellular supernatants were indeed readily detected when SARS-S expressing cells were mixed with TMPRSS2 expressing cells. No such effect was observed with TMPRSS4-positive cells or control transfected cells, indicating that cleavage was specific. However, differences in the relative amounts of cleavage products were noted on comparison of trans- and cis-cleavage of SARS-S by TMPRSS2. Thus, the SARS-S processing products of 45 kDa und 55 kDa observed upon cis-cleavage were usually not detected upon trans-cleavage, suggesting that TMPRSS2 might recognize the cleavage sites in SARS-S with different efficiencies, and only high-affinity sites might be cleaved in trans.

Expression of SARS-S on effector cells can allow fusion with receptor positive target cells, resulting in the formation of syncytia (36, 55, 64), which are also detected in infected patients (32, 46). Addition of trypsin to mixtures of SARS-S effector cells and ACE2-positive target cells is believed to be required for efficient cell-cell fusion (55, 64) and our results show that expression of the trypsin-like protease TMPRSS2 on target cells can functionally replace exogenous trypsin. Overexpression of ACE2 on 293T target cells, which produce low amounts of endogenous ACE2, also allowed efficient SARS-S-driven cell-cell fusion, indicating that proteolytic activation of SARS-S is only required for cell-cell fusion when receptor levels are limiting. Unexpectedly, expression of TMPRSS4 on target cells promoted SARS-S-driven cell-cell fusion with similar efficiency as TMPRSS2, but failed to produce detectable levels of SARS-S cleavage in the trans and cis settings. Although the molecular mechanism underlying SARS-S activation by TMPRSS4 is at present unclear, one can speculate that low levels of cleavage might be responsible. Importantly, TMPRSS2 but not TMPRSS4 promoted formation of syncytia in SARS-CoV infected cell cultures, indicating that only TMPRSS2 can activate SARS-CoV for spread in host cells.

Infectious SARS-CoV entry into target cells depends on the activity of the pH-dependent endosomal cysteine protease cathepsin L, and to a lesser degree on the related enzyme cathepsin B (53). Both proteases depend on low pH for their activity and SARS-CoV entry can therefore be blocked by lysosomotropic agents (which elevate endosomal pH) and by cathepsin inhibitors (26, 53, 55, 65). Previous studies indicate that the requirement for low pH and cathepsin activity for SARS-S-driven virus-cell fusion can be bypassed by treatment of cell-bound virions with trypsin (55) or insertion of an artificial cleavage site into SARS-S (61). Similarly to these findings,

expression of TMPRSS2 was sufficient to allow robust entry of SARS-S pseudotypes into cells treated with NH₄Cl and the cathepsin L inhibitor MDL 28170, a compound that was previously shown to inhibit SARS-S infectious entry (53), and the latter observation were confirmed with authentic SARS-CoV. In contrast, TMPRSS4 was inactive in this setting, suggesting that activation of SARS-S by this protease might only occur upon high expression of SARS-S and protease and/or upon interaction of large surfaces bearing these proteins - hallmarks of the cell-cell fusion assay. In sum, TMPRSS2 but not TMPRSS4 allows SARS-CoV to bypass a block otherwise imposed by cathepsin inhibitors. This observation, in conjunction with our finding that type II pneumocytes, which are major SARS-CoV target cells, coexpress TMPRSS2 and ACE2, suggests that cathepsin inhibitors might not be able to efficiently suppress viral spread in infected patients.

We report that TMPRSS2 can cleave SARS-S in cis and in trans, with different consequences for SARS-S function. It is noteworthy that TMPRSS2 is believed to cleave its substrates at the cell surface and/or in intracellular vesicles (7, 41) probably located close to the cell surface. However, a major fraction of SARS-S is retained in the ERGIC (44, 56, 59) in infected cells and might thus be inaccessible to TMPRSS2 for cis cleavage. Indeed, a recent study by Matsuyama and colleagues, which was published while the present manuscript was in revision, indicated that TMPRSS2 might not cleave SARS-S in cis in infected cell lines (42). Nevertheless, two reports demonstrated that some SARS-S is transported to the surface of infected cells (48, 59), where cis- and trans-cleavage by TMPRSS2 could occur, and it is possible that SARS-S is shed by type II pneumocytes, which might express higher levels of TMPRSS2 than the cell lines examined so far. While cis-cleavage of SARS-S awaits further investigation, our present results unambiguously demonstrate that SARS-S incorporated into both lentiviral pseudotypes and authentic SARS-CoV particles is activated by TMPRSS2 during host cell entry. Therefore, fully activated virions might be delivered to the endosomal compartment of type II pneumocytes and potentially other host cells, which would compromise the effectiveness of cathepsin inhibitors as antiviral agents, in agreement with recent findings (42, 52). Clearly, the role of TMPRSS2 in SARS-CoV spread and pathogenesis warrants further investigation, and tmprss2-knock-out mice, which do not display an obvious phenotype (31), might be a useful tool for these studies.

ACKNOWLEDGEMENTS

We thank T.F. Schulz for support, P. Nelson and J. Lucas for the kind gift of P5H9 antibody and K. Korn for p24-ELISA. This work was supported by BMBF (grant 01KI 0703), Center for Infection Biology (I.S.) and PhD program “Molecular Medicine” (T.S.T.).

REFERENCES

1. Babcock, G. J., D. J. Esshaki, W. D. Thomas, Jr., and D. M. Ambrosino. 2004. Amino acids 270 to 510 of the severe acute respiratory syndrome coronavirus spike protein are required for interaction with receptor. *J Virol* **78**:4552-4560.
2. Belouzard, S., V. C. Chu, and G. R. Whittaker. 2009. Activation of the SARS coronavirus spike protein via sequential proteolytic cleavage at two distinct sites. *Proc. Natl. Acad. Sci. U. S. A* **106**:5871-5876.
3. Bergeron, E., M. J. Vincent, L. Wickham, J. Hamelin, A. Basak, S. T. Nichol, M. Chretien, and N. G. Seidah. 2005. Implication of proprotein convertases in the processing and spread of severe acute respiratory syndrome coronavirus. *Biochem. Biophys. Res. Commun.* **326**:554-563.
4. Bertram, S., I. Glowacka, P. Blazejewska, E. Soilleux, P. Allen, S. Danisch, I. Steffen, S. Y. Choi, Y. Park, H. Schneider, K. Schughart, and S. Pöhlmann. 2010. TMPRSS2 and TMPRSS4 facilitate trypsin-independent spread of influenza virus in Caco-2 cells. *J Virol.* **84**:10016-10025.
5. Bertram, S., I. Glowacka, I. Steffen, A. Kuhl, and S. Pöhlmann. 2010. Novel insights into proteolytic cleavage of influenza virus hemagglutinin. *Rev. Med. Virol.* **20**:298-310.
6. Bottcher, E., T. Matrosovich, M. Beyerle, H. D. Klenk, W. Garten, and M. Matrosovich. 2006. Proteolytic activation of influenza viruses by serine proteases TMPRSS2 and HAT from human airway epithelium. *J. Virol.* **80**:9896-9898.
7. Bottcher-Friebertshauser, E., C. Freuer, F. Sielaff, S. Schmidt, M. Eickmann, J. Uhendorff, T. Steinmetzer, H. D. Klenk, and W. Garten. 2010. Cleavage of influenza virus hemagglutinin by airway proteases TMPRSS2 and HAT differs in subcellular localization and susceptibility to protease inhibitors. *J Virol.* **84**:5605-5614.

8. Chaipan, C., D. Kobasa, S. Bertram, I. Glowacka, I. Steffen, T. S. Tsegaye, M. Takeda, T. H. Bugge, S. Kim, Y. Park, A. Marzi, and S. Pöhlmann. 2009. Proteolytic activation of the 1918 influenza virus hemagglutinin. *J Virol.* **83**:3200-3211.
9. Chen, X., B. Zhou, M. Li, X. Liang, H. Wang, G. Yang, H. Wang, and X. Le. 2004. Serology of severe acute respiratory syndrome: implications for surveillance and outcome. *J Infect. Dis.* **189**:1158-1163.
10. Choi, S. Y., S. Bertram, I. Glowacka, Y. W. Park, and S. Pöhlmann. 2009. Type II transmembrane serine proteases in cancer and viral infections. *Trends Mol Med* **15**:303-312.
11. Connor, R. I., B. K. Chen, S. Choe, and N. R. Landau. 1995. Vpr is required for efficient replication of human immunodeficiency virus type-1 in mononuclear phagocytes. *Virology* **206**:935-944.
12. Dolnik, O., V. Volchkova, W. Garten, C. Carbonnelle, S. Becker, J. Kahnt, U. Stroher, H. D. Klenk, and V. Volchkov. 2004. Ectodomain shedding of the glycoprotein GP of Ebola virus. *EMBO J* **23**:2175-2184.
13. Du, L., R. Y. Kao, Y. Zhou, Y. He, G. Zhao, C. Wong, S. Jiang, K. Y. Yuen, D. Y. Jin, and B. J. Zheng. 2007. Cleavage of spike protein of SARS coronavirus by protease factor Xa is associated with viral infectivity. *Biochem. Biophys. Res. Commun.* **359**:174-179.
14. Eckert, D. M. and P. S. Kim. 2001. Mechanisms of viral membrane fusion and its inhibition. *Annu. Rev. Biochem.* **70**:777-810.
15. Follis, K. E., J. York, and J. H. Nunberg. 2006. Furin cleavage of the SARS coronavirus spike glycoprotein enhances cell-cell fusion but does not affect virion entry. *Virology* **350**:358-369.
16. Gao, F., Y. Li, J. M. Decker, F. W. Peyerl, F. Bibollet-Ruche, C. M. Rodenburg, Y. Chen, D. R. Shaw, S. Allen, R. Musonda, G. M. Shaw, A. J. Zajac, N. Letvin, and B. H. Hahn. 2003. Codon usage optimization of HIV type 1 subtype C gag, pol, env, and nef genes: in vitro expression and immune responses in DNA-vaccinated mice. *AIDS Res. Hum. Retroviruses* **19**:817-823.
17. Garten, W. and H. D. Klenk. 1999. Understanding influenza virus pathogenicity. *Trends Microbiol.* **7**:99-100.
18. Glowacka, I., S. Bertram, P. Herzog, S. Pfefferle, I. Steffen, M. O. Muench, G. Simmons, H. Hofmann, T. Kuri, F. Weber, J. Eichler, C. Drosten, and S. Pöhlmann.

2010. Differential downregulation of ACE2 by the spike proteins of severe acute respiratory syndrome coronavirus and human coronavirus NL63. *J Virol.* **84**:1198-1205.
19. **Guan, Y., B. J. Zheng, Y. Q. He, X. L. Liu, Z. X. Zhuang, C. L. Cheung, S. W. Luo, P. H. Li, L. J. Zhang, Y. J. Guan, K. M. Butt, K. L. Wong, K. W. Chan, W. Lim, K. F. Shortridge, K. Y. Yuen, J. S. Peiris, and L. L. Poon.** 2003. Isolation and characterization of viruses related to the SARS coronavirus from animals in southern China. *Science* **302**:276-278.
 20. **Hamming, I., W. Timens, M. L. Bulthuis, A. T. Lely, G. J. Navis, and H. van Goor.** 2004. Tissue distribution of ACE2 protein, the functional receptor for SARS coronavirus. A first step in understanding SARS pathogenesis. *J Pathol.* **203**:631-637.
 21. **He, Y., J. Li, S. Heck, S. Lustigman, and S. Jiang.** 2006. Antigenic and immunogenic characterization of recombinant baculovirus-expressed severe acute respiratory syndrome coronavirus spike protein: implication for vaccine design. *J Virol.* **80**:5757-5767.
 22. **He, Y., H. Lu, P. Siddiqui, Y. Zhou, and S. Jiang.** 2005. Receptor-binding domain of severe acute respiratory syndrome coronavirus spike protein contains multiple conformation-dependent epitopes that induce highly potent neutralizing antibodies. *J. Immunol.* **174**:4908-4915.
 23. **He, Y., Y. Zhou, S. Liu, Z. Kou, W. Li, M. Farzan, and S. Jiang.** 2004. Receptor-binding domain of SARS-CoV spike protein induces highly potent neutralizing antibodies: implication for developing subunit vaccine. *Biochem. Biophys. Res. Commun.* **324**:773-781.
 24. **He, Y., Y. Zhou, H. Wu, B. Luo, J. Chen, W. Li, and S. Jiang.** 2004. Identification of immunodominant sites on the spike protein of severe acute respiratory syndrome (SARS) coronavirus: implication for developing SARS diagnostics and vaccines. *J Immunol.* **173**:4050-4057.
 25. **Hofmann, H., M. Geier, A. Marzi, M. Krumbiegel, M. Peipp, G. H. Fey, T. Gramberg, and S. Pöhlmann.** 2004. Susceptibility to SARS coronavirus S protein-driven infection correlates with expression of angiotensin converting enzyme 2 and infection can be blocked by soluble receptor. *Biochem. Biophys. Res. Commun.* **319**:1216-1221.
 26. **Hofmann, H., K. Hattermann, A. Marzi, T. Gramberg, M. Geier, M. Krumbiegel, S. Kuate, K. Uberla, M. Niedrig, and S. Pöhlmann.** 2004. S protein of severe acute respiratory syndrome-associated coronavirus mediates entry into hepatoma cell lines and is targeted by neutralizing antibodies in infected patients. *J. Virol.* **78**:6134-6142.

27. **Hofmann, H. and S. Pöhlmann.** 2004. Cellular entry of the SARS coronavirus. *Trends Microbiol.* **12**:466-472.
28. **Hofmann, H., G. Simmons, A. J. Rennekamp, C. Chaipan, T. Gramberg, E. Heck, M. Geier, A. Wegele, A. Marzi, P. Bates, and S. Pöhlmann.** 2006. Highly conserved regions within the spike proteins of human coronaviruses 229E and NL63 determine recognition of their respective cellular receptors. *J. Virol.* **80**:8639-8652.
29. **Jung, H., K. P. Lee, S. J. Park, J. H. Park, Y. S. Jang, S. Y. Choi, J. G. Jung, K. Jo, D. Y. Park, J. H. Yoon, J. H. Park, D. S. Lim, G. R. Hong, C. Choi, Y. K. Park, J. W. Lee, H. J. Hong, S. Kim, and Y. W. Park.** 2008. TMPRSS4 promotes invasion, migration and metastasis of human tumor cells by facilitating an epithelial-mesenchymal transition. *Oncogene* **27**:2635-2647.
30. **Kam, Y. W., Y. Okumura, H. Kido, L. F. Ng, R. Bruzzone, and R. Altmeyer.** 2009. Cleavage of the SARS coronavirus spike glycoprotein by airway proteases enhances virus entry into human bronchial epithelial cells in vitro. *PLoS. One.* **4**:e7870.
31. **Kim, T. S., C. Heinlein, R. C. Hackman, and P. S. Nelson.** 2006. Phenotypic analysis of mice lacking the Tmprss2-encoded protease. *Mol Cell Biol.* **26**:965-975.
32. **Kuiken, T., R. A. Fouchier, M. Schutten, G. F. Rimmelzwaan, G. van Amerongen, D. van Riel, J. D. Laman, T. de Jong, G. van Doornum, W. Lim, A. E. Ling, P. K. Chan, J. S. Tam, M. C. Zambon, R. Gopal, C. Drosten, W. S. van der, N. Escriou, J. C. Manuguerra, K. Stohr, J. S. Peiris, and A. D. Osterhaus.** 2003. Newly discovered coronavirus as the primary cause of severe acute respiratory syndrome. *Lancet* **362**:263-270.
33. **Lau, S. K., P. C. Woo, K. S. Li, Y. Huang, H. W. Tsoi, B. H. Wong, S. S. Wong, S. Y. Leung, K. H. Chan, and K. Y. Yuen.** 2005. Severe acute respiratory syndrome coronavirus-like virus in Chinese horseshoe bats. *Proc Natl Acad Sci U. S A* **102**:14040-14045.
34. **Li, F., M. Berardi, W. Li, M. Farzan, P. R. Dormitzer, and S. C. Harrison.** 2006. Conformational states of the severe acute respiratory syndrome coronavirus spike protein ectodomain. *J. Virol.* **80**:6794-6800.
35. **Li, F., W. Li, M. Farzan, and S. C. Harrison.** 2005. Structure of SARS coronavirus spike receptor-binding domain complexed with receptor. *Science* **309**:1864-1868.
36. **Li, W., M. J. Moore, N. Vasilieva, J. Sui, S. K. Wong, M. A. Berne, M. Somasundaran, J. L. Sullivan, K. Luzuriaga, T. C. Greenough, H. Choe, and M. Farzan.** 2003. Angiotensin-converting enzyme 2 is a functional receptor for the SARS coronavirus. *Nature* **426**:450-454.

37. Li, W., Z. Shi, M. Yu, W. Ren, C. Smith, J. H. Epstein, H. Wang, G. Crameri, Z. Hu, H. Zhang, J. Zhang, J. McEachern, H. Field, P. Daszak, B. T. Eaton, S. Zhang, and L. F. Wang. 2005. Bats are natural reservoirs of SARS-like coronaviruses. *Science* **310**:676-679.
38. Li, W., S. K. Wong, F. Li, J. H. Kuhn, I. C. Huang, H. Choe, and M. Farzan. 2006. Animal origins of the severe acute respiratory syndrome coronavirus: insight from ACE2-S-protein interactions. *J. Virol.* **80**:4211-4219.
39. Li, W., C. Zhang, J. Sui, J. H. Kuhn, M. J. Moore, S. Luo, S. K. Wong, I. C. Huang, K. Xu, N. Vasilieva, A. Murakami, Y. He, W. A. Marasco, Y. Guan, H. Choe, and M. Farzan. 2005. Receptor and viral determinants of SARS-coronavirus adaptation to human ACE2. *EMBO J* **24**:1634-1643.
40. Lubisch, W., H. P. Hofmann, H. J. Treiber, and A. Moller. 2000. Synthesis and biological evaluation of novel piperidine carboxamide derived calpain inhibitors. *Bioorg. Med Chem. Lett.* **10**:2187-2191.
41. Lucas, J. M., L. True, S. Hawley, M. Matsumura, C. Morrissey, R. Vessella, and P. S. Nelson. 2008. The androgen-regulated type II serine protease TMPRSS2 is differentially expressed and mislocalized in prostate adenocarcinoma. *J Pathol.* **215**:118-125.
42. Matsuyama, S., N. Nagata, K. Shirato, M. Kawase, M. Takeda, and F. Taguchi. 2010. Efficient activation of SARS coronavirus spike protein by the transmembrane protease, TMPRSS2. *J Virol.*
43. Matsuyama, S., M. Ujike, S. Morikawa, M. Tashiro, and F. Taguchi. 2005. Protease-mediated enhancement of severe acute respiratory syndrome coronavirus infection. *Proc. Natl. Acad. Sci. U. S. A* **102**:12543-12547.
44. McBride, C. E., J. Li, and C. E. Machamer. 2007. The cytoplasmic tail of the severe acute respiratory syndrome coronavirus spike protein contains a novel endoplasmic reticulum retrieval signal that binds COPI and promotes interaction with membrane protein. *J. Virol.* **81**:2418-2428.
45. Mossel, E. C., J. Wang, S. Jeffers, K. E. Edeen, S. Wang, G. P. Cosgrove, C. J. Funk, R. Manzer, T. A. Miura, L. D. Pearson, K. V. Holmes, and R. J. Mason. 2008. SARS-CoV replicates in primary human alveolar type II cell cultures but not in type I-like cells. *Virology* **372**:127-135.
46. Nicholls, J. M., L. L. Poon, K. C. Lee, W. F. Ng, S. T. Lai, C. Y. Leung, C. M. Chu, P. K. Hui, K. L. Mak, W. Lim, K. W. Yan, K. H. Chan, N. C. Tsang, Y. Guan, K. Y. Yuen,

- and J. S. Peiris. 2003. Lung pathology of fatal severe acute respiratory syndrome. Lancet **361**:1773-1778.
47. Nie, Y., P. Wang, X. Shi, G. Wang, J. Chen, A. Zheng, W. Wang, Z. Wang, X. Qu, M. Luo, L. Tan, X. Song, X. Yin, J. Chen, M. Ding, and H. Deng. 2004. Highly infectious SARS-CoV pseudotyped virus reveals the cell tropism and its correlation with receptor expression. Biochem. Biophys. Res. Commun. **321**:994-1000.
48. Ohnishi, K., M. Sakaguchi, T. Kaji, K. Akagawa, T. Taniyama, M. Kasai, Y. Tsunetsugu-Yokota, M. Oshima, K. Yamamoto, N. Takasuka, S. Hashimoto, M. Ato, H. Fujii, Y. Takahashi, S. Morikawa, K. Ishii, T. Sata, H. Takagi, S. Itamura, T. Odagiri, T. Miyamura, I. Kurane, M. Tashiro, T. Kurata, H. Yoshikura, and T. Takemori. 2005. Immunological detection of severe acute respiratory syndrome coronavirus by monoclonal antibodies. Jpn. J Infect. Dis. **58**:88-94.
49. Peiris, J. S., Y. Guan, and K. Y. Yuen. 2004. Severe acute respiratory syndrome. Nat Med **10**:S88-S97.
50. Radonic, A., S. Thulke, I. M. Mackay, O. Landt, W. Siegert, and A. Nitsche. 2004. Guideline to reference gene selection for quantitative real-time PCR. Biochem. Biophys. Res. Commun. **313**:856-862.
51. Shirogane, Y., M. Takeda, M. Iwasaki, N. Ishiguro, H. Takeuchi, Y. Nakatsu, M. Tahara, H. Kikuta, and Y. Yanagi. 2008. Efficient multiplication of human metapneumovirus in Vero cells expressing the transmembrane serine protease TMPRSS2. J. Virol. **82**:8942-8946.
52. Shulla, A., T. Heald-Sargent, G. Subramanya, J. Zhao, S. Perlman, and T. Gallagher. 2011. A transmembrane serine protease is linked to the severe acute respiratory syndrome coronavirus receptor and activates virus entry. J. Virol. **85**:873-882.
53. Simmons, G., D. N. Gosalia, A. J. Rennekamp, J. D. Reeves, S. L. Diamond, and P. Bates. 2005. Inhibitors of cathepsin L prevent severe acute respiratory syndrome coronavirus entry. Proc Natl Acad Sci U. S A **102**:11876-11881.
54. Simmons, G., J. D. Reeves, C. C. Grogan, L. H. Vandenberghe, F. Baribaud, J. C. Whitbeck, E. Burke, M. J. Buchmeier, E. J. Soilleux, J. L. Riley, R. W. Doms, P. Bates, and S. Pöhlmann. 2003. DC-SIGN and DC-SIGNR bind ebola glycoproteins and enhance infection of macrophages and endothelial cells. Virology **305**:115-123.
55. Simmons, G., J. D. Reeves, A. J. Rennekamp, S. M. Amberg, A. J. Piefer, and P. Bates. 2004. Characterization of severe acute respiratory syndrome-associated

- coronavirus (SARS-CoV) spike glycoprotein-mediated viral entry. Proc. Natl. Acad. Sci. U. S. A **101**:4240-4245.
56. **Stertz, S., M. Reichelt, M. Spiegel, T. Kuri, L. Martinez-Sobrido, A. Garcia-Sastre, F. Weber, and G. Kochs.** 2007. The intracellular sites of early replication and budding of SARS-coronavirus. Virology **361**:304-315.
 57. **Szabo, R., S. Netzel-Arnett, J. P. Hobson, T. M. Antalis, and T. H. Bugge.** 2005. Matriptase-3 is a novel phylogenetically preserved membrane-anchored serine protease with broad serpin reactivity. Biochem. J. **390**:231-242.
 58. **To, K. F., J. H. Tong, P. K. Chan, F. W. Au, S. S. Chim, K. C. Chan, J. L. Cheung, E. Y. Liu, G. M. Tse, A. W. Lo, Y. M. Lo, and H. K. Ng.** 2004. Tissue and cellular tropism of the coronavirus associated with severe acute respiratory syndrome: an in-situ hybridization study of fatal cases. J Pathol. **202**:157-163.
 59. **Voss, D., S. Pfefferle, C. Drosten, L. Stevermann, E. Traggiai, A. Lanzavecchia, and S. Becker.** 2009. Studies on membrane topology, N-glycosylation and functionality of SARS-CoV membrane protein. Virol. J **6**:79.
 60. **Wang, P., J. Chen, A. Zheng, Y. Nie, X. Shi, W. Wang, G. Wang, M. Luo, H. Liu, L. Tan, X. Song, Z. Wang, X. Yin, X. Qu, X. Wang, T. Qing, M. Ding, and H. Deng.** 2004. Expression cloning of functional receptor used by SARS coronavirus. Biochem. Biophys. Res. Commun. **315**:439-444.
 61. **Watanabe, R., S. Matsuyama, K. Shirato, M. Maejima, S. Fukushi, S. Morikawa, and F. Taguchi.** 2008. Entry from the cell surface of severe acute respiratory syndrome coronavirus with cleaved s protein as revealed by pseudotype virus bearing cleaved s protein. J. Virol. **82**:11985-11991.
 62. **Wong, S. K., W. Li, M. J. Moore, H. Choe, and M. Farzan.** 2004. A 193-amino acid fragment of the SARS coronavirus S protein efficiently binds angiotensin-converting enzyme 2. J Biol. Chem. **279**:3197-3201.
 63. **Wu, X. D., B. Shang, R. F. Yang, H. Yu, Z. H. Ma, X. Shen, Y. Y. Ji, Y. Lin, Y. D. Wu, G. M. Lin, L. Tian, X. Q. Gan, S. Yang, W. H. Jiang, E. H. Dai, X. Y. Wang, H. L. Jiang, Y. H. Xie, X. L. Zhu, G. Pei, L. Li, J. R. Wu, and B. Sun.** 2004. The spike protein of severe acute respiratory syndrome (SARS) is cleaved in virus infected Vero-E6 cells. Cell Res. **14**:400-406.
 64. **Xiao, X., S. Chakraborti, A. S. Dimitrov, K. Gramatikoff, and D. S. Dimitrov.** 2003. The SARS-CoV S glycoprotein: expression and functional characterization. Biochem Biophys Res Commun. **312**:1159-1164.

65. **Yang, Z. Y., Y. Huang, L. Ganesh, K. Leung, W. P. Kong, O. Schwartz, K. Subbarao, and G. J. Nabel.** 2004. pH-dependent entry of severe acute respiratory syndrome coronavirus is mediated by the spike glycoprotein and enhanced by dendritic cell transfer through DC-SIGN. *J. Virol.* **78**:5642-5650.
66. **Yang, Z. Y., W. P. Kong, Y. Huang, A. Roberts, B. R. Murphy, K. Subbarao, and G. J. Nabel.** 2004. A DNA vaccine induces SARS coronavirus neutralization and protective immunity in mice. *Nature* **428**:561-564.
67. **Yao, Y. X., J. Ren, P. Heinen, M. Zambon, and I. M. Jones.** 2004. Cleavage and serum reactivity of the severe acute respiratory syndrome coronavirus spike protein. *J. Infect. Dis.* **190**:91-98.

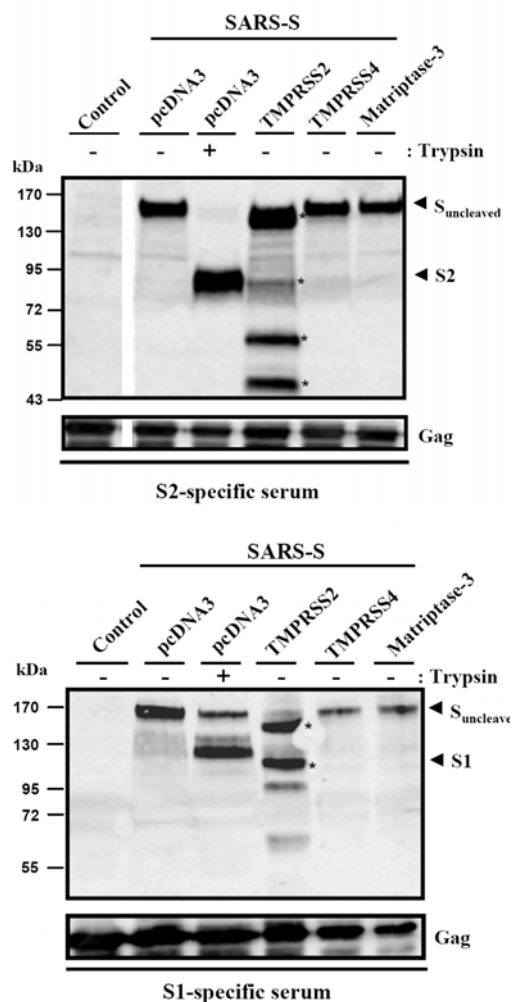


Figure 1. Proteolytic processing of SARS-S by TMPRSS2. Top panel: Virus-like particles (VLPs) were produced by coexpression of HIV p55 Gag and SARS-S in the absence and presence of coexpressed human TMPRSS2, TMPRSS4 or murine matriptase-3, treated with trypsin or PBS and analyzed for S-protein and HIV p55 Gag content as indicated, using a serum specific for the S2-subunit of SARS-S. (B) The experiment was carried out as described for (A). However, an S1-specific antiserum was used for SARS-S-protein detection.

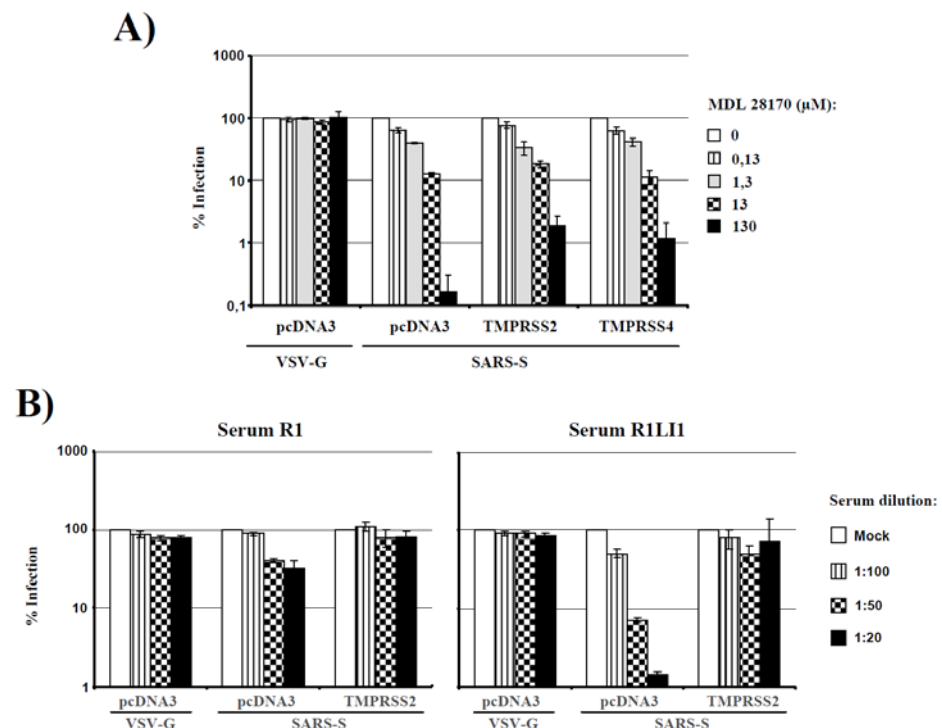


Figure 2. Impact of SARS-S processing by TMPRSS2 on cathepsin-dependence and neutralization sensitivity. (A) 293T cells engineered to express large amounts of ACE2 were incubated with the indicated concentrations of the cathepsin B/L inhibitor MDL 28170, inoculated with pseudotypes in triplicate and luciferase-activities were determined at 72 h post infection. Activities measured in the absence of inhibitor were set as 100%. A representative experiment out of three is shown, error bars indicate SD. In the absence of inhibitor, the following luciferase counts were measured. VSV-G: 55642 – 4877 c.p.s., SARS-S + pcDNA3: 64751 – 11505 c.p.s., SARS-S + TMPRSS2: 59071 – 5087 c.p.s., SARS + TMPRSS4: 94684 – 4576 c.p.s. (B) Equal volumes of pseudotypes bearing SARS-S wt were incubated for 60 min with the indicated dilutions of the sera R1 and R1LI1 in triplicate, and then added to ACE2-expressing 293T cells. Luciferase-activities in cell lysates were determined after 72 h, and activities measured in the absence of serum were set as 100%. The results – SD of a representative experiment are shown. Similar results were obtained in two independent experiments. In the absence of serum, the following luciferase counts were measured. VSV-G: 9037372 – 330551 c.p.s.; SARS-S + pcDNA3: 5411448 – 304990 c.p.s.; SARS-S + TMPRSS2: 444923 – 27314 c.p.s. C.p.s.: counts per second.

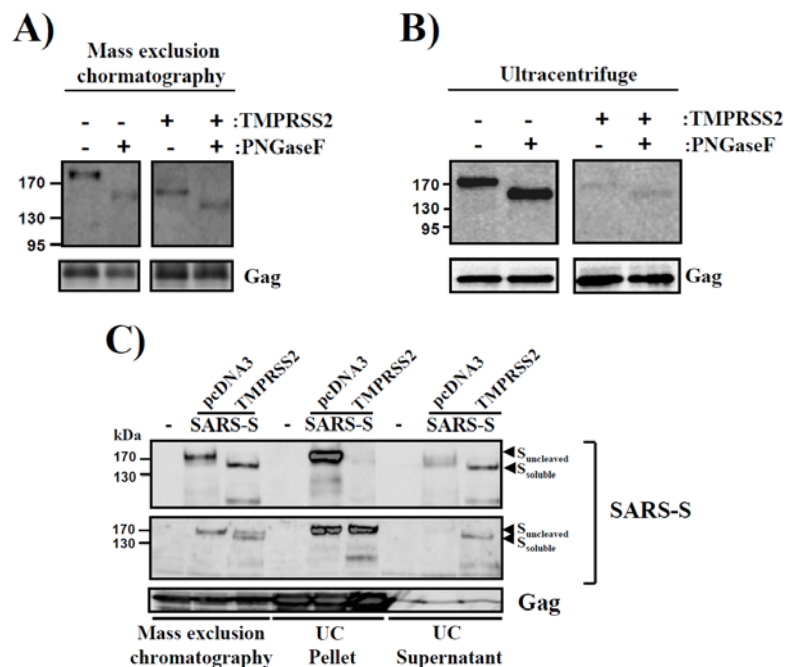


Figure 3. Cleavage by TMPRSS2 induces SARS-S shedding. (A) VLPs were produced in 293T cells in the absence and presence of TMPRSS2, concentrated by ultrafiltration, treated with PNGaseF to remove N-linked glycans and analyzed for SARS-S and Gag protein content by Western blot. Results of a single gel are shown, from which irrelevant lanes were removed. (B) The experiment was carried out as in (A) but VLPs were additionally concentrated by ultracentrifugation through a 20% sucrose cushion. (C) VLPs were produced as described in (A) and then subjected to ultrafiltration followed by ultracentrifugation. Western blot analysis was employed to determine the effect of these procedures on the concentrations of SARS-S and Gag protein in the VLP preparations. Ultrafiltration: VLP preparation subjected ultrafiltration, UC pellet: VLP preparation subjected to ultrafiltration followed by ultracentrifugation and Western blot analysis of the pellets, UC supernatant: VLP preparation subjected to ultrafiltration followed by ultracentrifugation and Western blot analysis of the supernatants of ultracentrifuge reactions.

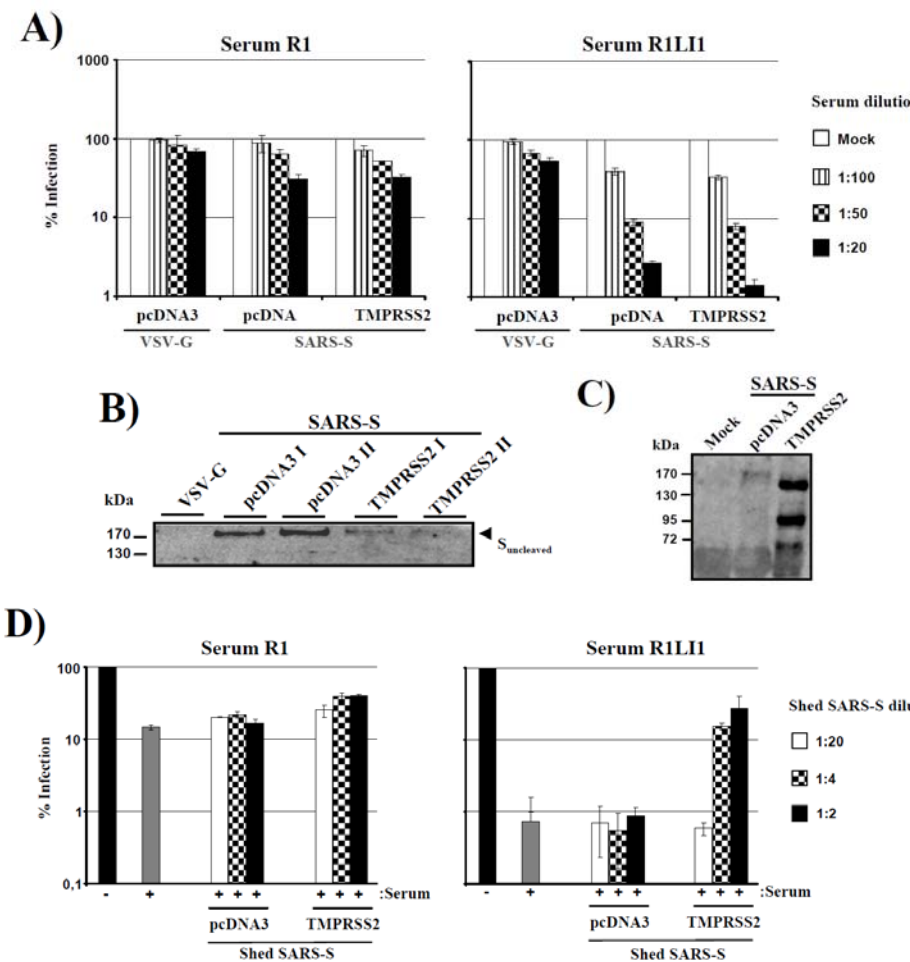


Figure 4. Shedding of SARS-S by TMPRSS2 confers neutralization resistance. (A) The pseudoparticles indicated were produced in 293T cells in the presence or absence of TMPRSS2, concentrated by ultracentrifugation through a 20% sucrose cushion, preincubated with the indicated dilutions of the sera R1 and R1LI1 and then used for triplicate infections of 293T-ACE2 cells. Luciferase-activities in cell lysates were determined after 72 h and activities measured in the absence of serum were set as 100%. The results of a representative experiment are shown, error bars indicate SD. The results were confirmed in two independent experiments. In the absence of serum, the following luciferase counts were measured. VSV-G: 509961 ± 37823 c.p.s.; SARS-S + pcDNA3: 497873 ± 52794 c.p.s.; SARS-S + TMPRSS2: 608600 ± 97835 c.p.s. (B) The concentrated pseudotypes described in (A) were analyzed by Western blot for the presence of SARS-S (employing an S1-specific rabbit serum). (C) 293T cells were transiently cotransfected with expression plasmids for SARS-S and TMPRSS2 or cotransfected with SARS-S plasmid and empty vector (pcDNA3) and culture supernatants were harvested at 48 h after transfection. Subsequently, the supernatants were concentrated by ultrafiltration followed by ultracentrifugation through a 20% sucrose cushion. The presence of soluble SARS-S-protein in the supernatants of ultracentrifuged samples was analyzed by immunoblotting, as described in (A). (D) Pseudoparticles bearing SARS-S and purified by ultracentrifugation through a sucrose cushion were preincubated with the indicated dilutions of supernatants described in (C) and a 1:50 dilution of the sera R1 and R1LI1 for 60 min before

addition to target cells (pcDNA3: supernatants from cells cotransfected with SARS-S and empty plasmid, TMPRSS2: supernatants from cells cotransfected with TMPRSS2 and SARS-S expression plasmids). Luciferase-activities in cell lysates were determined after 72 h. The results \pm SD of a representative experiment carried out in triplicate are shown, activities measured in the absence of serum, 1307409 ± 328118 c.p.s., were set as 100%. The results were confirmed in two separate experiments. C.p.s.: counts per second.

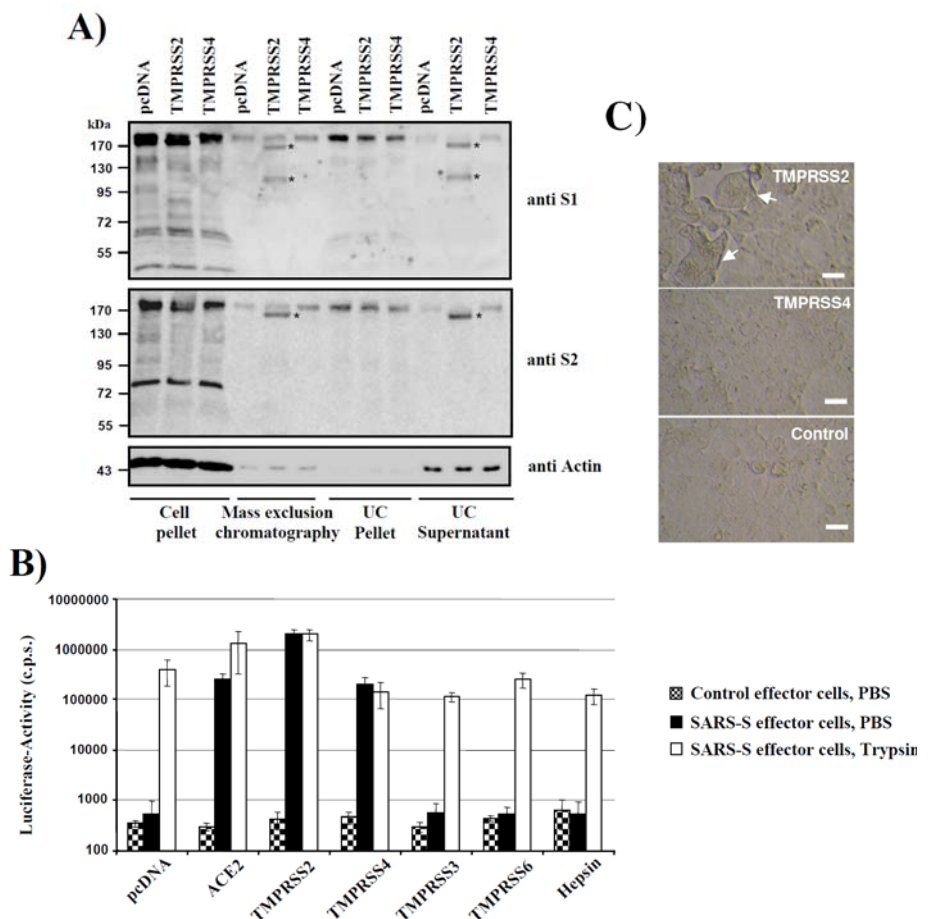


Figure 5. TMPRSS2 cleaves SARS-S in trans and activates SARS-S for cell-cell fusion. (A) Effector cells were transfected with SARS-S expression plasmid and mixed with target cells transfected with empty plasmid (pcDNA) or plasmids encoding TMPRSS2 or TMPRSS4. Lysates and supernatants of these cell mixtures were analyzed for SARS-S cleavage by Western blot, employing sera directed against the S1 and the S2 portions of SARS-S for detection. Before analysis by Western blot, supernatants were concentrated by ultrafiltration and ultracentrifugation. (B) Effector cells cotransfected with pGAL4-VP16 expression plasmid and either empty plasmid or SARS-S expression plasmid were mixed with target cells cotransfected with the indicated plasmids and a plasmid encoding luciferase under the control of a promoter with multiple GAL4 binding sites. The cell mixtures were then treated with either PBS or trypsin and the luciferase activities in cell lysates quantified at 48 h after cell mixing. The results of a representative experiment performed in triplicates are shown; error bars indicate SD. Similar results were observed in two independent experiments. Cell pellet: Lysates of transfected cells analyzed by Western blot. Ultrafiltration: Culture supernatants subjected to ultrafiltration followed by Western blot analysis. UC pellet: Culture supernatants subjected to ultrafiltration followed by ultracentrifugation and Western blot analysis of the pellets, UC supernatant: Culture supernatants subjected to ultrafiltration followed by ultracentrifugation and Western blot analysis of the supernatants of ultracentrifuge reactions. (C) Vero E6 cells transfected with TMPRSS2- or TMPRSS4-expression plasmid or empty vector (pcDNA) were infected with SARS-CoV (Frankfurt strain 1) at an MOI of 0.1. At 29 h post infection the cells

were fixed and analyzed by microscopy. Bars indicate 20 µm, arrows indicate syncytia. Similar results were obtained in an independent experiment.

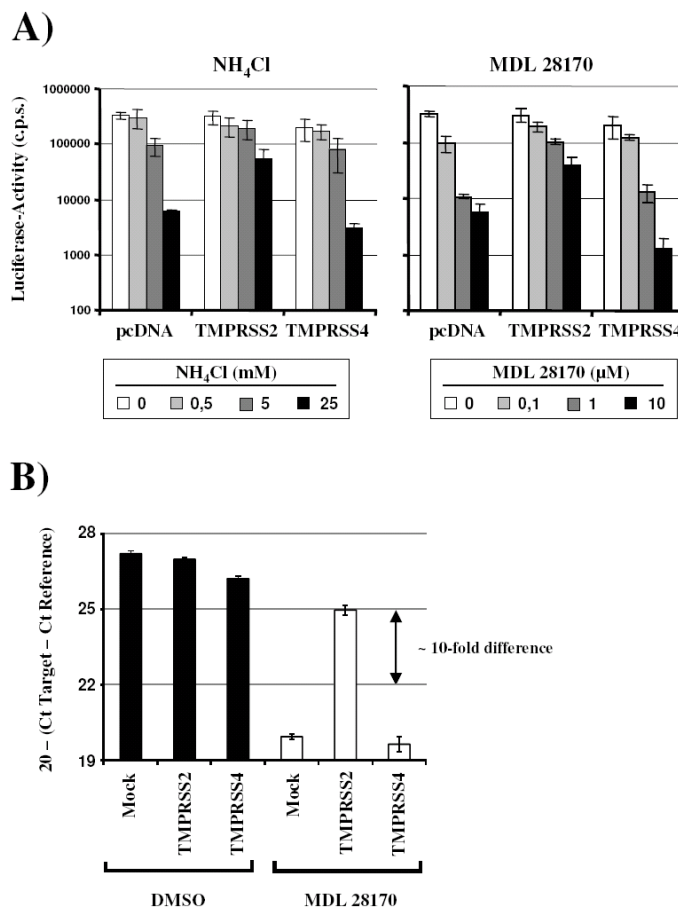


Figure 6. Expression of TMPRSS2 on target cells reduces the requirement for acidic pH and cathepsin activity for SARS-S-driven infectious entry. (A) The indicated proteases were expressed in 293T-hACE2 cells and the cells were pretreated with medium containing the indicated concentrations of NH₄Cl and MDL 28170, respectively. Subsequently, the cells were infected with pseudotypes bearing SARS-S in the presence of inhibitor. The infection medium was replaced by fresh medium without inhibitor at 16 h post infection and the luciferase activities in cell lysates analyzed at 72 h post infection. The results of representative experiments performed in triplicates are shown; error bars indicate SD. Similar results were obtained in two independent experiments. hACE2: human ACE2. (B) The indicated proteases were expressed in 293T-hACE2 cells and the cells treated with the cathepsin inhibitor MDL 28170 before infection with SARS-CoV (Frankfurt strain 1) at an MOI of 0.1. At five hours post infection the cells were washed with PBS, lysed and total RNA was extracted. SARS-CoV entry was analyzed by real-time RT-PCR specific for the N-gene mRNA. Average Ct values of a single experiment performed in triplicates were normalized by subtracting the respective Ct values for Tata-box binding protein (reference gene). For clarity, values were subtracted by a fixed number (20). A Ct difference of 3 correlated approximately with a 10-fold increase in transcripts as determined by a dilution series of both targets. Similar results were obtained in an independent experiment.

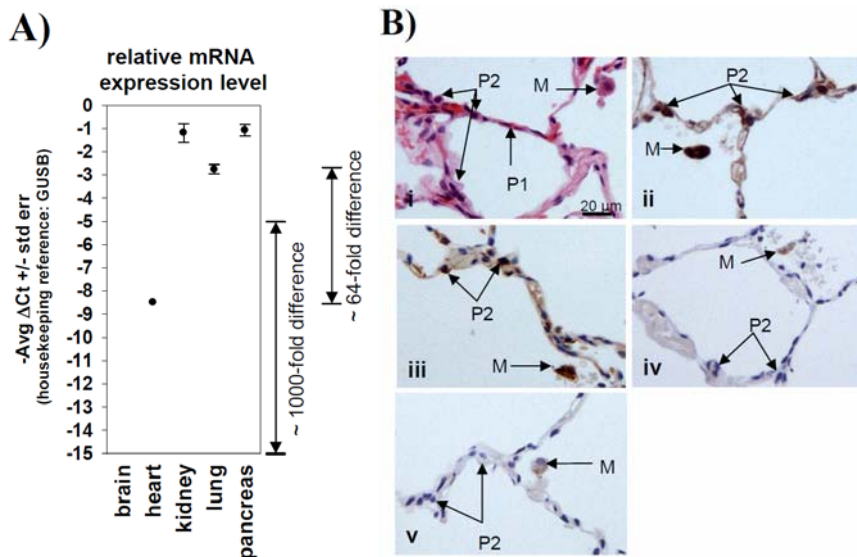


Figure 7. Coexpression of ACE2 and TMPRSS2 on type II pneumocytes. (A) The amount of tmprss2 transcript in the indicated organs was quantified by PCR, employing GUSB as housekeeping reference. The average of three independent experiments are shown, error bars indicate SD. No specific signal was measured for brain in three out of three experiments. A specific signal was measured for heart in one out of three independent experiments. (B) (i) Haematoxylin and eosin stained section of normal lung showing several alveolar spaces, in which alveolar macrophages (M), type I pneumocytes (P1) and type II pneumocytes (P2) are labelled. Scale bar (lower right corner) represents 20 microns. (ii) Serial section of i immunostained for TMPRSS2 using the peroxidase technique (brown) shows strong positive staining in type II pneumocytes (P2) and alveolar macrophages (M). (iii) Serial section of ii immunostained for ACE-2 shows strong positive staining in type II pneumocytes (P2) and alveolar macrophages (M). (iv) Serial section of iii immunostained with an irrelevant mouse primary antibody (melan-A), as a negative control for (ii), shows no immunostaining. Alveolar macrophages (M) show a faint brown tint, due to the presence of carbon, but not the strong brown staining of macrophages seen in (ii). (v) Serial section of (iv) immunostained using goat polyclonal serum as a primary antibody, as a negative control for (iii). Alveolar macrophages (M) show a faint brown tint, due to the presence of carbon, but not the strong brown staining of macrophages seen in (ii) and (iii).

4. Diskussion

Virale Oberflächenproteine stellen den Schlüssel des Virus zur Wirtszelle dar: Sie erkennen Rezeptoren auf der Oberfläche von Wirtszellen und vermitteln die Fusion der viralen Membran mit der Wirtszellmembran [Nagai und Klenk, 1977; de Haan *et al.*, 2004]. Viele virale Oberflächenproteine werden in einer inaktiven Form synthetisiert und anschließend durch Wirtszellproteasen durch Spaltung aktiviert [Nagai und Klenk, 1977; Stieneke-Gröber *et al.*, 1992; Hallenberger *et al.*, 1992, 1997; de Haan *et al.*, 2004; Chandran *et al.*, 2005; Böttcher *et al.*, 2006; Bertram *et al.*, 2010]. Alternativ kann die Spaltung viraler Oberflächenproteine durch zelluläre Proteasen zur Freisetzung löslicher Formen der Oberflächenproteine führen, die immunmodulatorische Wirkung ausüben oder als *antibody decoys* fungieren können [Dolnik *et al.*, 2004]. In der vorliegenden Arbeit wurde die Bedeutung von Wirtszellproteasen für die Aktivität des Oberflächenproteins, Spike (S), des SARS-CoV untersucht. Es konnte gezeigt werden, dass die Bindung von SARS-S an den zellulären Rezeptor ACE2 dessen Abspaltung durch die zelluläre Protease TACE/ADAM17 induziert [Haga *et al.*, 2008, 2010]. Die TACE-vermittelte Abspaltung von ACE2 könnte für die Herabregulierung der ACE2-Expression im Kontext der SARS-CoV-Infektion verantwortlich sein und wesentlich zur SARS-Entwicklung beitragen [Kuba *et al.*, 2005]. Weiterhin konnten Aminosäuresequenzen im SARS-S definiert werden, die bei der proteolytischen Aktivierung vom SARS-S eine Rolle spielen. Zudem konnte demonstriert werden, dass eine unbekannte Wirtszellprotease das SARS-S für die Zell-Zellfusion aktivieren kann. Schließlich wurde gezeigt, dass die zelluläre Protease TMPRSS2 auf wichtigen Zielzellen der SARS-CoV-Infektion exprimiert wird und das SARS-S für die Virus-Zell- und Zell-Zellfusion aktiviert. Diese Ergebnisse liefern wichtige Einblicke in die Interaktion von SARS-CoV mit Wirtszellen und definieren neue Ansatzpunkte für die antivirale Therapie.

Manuskript: Differential Downregulation of ACE2 by the Spike Proteins of Severe Acute Respiratory Syndrome Coronavirus and Human Coronavirus NL63

Das SARS-CoV ist ein hochpathogenes Virus, etwa 10% der Infizierten versterben an SARS [To und Lo, 2004]. Das humane Coronavirus-NL63 (HCoV-NL63) hingegen verursacht in den meisten Fällen nur eine Erkältung [van der Hoek *et al.*, 2007]. Beide Viren verwenden die Karboxypeptidase ACE2 als zellulären Rezeptor für den Eintritt in

Wirtszellen [Li *et al.*, 2003; Hofmann *et al.*, 2005]. Die Interaktion vom SARS-S mit ACE2 ist für die virale Ausbreitung im Wirt von zentraler Bedeutung, da ACE2-knockout Mäuse kaum permissiv für die SARS-CoV-Infektion sind [Kuba *et al.*, 2005] Zudem korreliert die ACE2-Expression in Zelllinien mit der Empfänglichkeit gegenüber dem SARS-S-getriebenen Zelleintritt [Li *et al.*, 2003; Nie *et al.*, 2004; Hofmann *et al.*, 2004a]. Die Interaktion von rekombinantem SARS-S induziert die Herabregulierung der ACE2-Expression [Kuba *et al.*, 2005] und dieser Prozess ist möglicherweise auf die Abspaltung von ACE2 durch die zelluläre Protease TACE/ADAM17 zurückzuführen [Haga *et al.*, 2008]. Die Expression von ACE2 schützt vor experimentell induzierter Lungenpathogenese [Imai *et al.*, 2005; Kuba *et al.*, 2005]. Es ist daher denkbar, dass die SARS-S-vermittelte Inhibition der ACE2-Expression die Entstehung von SARS fördert. Analog dazu könnte die geringe Pathogenität vom HCoV-NL63 auf eine im Vergleich zum SARS-CoV weniger effiziente Interaktion mit ACE2 zurückzuführen sein. Es sollte daher geklärt werden, ob das SARS-S und NL63-S mit unterschiedlicher Effizienz an ACE2 binden und die ACE2-Expression reduzieren. Im Kontext der ACE2-Herabregulierung sollte insbesondere die mögliche Rolle der Wirtszellprotease TACE/ADAM17 geklärt werden.

Zur Analyse der Effizienz der SARS-S- und NL63-S-Bindung an ACE2 benutzten wir die S1-Untereinheiten dieser Proteine, da sie die Rezeptorbindungsdomänen (RBD) tragen (SARS-S: Aminosäuren (AS) 13 -714; NL63-S AS 16-741) [Hofmann *et al.*, 2005; Li *et al.*, 2007; Mathewson *et al.*, 2008]. Dazu wurden die rekombinanten Proteine, gekoppelt an die Fc-Einheit des humanen Immunoglobulins, aufgereinigt und die Bindung an ACE2 überprüft. FACS- und ELISA-Analysen zeigten, dass das SARS-S effizienter an ACE2 bindet als das NL63-S. Diese Beobachtungen wurden in BIACore-Experimenten bestätigt. In Infektionsexperimenten mit SARS-S- bzw. NL63-S-Pseudotypen inhibierte schließlich rekombinantes SARS-S den Viruseintritt wirksamer als rekombinantes NL63-S. Diese Ergebnisse deuten auf eine effizientere ACE2-Bindung vom SARS-S im Vergleich zum NL63-S hin. Die unterschiedlich starke Bindung an ACE2 könnte darauf beruhen, dass das NL63-S und SARS-S mit unterschiedlichen Bindungsregionen im ACE2 interagieren [Hofmann *et al.*, 2006], die jedoch überlappen [Li *et al.*, 2007; Wu *et al.*, 2009]. Außerdem zeigten Kristallstrukturanalysen, dass die ACE2-Bindungsmotive im SARS-S und NL63-S keine strukturellen Gemeinsamkeiten aufweisen [Wu *et al.*, 2009].

Im nächsten Schritt wurde untersucht, ob sich die unterschiedliche ACE2-Bindungseffizienz vom SARS-S und NL63-S in einer unterschiedlichen ACE2-Herabregulierung widerspiegelt. Dazu wurden Vero E6-Zellen mit replikationsfähigem SARS-CoV und HCoV-NL63 infiziert und die ACE2-Expression per Immunoblot in

Zelllysaten analysiert. Als Replikationskontrolle wurde die Viruslast in den Überständen bestimmt. In SARS-CoV-infizierten Zellen wurde eine markante Abnahme der ACE2-Expression beobachtet, die mit der Menge an viraler RNS im Zellkulturüberstand bzw. der Expression des viralen Proteins Nsp8 in Zelllysaten korrelierte. Im Gegensatz dazu hatte die HCoV-NL63-Replikation keine Auswirkung auf die ACE2-Expression. Es ist daher denkbar, dass die relativ ineffiziente ACE2-Bindung von NL63-S nicht zur Herabregulierung der ACE2-Expression führt. Da das HCoV-NL63 jedoch weniger effizient replizierte als das SARS-CoV, konnte der Einfluss der beiden Viren auf die ACE2-Expression nicht direkt verglichen werden. Wahrscheinlich steht jedoch die relativ ineffiziente ACE2-Bindung von NL63-S im Vergleich zum SARS-S mit der ineffizienten viralen Ausbreitung und Herabregulierung der ACE2-Expression in Vero E6-Zellen in Zusammenhang. Es ist daher möglich, dass der Erwerb einer höheren ACE2-Bindungskapazität mit einer Zunahme der Pathogenität von HCoV-NL63-Varianten einhergeht. Die Möglichkeit diese Hypothese zu untersuchen, wäre die Konstruktion von chimären Viren und deren Analyse im Mausmodel. Für diese Studien könnten ein bereits etabliertes reverses genetisches System für HCoV-NL63 [Donaldson *et al.*, 2008] und ein Mausmodel für die SARS-Pathogenese [Roberts *et al.*, 2005] dienen.

Es ist bekannt, dass virale Oberflächenproteine mit ihrem zellulären Rezeptor während der Biogenese interagieren können und dies zur Verringerung der Rezeptorexpression an der Zelloberfläche führen kann [Hoxie *et al.*, 1986]. Beispielsweise erfolgt die CD4-Herabregulierung durch das HIV-1 Protein Env (*envelope*) [Lama, 2003]. Im späten Stadium der Infektion wird das Env-Protein synthetisiert, wobei es den Transport von neu gebildetem CD4 zur Zellmembran blockiert [Levesque *et al.*, 2004]. Um den Mechanismus der ACE2-Herabregulierung zu klären, wurde daher zunächst der Einfluss der Koexpression vom SARS-S, NL63-S, den SARS-CoV-Nichtstrukturproteinen und den Proteinen kodiert durch die SARS-CoV-ORFs (N, 3a, 3b, 6, 7a, 7b, 8a, 8b, 9b) auf die ACE2-Expression untersucht. Die acht akzessorischen Proteine des SARS-CoV [Marra *et al.*, 2003; Rota *et al.*, 2003] wurden zu den Analysen herangezogen, da das HCoV-NL63-Genom nur für ein akzessorisches Protein kodiert [van der Hoek *et al.*, 2004; Fouchier *et al.*, 2004]. Die zusätzlichen akzessorischen Proteine des SARS-CoV könnten somit als Pathogenitätsfaktor in Frage kommen. Es konnte gezeigt werden, dass nur die SARS-S-Expression die ACE2-Konzentration reduzierte. Es ist daher wahrscheinlich, dass auch in infizierten Zellen lediglich das SARS-S und kein anderes virales Protein mit der ACE2-Expression interferiert. Vorstellbar wäre, dass das SARS-S-Protein während

seiner Biogenese im konstitutiven sekretorischen Weg den Transport von ACE2 zur Zelloberfläche verhindert oder im Zellinneren die Degradierung von ACE2 herbeiführt. Kuba *et al.* demonstrierten, dass rekombinantes SARS-S mit der ACE2-Expression interferiert [Kuba *et al.*, 2005]. Zudem zeigten Haga *et al.*, dass die Bindung vom SARS-S an ACE2 die Abspaltung des Rezeptors durch die zelluläre Protease TACE/ADAM17 bewirkt [Lambert *et al.*, 2005; Haga *et al.*, 2008]. Deren Aktivität könnte wiederum für die Reduktion der ACE2-Oberflächenexpression verantwortlich sein. Wir haben zunächst untersucht, ob das SARS-S und NL63-S die ACE2-Abspaltung induzieren. Für diese Untersuchungen verwendeten wir Vero E6-Zellen, die endogenes ACE2 exprimieren, und *virus-like particles* (VLPs), die SARS-S oder NL63-S in ihrer Hülle tragen, aber nicht replikationsfähig sind. Die Behandlung von Vero E6-Zellen mit Phorbol-Myristat-Acetat (PMA) diente als Positivkontrolle, da Lambert *et al.* zeigten, dass PMA die Abspaltung von ACE2 über TACE/ADAM17 induziert [Lambert *et al.*, 2005; Jia *et al.*, 2009]. In Immunoblotanalysen von SARS-S-VLP- wie auch PMA-behandelten Vero E6-Zellen verzeichneten wir eine Zunahme der ACE2-Menge im Überstand. Dieser Effekt wurde nach Inkubation mit Kontroll-VLPs ohne Glycoprotein nicht beobachtet. Auch NL63-S-VLPs bewirkten die Abspaltung von ACE2, allerdings mit geringerer Effizienz als SARS-S-VLPs. Nur in PMA-behandelten Zellen kam es zu einer Reduktion der ACE2-Menge in Zelllysaten, was darauf hindeutet, dass das PMA die ACE2-Abspaltung deutlich effizienter induzierte als das SARS-S. Diese Ergebnisse wurden mit rekombinanten S-Proteinen bestätigt und zeigen, dass die ACE2-Bindung die Wirkkraft der ACE2-Herabregulierung durch das SARS-S und NL63-S widerspiegelt.

Um zu untersuchen, ob die ACE2-Abspaltung durch das SARS-S auf die Aktivität von TACE/ADAM17 zurückzuführen ist, bedienten wir uns des TACE-Inhibitors TAPI-0 [Black *et al.*, 1997, 2002]. Mit Hilfe eines publizierten FACS-basierenden Testsystems [Kuba *et al.*, 2005] konnten wir zeigen, dass lösliches SARS-S die ACE2-Expression auf der Zelloberfläche reduziert und, dass dieser Effekt nicht eintritt, wenn die Zellen mit TAPI-0 behandelt werden. Die von Kuba und Kollegen beschriebene Reduktion der ACE2-Expression durch lösliches SARS-S ist daher mit hoher Wahrscheinlichkeit auf die TACE/ADAM17-abhängige Abspaltung von ACE2 zurückzuführen. Die Bindung von NL63-S an Vero E6-Zellen wurde im Einklang mit der ineffizienten Bindung von NL63-S an rekombinantes ACE2 nicht beobachtet. Schlussfolgernd lässt sich sagen, dass die SARS-S-Interaktion mit ACE2 zur TACE/ADAM17-vermittelten ACE2-Abspaltung führt. Diese könnte möglicherweise für die reduzierte Oberflächenexpression von ACE2 in SARS-CoV-infizierten Zellen verantwortlich sein.

Haga *et al.* postulierten, dass die SARS-S-induzierte ACE2-Abspaltung durch TACE/ADAM17 für den viralen Eintritt vom SARS-CoV in Zielzellen wichtig ist [Haga *et al.*, 2008]. Allerdings wurde ein experimentelles System gewählt, das nicht zwischen infektiösem und nicht-infektiösem Zelleintritt unterscheidet. Um die Bedeutung der ACE2-Abspaltung für den SARS-S-getriebenen Eintritt zu untersuchen, wurden ACE2-exprimierende Zellen mit TAPI-0 vorinkubiert und mit SARS-S- bzw. NL63-S-Pseudotypen infiziert. Ein ähnlicher Versuchsaufbau wurde auch mit replikationsfähigen Viren durchgeführt. Die Behandlung von Zielzellen mit TAPI-0 hatte weder Einfluss auf die Transduktion mit Pseudotypen noch auf die Replikation vom SARS-CoV und HCoV-NL63. Diese Ergebnisse deuten daraufhin, dass die S-induzierte ACE2-Abspaltung für die Replikation beider Viren nicht notwendig ist. Aktuelle Beobachtungen von Haga und Kollegen zeigen allerdings, dass die Blockierung von TACE/ADAM17 in Zellkultur und in infizierten Mäusen den Eintritt vom SARS-CoV leicht inhibiert [Haga *et al.*, 2010]. Es ist jedoch unklar, ob der virale Eintritt im Einklang mit der viralen Replikation steht. Beispielsweise erfolgt die Internalisierung von HIV-1 in HeLa-Zellen, jedoch resultiert die Aufnahme des Virus nicht in einer produktiven Infektion [Maréchal *et al.*, 1998].

Zusammenfassend haben die Untersuchungen gezeigt, dass das SARS-S effizienter an ACE2 bindet als NL63-S und die stärkere ACE2-Bindung mit einer höheren Induktion der ACE2-Abspaltung einhergeht. Zudem ist die reduzierte ACE2-Expression in SARS-CoV-infizierten Zellen wahrscheinlich auf eine TACE/ADAM17-vermittelte ACE2-Abspaltung zurückzuführen, wobei auch die intrazelluläre Interaktion vom SARS-S mit ACE2 eine Rolle spielen könnte. Die ACE2-Abspaltung ist für den viralen Eintritt und die virale Vermehrung wahrscheinlich nicht essentiell, eine moderate Reduktion des SARS-CoV-Eintritts durch TACE-Inhibitoren ist jedoch möglich. Das abgespaltene ACE2 könnte mit dem S-Protein austretender Viren interagieren und somit vor einer Reinfektion schützen. Diese Vermutung wird durch die Beobachtung gestützt, dass lösliches ACE2 den SARS-S-getriebenen Eintritt blockiert [Hofmann *et al.*, 2004].

Manuskript: Different host cell proteases activate the SARS-coronavirus spike-protein for cell-cell and virus-cell fusion

Virale Glykoproteine werden posttranslational für die Fusion mit der Wirtszellmembran aktiviert [Nagai und Klenk, 1977; de Haan *et al.*, 2004]. Die Spaltung kann dabei in verschiedenen zellulären Kompartimenten bzw. zu verschiedenen Stadien des viralen

Vermehrungszyklus ablaufen. Die proteolytische Spaltung von Coronavirus Spike-Proteinen durch Wirtszellproteasen ist essentiell für die Spike-Proteinaktivierung [Gallagher und Buchmeier, 2001]. Die Spike-Proteine bestimmter Maus-Hepatitis-Viren (MHV) werden im konstitutiven sekretorischen Weg infizierter Zellen durch Furin gespalten [de Haan *et al.*, 2004]. Diese Viren tragen somit ein aktiviertes Spike-Protein und die Interaktion des Spike-Proteins mit den Rezeptor ist ausreichend, um die Spike-Protein-getriebene Fusion der viralen Membran mit der Plasmamembran auszulösen [de Haan *et al.*, 2004; Nash und Buchmeier, 1997]. Im Gegensatz dazu wird das S-Protein des MHV Typ 2-Stammes in infizierten Zellen nicht gespalten. Diese Viren müssen zunächst in Endosomen von Wirtszellen aufgenommen werden, wo sie durch Proteasen der Cathepsinfamilie aktiviert werden [Qiu *et al.*, 2006]. Auch das SARS-Spike-Protein wird durch Cathepsine aktiviert [Simmons *et al.*, 2005], jedoch sind die Spaltstellen im SARS-S nicht klar definiert.

Das S-Protein beinhaltet mehrere Aminosäuremotive, die durch Wirtszellproteasen gespalten werden könnten [Follis *et al.*, 2006; Belouzard *et al.*, 2009; Kam *et al.*, 2009]. Das Arginin 667 (R667) im SARS-S-Protein scheint für die Aktivierung der SARS-S-getriebene Zell-Zell- und Virus-Zellfusion durch exogenes Trypsin essentiell zu sein [Bergeron *et al.*, 2005; Follis *et al.*, 2006; Belouzard *et al.*, 2009]. Es ist allerdings unklar, ob dieses Spaltmotiv auch für die SARS-S-Aktivierung durch Cathepsin L nötig ist. Studien zeigten zudem, dass die Position R797 im Spike-Protein eine zweite Spaltstelle darstellen könnte [Folis *et al.*, 2006; Belouzard *et al.*, 2009]. Ähnlich zu R667 ist R797 in der SARS-S-Aktivierung für die Membranfusion durch exogenes Trypsin von Bedeutung [Belouzard *et al.*, 2009]. Weiterhin wurden die Aminosäuren K672 [Bergeron *et al.*, 2005; Follis *et al.*, 2006] und T678 [Bosch *et al.*, 2008] als Spaltstellen diskutiert, wobei die Bedeutung dieser Aminosäuren für die SARS-S-Aktivierung noch unbekannt ist. Schließlich beinhaltet das SARS-S die Aminosäuresequenz 758-RNTR-761, die in Peptidform durch Furin gespalten wird [Bergeron *et al.*, 2005]. Auch die Relevanz dieser Sequenz für die Aktivierung vom SARS-S ist unklar.

Es wurde untersucht, welche Bedeutung die Aminosäuren R667 und K672 für die proteolytische Aktivierung vom SARS-S haben. In Immunoblotanalysen war die Prozessierung des S-Proteins nur von der Aminosäure R667, aber nicht von K672, abhängig. Die Mutation dieser Aminosäuren (R667A, K672L) hatte kaum Auswirkung auf den Zelleintritt von SARS-S-Pseudotypen. Somit ist es wahrscheinlich, dass die Aminosäuren R667 und K672 für die Aktivierung vom SARS-CoV verzichtbar sind. Die Behandlung von zellfreien SARS-S-Pseudotypen mit Trypsin reduziert die virale Infektiosität [Simmons *et al.*, 2004, 2005]. Es wurde daher untersucht, ob die

Mutationen R667A und K672L die Inaktivierung von SARS-S-Pseudotypen durch Trypsin beeinflussen. Die Mutation K672L hatte keine Auswirkung auf die Inaktivierung durch Trypsin. Im Gegensatz dazu war die SARS-S R667A-Mutante in Übereinstimmung mit publizierten Daten [Follis *et al.*, 2006; Belouzard *et al.*, 2009] resistent gegenüber der Inaktivierung durch Trypsin und durch andere Proteasen wie Plasmin, Faktor Xa und Thrombin. Diese Ergebnisse zeigen, dass die Aminosäure R667 effizient durch unterschiedliche Proteasen erkannt werden kann und, dass die Spaltung vom SARS-S an dieser Position die Infektiosität von zellfreien Viren vermindert. Eine Ursache dafür könnte die vorzeitige Auslösung der Fusionsaktivität des S-Proteins sein. Alternativ könnte die Prozessierung eine Konformationsänderung des S-Proteins auslösen, die mit der Bindung an ACE2 oder der nachfolgenden Fusion mit der Wirtszellmembran nicht kompatibel ist.

Die Aktivierung vom SARS-S durch die Protease Cathepsin L, die nur im sauren Milieu endo- bzw. lysosomaler Vesikel aktiv ist, ist für den SARS-S-vermittelten Zelleintritt essentiell. Daher wird der SARS-S-getriebene Zelleintritt durch lysosomotrope Agenzien wie Ammoniumchlorid blockiert, die den pH-Wert in endo- und lysosomalen Vesikeln erhöhen [Yang *et al.*, 2004; Hofmann *et al.*, 2004b; Simmons *et al.*, 2004]. Trypsin ist in der Lage zellgebundene Viren für den SARS-S-getriebenen Eintritt in Ammoniumchlorid-behandelte Zellen zu aktivieren, indem es die Wirkung von Cathepsin L substituiert [Simmons *et al.*, 2004]. Es wurde daher untersucht, ob die Spaltstelle R667 im SARS-S für den Trypsin-induzierten, SARS-S-getriebenen Eintritt in Ammoniumchlorid-behandelte Zellen wichtig ist. Im Einklang mit publizierten Daten konnte demonstriert werden, dass R667 nicht nur für die Trypsininaktivierung von zellfreien [Follis *et al.*, 2006; Belouzard *et al.*, 2009], sondern auch für die Trypsinaktivierung von zellgebundenen Viren essentiell ist.

Die bis dahin erhobenen Daten belegten, dass R667 für die Spaltung vom SARS-S durch Trypsin wichtig ist. Die Ergebnisse lieferten jedoch keine Information über die Bedeutung dieser Aminosäure für die SARS-S-Aktivierung durch Cathepsin L. Um diese Frage zu beantworten, wurde ein Virus-Virus-Membranfusionsexperiment durchgeführt, bei dem die Fusion von Pseudotypen, die neben dem SARS-S auch das Hüllprotein des aviären Leukosevirus-A (EnvA) tragen, mit Viren gemessen wird, die ACE2 auf ihrer Oberfläche tragen. Die Quantifizierung der Fusionsaktivität erfolgt über ein Reportergen, das im Genom der ACE2-tragenden Viren inseriert wurde. Dieses wird nur nach Virus-Virusfusion und nachfolgender Infektion von Zellen, die den EnvA-Rezeptor T_vA auf ihrer Oberfläche tragen, abgelesen. Damit ein Einfluss von Wirtszellproteasen in diesem System ausgeschlossen werden kann, wurden die Zielzellen vor der Infektion mit dem Proteaseinhibitor Leupeptin behandelt. Schließlich

ist hervorzuheben, dass Zielzellen gewählt wurden, die für den SARS-S-vermittelten Zelleintritt nicht permissiv sind und somit Infektionsereignisse die vorangegangene Virus-Virusfusion voraussetzen [Simmons *et al.*, 2005]. Der wesentliche Vorteil dieses experimentellen Systems ist, dass die SARS-S-Interaktion mit ACE2, die proteolytische Aktivierung vom SARS-S und die nachfolgende Membranfusion unter zellfreien Bedingungen analysiert werden können. Interessanterweise war in diesem System die Aminosäure R667 für die Aktivierung vom SARS-S durch sowohl Trypsin als auch Cathepsin L verzichtbar. Gründe für diese Beobachtung könnten auf den unterschiedlichen Eigenschaften wie etwa Rezeptorkonzentration oder Proteaseexpression von Wirtszellmembranen und viraler Membranen beruhen. Die Beobachtung, dass R667 möglicherweise für die Aktivierung vom SARS-CoV nicht nötig ist, würde schließlich publizierte Daten stützen, in denen die Spaltstelle für Cathepsin L an Position T678 im SARS-S kartiert wurde [Bosch *et al.*, 2008].

Im nächsten Teil dieser Arbeit wurde untersucht, ob die Sequenz 758-RNTR-761 für die Aktivierung vom SARS-S wichtig ist, da gezeigt wurde, dass ein Peptid mit diesem Motiv durch Furin gespalten wird [Bergeron *et al.*, 2005]. Hinweise zur Bedeutung der proteolytischen Aktivierung vom SARS-S an dieser Stelle wurden jedoch nicht erbracht. Es ist daher denkbar, dass das 758-RNTR-761 Motiv im SARS-S nur ineffizient durch Furin gespalten wird, die Spaltung aber für die Aktivierung vom SARS-S wichtig ist. Zur Überprüfung dieser Hypothese wurde die potentielle Spaltstelle durch den Austausch T670R optimiert und die resultierende SARS-S-Variante funktionell charakterisiert. Die Mutation hatte keinen Einfluss auf die SARS-S-Expression, sie erhöhte jedoch die Effizienz der SARS-S-getriebenen Virus-Zell- und Zell-Zellfusion. Ähnliche Effekte wurden auch nach Furinüberexpression beobachtet. Diese Beobachtungen weisen auf einen Beitrag des 758-RNTR-761 Motivs zur SARS-S-Aktivierung hin. Zudem deuten die Ergebnisse an, dass die Expression von Furin in infizierten Zellen bei der SARS-S-Aktivierung eine Rolle spielen könnte. Weder die Anwesenheit des 758-RNTR-761 Motivs noch die Überexpression von Furin führte jedoch zu detektierbarer SARS-S-Spaltung. Somit ist es möglich, dass Furin bzw. 758-RNTR-761 nur indirekt an der SARS-S-Spaltung beteiligt sind. Außerdem ist es denkbar, dass der Austausch T760R die Proteasesensitivität anderer Positionen im SARS-S und damit die SARS-S-Aktivität erhöht.

Zell-Zellfusionsexperimente werden zur Analyse der potentiellen Spaltstellen im SARS-S genutzt [Simmons *et al.*, 2003; Belouzard *et al.*, 2009; Follis *et al.*, 2006; Hofmann *et al.*, 2006]. In den meisten Studien wurde die Aktivierung des Spike-Proteins für die Zell-Zellfusion durch exogenes Trypsin beobachtet. Bisher wurde noch nicht untersucht, ob auch eine Wirtszellprotease das SARS-S für die Zell-Zellfusion

aktivieren kann. Unsere Beobachtungen zeigen, dass die SARS-S-Aktivierung durch Trypsin für die Fusion mit den Zielzellen nur bei geringer Expression des Rezeptors ACE2 nötig ist und, dass die Fusion bei hoher ACE2-Konzentration Trypsin-unabhängig verläuft. Somit erfolgt die Membranfusion bei hoher ACE2-Expression in der Abwesenheit von Trypsin und könnte daher auf der SARS-S-Aktivierung durch eine Wirtszellprotease beruhen.

In der Literatur ist eine wichtige Rolle von Cathepsin L bei der Aktivierung vom SARS-S für die Virus-Zellfusion dokumentiert. Ob diese Protease das SARS-S auch für die Zell-Zellfusion aktiviert, ist jedoch unbekannt. Die Behandlung von Zielzellen mit einem Cathepsin L-Inhibitor reduzierte die Virus-Zellfusion markant, hatte jedoch keinen Einfluss auf die Zell-Zellfusion. Daher wurde die Bedeutung anderer Wirtszellproteasen für die SARS-S-getriebene Zell-Zellfusion überprüft. Für diese Studien wurden Inhibitoren wie Leupeptin (Inhibitor für Cystein- und Serinproteasen), AEBSF (Inhibitor für Serinproteasen), E64c und MDL 28170 (Inhibitoren für Cathepsine) eingesetzt. Von diesen Inhibitoren hatte nur Leupeptin eine inhibierende Wirkung auf die SARS-S-getriebene Zell-Zellfusion. Diese Ergebnisse zeigen, dass das SARS-S von einer bisher unbekannten Cystein- oder Serinprotease für die Zell-Zellfusion aktiviert wird, während die Virus-Zellfusion die Aktivität von Cathepsin L benötigt. Du und Mitarbeiter zeigten, dass Faktor Xa, eine Serinprotease, eine Rolle in der SARS-CoV-Infektiosität und der SARS-S-Spaltung spielen könnte [Du *et al.*, 2007]. Zudem gibt es Hinweise, dass Typ II Transmembran-Serinproteasen das Influenza Hämagglutinin durch Spaltung aktivieren.

Zusammenfassend und im Einklang mit dem postulierten Modell zweier Aktivierungsstellen [Belouzard *et al.*, 2009] zeigen auch unsere Ergebnisse, dass zwei Schnittstellen im SARS-S für die proteolytischen Aktivierung nötig sein könnten. Der stromaufwärts im SARS-S-liegende Spaltbereich könnte die Aminosäuren 657 bis 676 umfassen. Zudem führen unsere Beobachtungen zu der Hypothese, dass zusätzlich zum R797 Motiv eine alternative stromabwärtsliegende Spaltstelle (Aminosäuren 758-761) bestehen könnte, wobei die Interaktion dieser beiden Spaltbereiche noch aufgeklärt werden muss.

Manuskript: Evidence that TMPRSS2 activates the SARS-coronavirus spike-protein for membrane fusion and reduces viral control by the humoral immune response

Ein Merkmal viraler Klasse I Fusionsproteine ist die Spaltung durch Wirtszellproteasen während der Biogenese im konstitutiven sekretorischen Weg infizierter Zellen [Kielian und Rey, 2006]. Die Proteolyse erlaubt den Übergang der Fusionsproteine in einen aktivierten, metastabilen Zustand, der für die Fusion mit der Wirtszellmembran essentiell ist [Nagai und Klenk, 1977; de Haan *et al.*, 2004; Matsuyama und Taguchi, 2009]. Ausnahmen bilden die Oberflächenproteine des SARS-CoV und des Ebola Virus, die während des viralen Eintritts in Zielzellen durch endosomale Proteasen, Cathepsin B und L, aktiviert werden [Simmons *et al.*, 2005; Chandran *et al.*, 2005]. Ob das SARS-S auch in produktiv infizierten Zellen durch Wirtszellproteasen gespalten wird und, ob eine mögliche Spaltung für die SARS-S-Funktion wichtig ist, ist jedoch unklar. Typ II Transmembran-Serinproteasen (TTSPs) wie TMPRSS2 oder TMPRSS4 können das Influenza Virus Hämagglyutinin durch Spaltung aktivieren [Böttcher *et al.*, 2006; Chaipan *et al.*, 2009; Bertram *et al.*, 2010]. TMPRSS2 wird in humanen Epithelzellen der Lunge exprimiert und könnte bei der Ausbreitung von Influenza Viren im infizierten Wirt eine wichtige Rolle spielen [Paoloni-Giacobino *et al.*, 1997; Donaldson *et al.*, 2002; Bertram *et al.*, 2010]. Zusätzlich wurde gezeigt, dass TMPRSS11a, eine weitere TTSP, rekombinantes SARS-S spaltet [Kam *et al.*, 2009]. Ob Spaltung von zellulärem oder Virus-assoziiertem SARS-S durch TMPRSS11a erfolgt, wurde jedoch nicht untersucht. Da die Lunge, analog zum Influenza Virus, auch für das SARS-CoV das wichtigste Zielorgan darstellt, sollte im Folgenden untersucht werden, ob TMPRSS2 und verwandte TTSPs das SARS-S spalten und den SARS-S-getriebenen Zelleintritt beeinflussen.

Die Analyse der Spaltung von Zell- und Virus-assoziiertem SARS-S ergab, dass das SARS-S durch koexprimierte TMPRSS2 jedoch nicht durch TMPRSS4 in mehrere Fragmente (150, 110, 85, 55 und 45 kDa) gespalten wird. Im Gegensatz dazu wurde das SARS-S im Einklang mit publizierten Daten [Yao *et al.*, 2004; Bergeron *et al.*, 2005; Matsuyama *et al.*, 2005; Belouzard *et al.*, 2009] durch Trypsinbehandlung in zwei Fragmente, die Untereinheiten S1 und S2, gespalten. Die Spaltstellen für Trypsin im SARS-S-Protein liegen an Position R667 [Bergeron *et al.*, 2005; Follis *et al.*, 2006; Belouzard *et al.*, 2009] und vermutlich an Position R797 [Watanabe *et al.*, 2008; Belouzard *et al.*, 2009]. Erstere Schnittstelle liegt in der C-terminalen Region der S1-Untereinheit und Letztere in der N-terminalen Region der S2-Untereinheit. Mit Hilfe von Antikörpern, die verschiedene Abschnitte im SARS-S-Protein erkennen, konnte eine Schnittstelle von TMPRSS2 auf die Aminosäuren 1152-1200 eingeschränkt werden. Die entsprechende Spaltung ist für die Generierung des 150 kDa Fragments verantwortlich.

Als nächstes wurde untersucht, ob die Spaltung vom SARS-S durch TMPRSS2 in Virus-produzierenden Zellen das S-Protein aktiviert und daher den Eintritt in Zielzellen ermöglicht, die mit einem Cathepsininhibitor behandelt wurden. Dazu wurden die Zielzellen mit dem Cathepsininhibitor MDL 28170 vorinkubiert und nachfolgend mit SARS-S-Pseudotypen infiziert. Die inhibierende Wirkung von MDL 28170 auf die Infektion durch SARS-S-Pseudotypen wurde jedoch durch die Spaltung vom SARS-S durch TMPRSS2 nicht aufgehoben. Die Koexpression des SARS-S und TMPRSS2 führt also nicht zur SARS-S-Aktivierung.

Im nächsten Schritt wurde die Auswirkung der SARS-S-Spaltung durch TMPRSS2 auf die Neutralisierung durch Antikörper untersucht. Dazu wurden SARS-S-Pseudotypen in TMPRSS2-positiven und -negativen Zellen generiert und vor der Infektion von Zielzellen mit Seren inkubiert, die nach der Immunisierung von Mäusen mit löslichem S-Protein erhalten wurden. Viren, die in TMPRSS2-negativen Zellen generiert wurden, wurden effizient durch die Maus-Seren gehemmt. Während Viren, die in TMPRSS2-positiven Zellen produziert wurden, nach Inkubation mit den Seren kaum an Infektiosität verloren. Die Spaltung des SARS-S durch TMPRSS2 scheint daher den Angriff von neutralisierenden Antikörpern zu erschweren.

Die Spaltung des Ebola Virus Glykoproteins durch TACE/ADAM17 führt zur Bildung einer löslichen Form des Glykoproteins, die mit der Virusneutralisierung durch Antikörper interferiert [Dolnik *et al.*, 2004]. Es wurde daher untersucht, ob die SARS-S-Spaltung durch TMPRSS2 zur Bildung von löslichem SARS-S führt. In der Tat zeigte die Analyse von Zellkulturüberständen nach Ultrazentrifugation, dass TMPRSS2 die Abgabe von löslichem SARS-S in den Zellkulturüberstand induziert. Um die Bedeutung des löslichen SARS-S für die Neutralisationseffizienz zu bestimmen, wurden SARS-Pseudotypen, generiert in TMPRSS2-positiven und -negativen Zellen generiert, durch ein 20%-iges Sukrosekissen zentrifugiert. Somit wurde lösliches SARS-S aus der Virus-Präparation entfernt. Unter diesen Bedingungen zeigten beide Viren nach Inkubation mit Antiseren eine deutlich abfallende Infektiosität. Diese Beobachtung zeigt, dass lösliches SARS-S, erzeugt durch die Koexpression von TMPRSS2, Resistenz gegenüber der Neutralisierung mit Antikörpern vermittelt. Um diese Hypothese zu untermauern, wurde lösliches S-Protein durch TMPRSS2-Spaltung erzeugt, ankonzentriert und in Neutralisationsexperimenten untersucht. Nach der Zugabe von löslichem SARS-S zu SARS-S-Pseudotypen, die in der An- und Abwesenheit von TMPRSS2 generiert und anschließend durch ein Sukrosekissen pelletiert wurden, wiesen beide Viren Resistenz gegen die Antikörper-vermittelte Neutralisation auf. Diese Ergebnisse belegen, dass eines oder mehrere der nach SARS-S-Spaltung durch TMPRSS2 generierten Fragmente als Antikörper-decoy

fungiert/fungieren. Ein wichtiger Kandidat ist das 150 kDa-Produkt, da es die Rezeptor-Bindungsdomäne trägt, die das Hauptziel neutralisierenden Antikörper darstellt [He *et al.*, 2004a, b, 2005]. Die humorale Immunantwort ist wesentlich an der Kontrolle der SARS-CoV-Infektion beteiligt [Chen *et al.*, 2004; Yang *et al.*, 2004b; Hofmann *et al.*, 2004b]. Eine verringerte Antikörpererkennung vom SARS-CoV durch TMPRSS2-vermittelte Bildung von löslichem SARS-S könnte die virale Ausbreitung und damit die Entwicklung von SARS in infizierten Patienten begünstigen. Allerdings muss vor einer Aussage zur biologischen Relevanz dieses Prozesses geprüft werden, ob das SARS-S auch durch TMPRSS2 in infizierten Zellen gespalten wird. Neue Daten weisen darauf hin, dass die Spaltung in infizierten Zellen sehr ineffizient ist oder nicht stattfindet [Matsuyama *et al.*, 2010]. Es ist möglich, dass die in dieser Arbeit erhaltenen Ergebnisse auf TMPRSS2-Überexpression bzw. auf einen veränderten intrazellulären Transport des SARS-S in transfizierten relativ zu infizierten Zellen zurückzuführen sind. Allerdings ist ebenfalls unklar, ob die von Matsuyama und Kollegen verwendete Zelllinie ein adäquates Modell für die Expression und den intrazellulären Transport von TMPRSS2 und des SARS-S in Typ II Pneumozyten, den wichtigsten SARS-CoV-Zielzellen, darstellt. Um die biologische Relevanz dieser Vermutung zu veranschaulichen, konnte gezeigt werden, dass Typ II Pneumozyten ACE2 und TMPRSS2 koexprimieren.

Die Aktivierung des Influenza Virus Hämagglutinins durch TTSPs kann während der Biogenese von HA im konstitutiven sekretorischen Weg infizierter Zellen, im extrazellulären Raum [Kido *et al.*, 1992; Murakami *et al.*, 2001; Kido *et al.*, 2007] oder während des viralen Eintritts in Zielzellen erfolgen [Böttcher-Friebertshäuser *et al.*, 2010]. Wir haben daher untersucht, ob das SARS-S durch TMPRSS2 nur nach Koexpression gespalten wird (*cis*-Spaltung) oder, ob Spaltung auch erfolgt, wenn das SARS-S und TMPRSS2 auf benachbarten Zellen exprimiert werden (*trans*-Spaltung). Nach Kokultivierung von SARS-S- und TMPRSS2-exprimierenden Zellen wurde SARS-S-Spaltung beobachtet, wobei Fragmente von 150 und 110 kDa entstehen, die vermutlich durch Spaltstellen in der S1- und S2-Untereinheiten hervorgerufen werden. Um die Bedeutung der *trans*-Spaltung vom SARS-S durch TMPRSS2 für die SARS-S-Funktion zu analysieren, wurden Zell-Zellfusionsstudien durchgeführt [Xiao *et al.*, 2003; Simmons *et al.*, 2004]. Diese zeigten, dass TMPRSS2 durch *trans*-Spaltung in der Lage ist das S-Protein für die Zell-Zellfusion zu aktivieren. Entgegen den Erwartungen wurde SARS-S auch durch TMPRSS4 für die Zell-Zellfusion aktiviert, trotz nicht detektierbarer SARS-S-Spaltung durch diese Protease. Grund für diesen Effekt könnte eine ineffiziente aber funktionell wichtige *trans*-Spaltung vom SARS-S durch TMPRSS4

sein. Alternativ könnte TMPRSS4 die ACE2-Expression oder -Membranlokalisierung verändern.

Die Beobachtung, dass das SARS-S durch TMPRSS2 für die Zell-Zellfusion in trans aktiviert wird, legte die Vermutung nahe, dass das SARS-S durch TMPRSS2 auch für die Virus-Zellfusion aktiviert werden könnte. Die Expression von TMPRSS2 auf Zielzellen, die mit einem Cathepsininhibitor behandelt wurden, erlaubte den effizienten SARS-S-getriebenen Eintritt. Dies weist darauf hin, dass das SARS-S in TMPRSS2-exprimierenden Zellen während oder kurz nach dem Zelleintritt aktiviert wird und eine nachfolgende Spaltung vom SARS-S durch Cathepsine für den infektiösen Eintritt verzichtbar wird. Die Expression von TMPRSS4 hatte dagegen keine Auswirkung auf die Inhibition von SARS-S-Pseudotypen durch Cathepsininhibitoren. Diese Beobachtungen deuten darauf hin, dass Cathepsininhibitoren möglicherweise nicht in der Lage sind die Virusausbreitung in infizierten Patienten effizient zu unterdrücken. Die Expression von TMPRSS4 erlaubte dagegen nicht den Cathepsin-unabhängigen Zelleintritt. Da wahrscheinlich bei der Virus-Zellfusion im Vergleich zur Zell-Zellfusion deutlich kleinere Oberflächen interagieren und unter diesen Umständen eine Aktivierung vom SARS-S durch TMPRSS4 nicht erfolgen kann. Zusammenfassend deuten diese Beobachtungen auf eine Aktivierung des SARS-S durch TMPRSS2 in der frühen Phase des Zelleintritts hin, welche die Cathepsin L-induzierte SARS-S-Spaltung verzichtbar macht. Diese Vermutung wird durch die Beobachtungen gestützt, dass TMPRSS2 sein Substrat an der Zelloberfläche oder im Zellinneren in Vesikeln spaltet [Lucas *et al.*, 2008; Böttcher-Friebertshäuser *et al.*, 2010]. Da jedoch der größte SARS-S-Anteil in infizierten Zellen im ERGIC zurückgehalten wird [McBride *et al.*, 2007; Stertz *et al.*, 2007; Voss *et al.*, 2009], könnte das Spike-Protein für TMPRSS2 unzugänglich sein. Eine aktuelle Studie zeigt, dass TMPRSS2 vermutlich nicht in der Lage ist das Spike-Protein in *cis* und somit an der Zellmembran zu spalten [Matsuyama *et al.*, 2010]. Dennoch zeigen zwei Publikationen den Transport des Spike-Proteins in infizierten Zellen zur Zelloberfläche [Ohnishi *et al.*, 2005; Voss *et al.*, 2009], wo *cis*- und *trans*-Spaltung durch TMPRSS2 erfolgen könnte. Zudem ist die Abspaltung vom SARS-S in Typ II Pneumozyten denkbar, welche im Vergleich zu den verwendeten Zelllinien von Matsuyama und Kollegen TMPRSS2 in höheren Mengen exprimieren könnten. TMPRSS2 könnte daher die Ausbreitung vom SARS-CoV in infizierten Personen über unterschiedliche Mechanismen fördern: Die Expression von TMPRSS2 auf Zielzellen vermittelt die SARS-S-Aktivierung, während die Koexpression von TMPRSS2 und des SARS-S in infizierten Zellen die Produktion von löslichem SARS-S induzieren könnte, welches die Kontrolle vom SARS-CoV durch die humorale Immunantwort erschweren könnte. Zur weiteren Untersuchung der Bedeutung von

TMPRSS2 für die SARS-CoV-Vermehrung und -Pathogenese wären *tmprss2-knockout* Mäuse [Kim et al., 2006] von großem Nutzen.

5. Literaturverzeichnis

- A multicentre collaboration to investigate the cause of severe acute respiratory syndrome.** (2003) World Health Organization Multicentre Collaborative Network for Severe Acute Respiratory Syndrome Diagnosis. *Lancet* **361**:1730-1733
- Anderson ED, Molloy SS, Jean F, Fei H, Shimamura S, Thomas G.** (2002) The ordered and compartment-specific autoproteolytic removal of the furin intramolecular chaperone is required for enzyme activation. *J Biol Chem* **277**:12879–12890
- Babcock GJ, Esshaki DJ, Thomas WD Jr, Ambrosino DM.** (2004) Amino acids 270 to 510 of the severe acute respiratory syndrome coronavirus spike protein are required for interaction with receptor. *J Virol* **78**:4552–4560
- Backovic M, Jardetzky TS.** (2009) Class III viral membrane fusion proteins. *Curr Opin Struct Biol* **19**(2):189-196
- Baer GS, Ebert DH, Chung CJ, Erickson AH, Dermody TS.** (1999) Mutant cells selected during persistent reovirus infection do not express mature cathepsin L and do not support reovirus disassembly. *J Virol* **73**(11):9532-43
- Baker KA, Dutch RE, Lamb RA and Jardetzky TS.** (1999) Structural basis for paramyxovirus-mediated membrane fusion. *Mol Cell* **3**:309-319
- Barr PJ.** (1991) Mammalian subtilisins: the long-sought dibasic processing endoproteases. *Cell* **66**(1):1-3
- Barrett AJ.** (1994) Classification of peptidases. *Methods Enzymol* **244**:1-15
- Belouzard S, Chu VC, Whittaker GR.** (2009) Activation of the SARS coronavirus spike protein via sequential proteolytic cleavage at two distinct sites. *Proc Natl Acad Sci U S A* **106**(14):5871-5876
- Beniac DR, deVarennes SL, Andonov A, He R, Booth TF.** (2007) Conformational reorganization of the SARS coronavirus spike following receptor binding: implications for membrane fusion. *PLoS One* **2**(10):e1082
- Bergeron E, Vincent MJ, Wickham L, Hamelin J, Basak A, Nichol ST, Chrétien M, Seidah NG.** (2005) Implication of proprotein convertases in the processing and spread of severe acute respiratory syndrome coronavirus. *Biochem Biophys Res Commun.* **326**(3):554-563.
- Bertram S, Glowacka I, Steffen I, Kühl A, Pöhlmann S.** (2010) Novel insights into proteolytic cleavage of influenza virus hemagglutinin. *Rev Med Virol* **20**(5):298-310.
- Bertram S, Glowacka I, Blazejewska P, Soilleux E, Allen P, Danisch S, Steffen I, Choi SY, Park Y, Schneider H, Schughart K, Pöhlmann S.** (2010) TMPRSS2 and TMPRSS4

- facilitate trypsin-independent spread of influenza virus in Caco-2 cells. *J Virol* **84**(19):10016-10025
- Black RA, Rauch CT, Kozlosky CJ, Peschon JJ, Slack JL, Wolfson MF, Castner BJ, Stocking KL, Reddy P, Srinivasan S, Nelson N, Boiani N, Schooley KA, Gerhart M, Davis R, Fitzner JN, Johnson RS, Paxton RJ, March CJ, Cerretti DP.** (1997) A metalloproteinase disintegrin that releases tumour-necrosis factor-alpha from cells. *Nature* **385**(6618):729-733
- Black RA** (2002). "Tumor necrosis factor-alpha converting enzyme.". *Int J Biochem Cell Biol* **34**(1):1–5
- Böttcher E, Matrosovich T, Beyerle M, Klenk HD, Garten W, and Matrosovich M.** (2006) Proteolytic activation of influenza viruses by serine proteases TMPRSS2 and HAT from human airway epithelium. *J Virol* **80**:9896–9898
- Böttcher-Friebertshäuser E, Freuer C, Sielaff F, Schmidt S, Eickmann M, Uhlendorff J, Steinmetzer T, Klenk HD, Garten W.** (2010) Cleavage of influenza virus hemagglutinin by airway proteases TMPRSS2 and HAT differs in subcellular localization and susceptibility to protease inhibitors. *J Virol* **84**(11):5605-5614
- Bosch BJ, van der Zee R, de Haan CA, Rottier PJ.** (2003) The coronavirus spike protein is a class I virus fusion protein: structurall and functional characterization of the fusion core complexe. *J Virol* **77**:8801-8811
- Bosch BJ, Bartelink W, Rottier PJ.** (2008) Cathepsin L functionally cleaves the severe acute respiratory syndrome coronavirus class I fusion protein upstream of rather than adjacent to the fusion peptide. *J Virol* **82**:8887–8890
- Bosch FX, Garten W, Klenk HD, Rott R.** (1981) Proteolytic cleavage of influenza virus hemagglutinins: primary structure of the connecting peptide between HA1 and HA2 determines proteolytic cleavability and pathogenicity of Avian influenza viruses. *Virology* **113**(2):725-735.
- Carstens EB.** (2010) Ratification vote on taxonomie proposal to the International Committee on Taxonomy of Viruses (2009). *Arch Virol* **155**:133-146
- Cavanagh D.** (1997) Nidovirales: a new order comprising Coronaviridae and Arteriviridae. *Arch Virol* **142**:629–633
- Chaipan C, Kobasa D, Bertram S, Glowacka I, Steffen I, Tsegaye TS, Takeda M, Bugge TH, Kim S, Park Y, Marzi A, Pöhlmann S.** (2009) Proteolytic activation of the 1918 influenza virus hemagglutinin. *J Virol* **83**(7):3200-3211
- Chakraborti S, Prabakaran P, Xiao X, Dimitrov DS.** (2005) The SARS coronavirus S glycoprotein receptor binding domain: fine mapping and functional characterization. *Virol J* **2**:73

- Chan VS, Chan KY, Chen Y, Poon LL, Cheung AN, Zheng B, Chan KH, Mak W, Ngan HY, Xu X, Scream G, Tam PK, Austyn JM, Chan LC, Yip SP, Peiris M, Khoo US, Lin CL.** (2006) Homozygous L-SIGN (CLEC4M) plays a protective role in SARS coronavirus infection. *Nat Genet* **38**:38–46
- Chandran K, Sullivan NJ, Felbor U, Whelan SP, Cunningham JM.** (2005) Endosomal proteolysis of the Ebola virus glycoprotein is necessary for infection. *Science* **308**(5728):1643-1645
- Chen X, Zhou B, Li M, Liang X, Wang H, Yang G, Wang H, Le X.** (2004) Serology of severe acute respiratory syndrome: implications for surveillance and outcome. *J Infect Dis* **189**:1158-1163
- Chiu SS, Chan KH, Chu KW, Kwan SW, Guan Y, Poon LL & Peiris JS** (2005) Human coronavirus NL63 infection and other coronavirus infections in children hospitalized with acute respiratory disease in Hong Kong China. *Clin Infect Dis* **40**:1721–1729
- Choi SY, Bertram S, Glowacka I, Park YW, Pöhlmann S.** (2009) Type II transmembrane serine proteases in cancer and viral infections. *Trends Mol Med* **15**(7):303-312
- Colman PM and Lawrence MC.** (2003). The structural biology of type I viral membrane fusion. *Nat Rev Mol Cell Biol* **4**:309-319
- Corvol P, Williams TA, Soubrier F.** (1995) Peptidyl dipeptidase A: Angiotensin I-converting enzyme. *Methods Enzymol* **248**: 283–305
- de Groot RJ, Ziebuhr J, Poon LL, Woo PC, Talbot PJ, Rottier PJM, Holmes KV, Baric R, Perlman S, Enjuanes L, Gorbatenko AE.** (2008) Taxonomic proposal to the ICTV Executive Committee. Revision of the family Coronaviridae. International Committee on Taxonomy of Viruses. http://talk.ictvonline.org/files/ictv_official_taxonomy_updates_since_the_8th_report/m/vertebrate-2008/1230/download.aspx
- de Haan CA, Stadler K, Godeke GJ, Bosch BJ, Rottier PJ.** (2004) Cleavage inhibition of the murine coronavirus spike protein by a furin-like enzyme affects cell-cell but not virus-cell fusion. *J Virol* **78**(11):6048-6054
- Delmas B, Gelfi J, L'Haridon R, Vogel LK, Sjostrom H, Noren O & Laude H** (1992) Aminopeptidase N is a major receptor for the enteropathogenic coronavirus TGEV. *Nature* **357**:417–420
- Ding Y, He L, Zhang Q, Huang Z, Che X, Hou J, Wang H, Shen H, Qiu L, Li Z, Geng J, Cai J, Han H, Li X, Kang W, Weng D, Liang P, Jiang S** (2004) Organ distribution of severe acute respiratory syndrome (SARS) associated coronavirus (SARS-CoV) in SARS patients: implications for pathogenesis and virus transmission pathways. *J Pathol* **203**:622–630

- Dolnik O, Volchkova V, Garten W, Carbonnelle C, Becker S, Kahnt J, Ströher U, Klenk HD, Volchkov V.** (2004) Ectodomain shedding of the glycoprotein GP of Ebola virus. *EMBO J* **23**(10):2175-2184
- Donaldson EF, Yount B, Sims AC, Burkett S, Pickles RJ, Baric RS.** (2008) Systematic assembly of a full-length infectious clone of human coronavirus NL63. *J Virol* **82**(23):11948-11957
- Donaldson SH, Hirsh A, Li DC, Holloway G, Chao J, Boucher RC, Gabriel SE.** (2002) Regulation of the epithelial sodium channel by serine proteases in human airways. *J Biol Chem* **277**:8338-8345
- Donoghue M, Hsieh F, Baronas E, Godbout K, Gosselin M, Stagliano N, Donovan M, Woolf B, Robison K, Jeyaseelan R, Breitbart RE.** (2000) Acton SA novel angiotensin-converting enzyme-related carboxypeptidase (ACE2) converts angiotensin I to angiotensin 1-9. *Circ Res* **87**(5):E1-9
- Douglas GC, O'Bryan MK, Hedger MP, Lee DK, Yarski MA, Smith AI, Lew RA.** (2004) The novel angiotensin-converting enzyme (ACE) homolog, ACE2, is selectively expressed by adult Leydig cells of the testis. *Endocrinology* **145**:4703–4711
- Drosten C, Gunther S, Preiser W, van der Werf S, Brodt HR, Becker S, Rabenau H, Panning M, Kolesnikova L, Fouchier RA, Berger A, Burguiere AM, Cinatl J, Eickmann M, Escriou N, Grywna K, Kramme S, Manuguerra JC, Müller S, Rickerts V, Sturmer M, Vieth S, Klenk HD, Osterhaus AD, Schmitz H, Doerr H-W.** (2003) Identification of a novel coronavirus in patients with severe acute respiratory syndrome. *N Engl J Med* **348**(20):1967-76
- Du L, He Y, Zhou Y, Liu S, Zheng BJ, Jiang S.** (2009) The spike protein of SARS-CoV-a target for vaccine and therapeutic development. *Nat Rev Microbiol* **7**(3):226-236
- Dutch RE, Jardetzky TS, Lamb RA.** (2000) Virus membrane fusion proteins: biological machines that undergo a metamorphosis. *Biosci Rep* **20**(6):597-612
- Eckert DM, Kim PS.** (2001) Mechanism of viral membrane fusion and its inhibition. *Annu Rev Biochem* **70**:777-810
- Eickmann M, Becker S, Klenk HD, Doerr HW, Stadler K, Censini S, Guidotti S, Massignani V, Scarselli M, Mora M, Donati C, Han J.H, Song HC, Abrignani S, Covacci A, Rappuoli R.** (2003) Phylogeny of the SARS coronavirus. *Science* **302**(5650):1504-1505
- Follis KE, York J, Nunberg JH.** (2006) Furin cleavage of the SARS coronavirus spike glycoprotein enhances cell-cell fusion but does not affect virion entry. *Virology* **350**(2):358-69

- Fouchier RA M, Kuiken T, Schutten M, van Amerongen G, van Doornum GJJ, van den Hoogen BG, Peiris M, Lim W, Stöhr K, Osterhaus ADME.** (2003) Aetiology: Koch's postulates fulfilled for SARS virus. *Nature* **423**:240
- Fouchier RA, Hartwig NG, Bestebroer TM, Niemeyer B, de Jong JC, Simon JH, Osterhaus AD** (2004) A previously undescribed coronavirus associated with respiratory disease in humans. *Proc Natl Acad Sci U S A* **101**:6212–6216
- Gallagher TM, Buchmeier MJ.** (2001) Coronavirus spike proteins in viral entry and pathogenesis. *Virology* **279**(2):371-374
- Garten W, Klenk HD.** (1999) Understanding influenza virus pathogenicity. *Trend Microbiol* **7**:99-100
- Golden JW, Linke J, Schmeichel S, Thoemke K, Schiff LA.** (2002) Addition of exogenous protease facilitates reovirus infection in many restrictive cells. *J Virol* **76**(15):7430-7443
- Gonzalez JM, Gomez-Puertas P, Cavanagh D, Gorbelenya AE, Enjuanes L.** (2003) A comparative sequence analysis to revise the current taxonomy of the family Coronaviridae. *Arch Virol* **148**:2207–2235
- Gorbelenya AE, Enjuanes L, Ziebuhr J, Snijder EJ.** (2006). Nidovirales: Evolving the largest RNA virus genome. *Virus Research* **117**:17-37
- Guan Y, Zheng BJ, He YQ, Liu XL, Zhuang ZX, Cheung CL, Luo SW, Li PH, Zhang LJ, Guan YJ, Butt KM, Wong KL, Chan KW, Lim W, Shortridge KF, Yuen KY, Peiris JS, Poon LL.** (2003) Isolation and characterization of viruses related to the SARS coronavirus from animals in southern China. *Science* **302**:276-278
- Haga S, Yamamoto N, Nakai-Murakami C, Osawa Y, Tokunaga K, Sata T, Yamamoto N, Sasazuki T, Ishizaka Y.** (2008) Modulation of TNF-alpha-converting enzyme by the spike protein of SARS-CoV and ACE2 induces TNF-alpha production and facilitates viral entry. *Proc Natl Acad Sci U S A* **105**(22):7809-7814
- Haga S, Nagata N, Okamura T, Yamamoto N, Sata T, Yamamoto N, Sasazuki T, Ishizaka Y.** (2010) TACE antagonists blocking ACE2 shedding caused by the spike protein of SARS-CoV are candidate antiviral compounds. *Antiviral Res* **85**(3):551-555
- Hallenberger S, Bosch V, Angliker H, Shaw E, Klenk HD, Garten W.** (1992) Inhibition of furin-mediated cleavage activation of HIV-1 glycoprotein gp160. *Nature* **360**(6402):358-361
- Hallenberger S, Moulard M, Sordel M, Klenk HD, Garten W.** (1997) The role of eukaryotic subtilisin-like endoproteases for the activation of human immunodeficiency virus glycoproteins in natural host cells. *J Virol* **71**(2):1036-1045

- Hamming I, Timens W, Bulthuis ML, Lely AT, Navis GJ, van Goor H.** (2004) Tissue distribution of ACE2 protein, the functional receptor for SARS coronavirus. A first step in understanding SARS pathogenesis. *J Pathol* **203**:631–637
- Harrison SC.** (2005) Mechanism of membrane fusion by viral envelope proteins. *Adv Virus Res* **65**:231-269
- He Y, Zhou Y, Liu S, Kou Z, Li W, Farzan M, Jiang S** (2004a) Receptor-binding domain of SARS-CoV spike protein induces highly potent neutralizing antibodies: implication for developing subunit vaccine. *Biochem Biophys Res Commun* **324**:773–781
- He Y, Zhou Y, Wu H, Luo B, Chen J, Li W, Jiang S** (2004b) Identification of immunodominant sites on the spike protein of severe acute respiratory syndrome (SARS) coronavirus: implication for developing SARS diagnostics and vaccines. *J Immunol* **173**:4050–4057
- He Y, Lu H, Siddiqui P, Zhou Y, Jiang S** (2005) Receptor-binding domain of severe acute respiratory syndrome coronavirus spike protein contains multiple conformation-dependent epitopes that induce highly potent neutralizing antibodies. *J Immunol* **174**:4908–4915
- Hofmann H, Pöhlmann S.** (2004) Cellular entry of the SARS coronavirus. *Trends Microbiol* **12**(10):466-472
- Hofmann H, Geier M, Marzi A, Krumbiegel M, Peipp M, Fey GH, Gramberg T, Pöhlmann S.** (2004a) Susceptibility to SARS coronavirus S protein-driven infection correlates with expression of angiotensin converting enzyme 2 and infection can be blocked by soluble receptor. *Biochem Biophys Res Commun* **319**:1216–1221
- Hofmann H, Hattermann K, Marzi A, Gramberg T, Geier M, Krumbiegel M, Kuaté S, Überla K, Niedrig M, Pöhlmann S.** (2004b) S protein of severe acute respiratory syndrome-associated coronavirus mediates entry into hepatoma cell lines and is targeted by neutralizing antibodies in infected patients. *J Virol* **78**(12):6134-6142
- Hofmann H, Pyrc K, van der HL, Geier M, Berkhout B, Pöhlmann S.** (2005) Human coronavirus NL63 employs the severe acute respiratory syndrome coronavirus receptor for cellular entry. *Proc Natl Acad Sci USA* **102**:7988–7993
- Hofmann H, Simmons G, Rennekamp AJ, Chaipan C, Gramberg T, Heck E, Geier M, Wegele A, Marzi A, Bates P, Pöhlmann S.** (2006) Highly conserved regions within the spike proteins of human coronaviruses 229E and NL63 determine recognition of their respective cellular receptors. *J Virol* **80**(17):8639-52
- Holmes KV, Enjuanes L.** (2003) The SARS Coronavirus: A Postgenomic Era. *Science* **300**:1377-1378
- Holmes KV.** (2003) SARS coronavirus: a new challenge for prevention and therapy. *Journal of Clinical Investigation* **111**(11):1605-1609

- Holmes KV.** (2003). SARS-Assoziates Coronavirus. *N Engl J Med* **348**(20):194
- Hoxie JA, Alpers JD, Rackowski JL, Huebner K, Haggarty BS, Cedarbaum AJ, Reed JC.** (1986) Alterations in T4 (CD4) protein and mRNA synthesis in cells infected with HIV. *Science* **234**(4780):1123-1127
- Huang IC, Bosch BJ, Li F, Li W, Lee KH, Ghiran S, Vasilieva N, Dermody TS, Harrison SC, Dormitzer PR, Farzan M, Rottier PJ, Choe H.** (2006) SARS coronavirus, but not human coronavirus NL63, utilizes cathepsin L to infect ACE2-expressing cells. *J Biol Chem* **281**(6):3198-3203
- Imai Y, Kuba K, Rao S, Huan Y, Guo F, Guan B, Yang P, Sarao R, Wada T, Leong-Poi H, Crackower MA, Fukamizu A, Hui CC, Hein L, Uhlig S, Slutsky AS, Jiang C, Penninger JM.** (2005) Angiotensin-converting enzyme 2 protects from severe acute lung failure. *Nature* **436**:112–116
- Imai Y, Kuba K, Penninger JM.** (2008) The discovery of angiotensin-converting enzyme 2 and its role in acute lung injury in mice. *Exp Physiol* **93**:543–548
- Ingallinella P, Bianchi E, Finotto M, Cantoni G, Eckert DM, Supekar VM, Bruckmann C, Carfi A, Pessi A** (2004) Structural characterization of the fusion-active complex of severe acute respiratory syndrome (SARS) coronavirus. *Proc Natl Acad Sci USA* **101**:8709–8714
- Isaacs D, Flowers D, Clarke JR, Valman HB, MacNaughton MR.** (1983) Epidemiology of coronavirus respiratory infections. *Arch Dis Child* **58**:500–503
- Jia HP, Look DC, Tan P, Shi L, Hickey M, Gakhar L, Chappell MC, Wohlford-Lenane C, McCray P B Jr.** (2009) Ectodomain shedding of angiotensin converting enzyme 2 in human airway epithelia. *Am. J. Physiol. Lung Cell Mol Physiol* **297**:L84–L96
- Kam YW, Okumura Y, Kido H, Ng LF, Bruzzone R, Altmeier R.** (2009) Cleavage of the SARS coronavirus spike glycoprotein by airway proteases enhances virus entry into human bronchial epithelial cells in vitro. *PLoS One* **4**(11):e7870
- Kido H, Yokogoshi Y, Sakai K, Tashiro M, Kishino Y, Fukutomi A, Katunuma N.** (1992) Isolation and characterization of a novel trypsin-like protease found in rat bronchiolar epithelial Clara cells. A possible activator of the viral fusion glycoprotein. *J Biol Chem* **267**(19):13573-13579
- Kido H, Okumura Y, Yamada H, Le TQ, Yano M.** (2007) Proteases essential for human influenza virus entry into cells and their inhibitors as potential therapeutic agents. *Curr Pharm Des* **13**(4):405-414
- Kielian M** (2006) Class II virus membrane fusion proteins. *Virology* **344**:38–47
- Kielian M, Rey FA** (2006) Virus membrane-fusion proteins: more than one way to make a hairpin. *Nat Rev Microbiol* **4**:67–76

- Kim TS, Heinlein C, Hackman RC, Nelson PS.** (2006) Phenotypic analysis of mice lacking the Tmprss2-encoded protease. *Mol Cell Biol* **26**(3):965-975
- Kirschke H, Langner J, Wiederanders B, Ansorge S, Bohley P.** (1977) Cathepsin L. A new proteinase from rat-liver lysosomes. *Eur J Biochem* **74**(2):293-301
- Klenk HD and Garten W.** (1994) Host cell protease controlling virus pathogenicity; *Trends Microbiol* **2**:39-43
- Klumperman J, Locker JK, Meijer A, Horzinek MC, Geuze HJ, Rottier PJ.** (1994) Coronavirus M proteins accumulate in the Golgi complex beyond the site of virion budding. *J Virol* **68**:6523-6534
- Kominami E, Tsukahara T, Hara K, Katunuma N.** (1988) Biosyntheses and processing of lysosomal cysteine proteinases in rat macrophages. *FEBS Lett* **231**(1):225-228
- Ksiazek TG, Erdmann D, Goldsmith CS, Zaki SR, Peret T, Emery S, Tong S, Urbani C, Comer JA, Lim W, Rollin PE, Dowell SF, Ling AE, Humphrey CD, Shieh WJ, Guaner J, Paddock CD, Rota P, Fielda B, DeRisi J, Yang JY, Cox N, Hughes JM, LeDuc JW, Bellini WJ, Anderson LJ.** SARS Working Group. (2003) A novel coronavirus associated with severe acute respiratory syndrome; *N Engl J Med* **348**(20):1953-1966
- Kuba K, Imai Y, Rao S, Gao H, Guo F, Guan B, Huan Y, Yang P, Zhang Y, Deng W, Bao L, Zhang B, Liu G, Wang Z, Chappell M, Liu Y, Zheng D, Leibbrandt A, Wada T, Slutsky AS, Liu D, Qin C, Jiang C, Penninger JM.** (2005) A crucial role of angiotensin converting enzyme 2 (ACE2) in SARS coronavirus-induced lung injury. *Nat Med* **11**:875-879
- Kuba K, Imai Y, Rao S, Jiang C, Penninger JM.** (2006) Lessons from SARS: control of acute lung failure by the SARS receptor ACE2. *J Mol Med* **84**:814-820
- Kuhn JH, Li W, Choe H, Farzan M.** (2004) Angiotensin-converting enzyme 2: a functional receptor for SARS coronavirus. *Cell Mol Life Sci* **61**:2738-2743
- Kuiken T, Fouchier RA, Schutten M, Rimmelzwaan GF, van Amerongen G, van Riel D, Laman JD, de Jong T, van Doornum G, Lim W, Ling AE, Chan PK, Tam JS, Zambon MC, Gopal R, Drosten C, van der Werf S, Escriou N, Manuguerra JC, Stohr K, Peiris JS, Osterhaus AD.** (2003) Newly discovered coronavirus as the primary cause of severe acute respiratory syndrome. *Lancet* **362**(9380):263-270
- Lai MM, Cavanagh D.** (1997) The molecular biology of coronaviruses. *Adv Virus Res* **48**:1-100
- Lai, MMC, Holmes, KV,** 2001. Coronaviridae: the viruses and their replication, In: Knipe, D, Howley, PM, (Eds.), *Fields' Virology*, 4th ed. Lippincott Williams and Wilkins, Philadelphia, 1163-1185

- Lama J.** (2003) The physiological relevance of CD4 receptor down-modulation during HIV infection. *Curr HIV Res* **1**:167-184
- Lambert DW, Yarski M, Warner FJ, Thornhill P, Parkin ET, Smith AI, Hooper NM, Turner AJ.** (2005) Tumor necrosis factor-alpha convertase (ADAM17) mediates regulated ectodomain shedding of the severe-acute respiratory syndrome-coronavirus (SARS-CoV) receptor, angiotensin-converting enzyme-2 (ACE2). *J Biol Chem* **280**(34):30113-30119
- Larson HE, Reed SE, Tyrrell DA.** (1980) Isolation of rhinoviruses and coronaviruses from 38 colds in adults. *J Med Virol* **5**:221–229
- Lau SK, Woo PC, Li KS, Huang Y, Tsui HW, Wong BH, Wong SS, Leung SY, Chan KH, Yuen KY.** (2005) Severe acute respiratory syndrome coronavirus-like virus in Chinese horseshoe bats. *Proc Natl Acad Sci U S A* **102**:14040-14045
- Levesque K, Finzi A, Binette J, Cohen EA.** (2004) Role of CD4 receptor downmodulation during HIV-1 infection. *Curr HIV Res* **2**(1):51-59
- Li W, Moore MJ, Vasilieva N, Sui J, Wong SK, Berne MA, Somasundaran M, Sullivan JL, Luzuriaga K, Greenough TC, Choe H, Farzan M** (2003) Angiotensin-converting enzyme 2 is a functional receptor for the SARS coronavirus. *Nature* **426**:450–454
- Li W, Greenough TC, Moore MJ, Vasilieva N, Somasundaran M, Sullivan JL, Farzan M, Choe H.** (2004) Efficient replication of severe acute respiratory syndrome coronavirus in mouse cells is limited by murine angiotensin-converting enzyme 2. *J Virol* **78**:11429–11433
- Li F, Li W, Farzan M, Harrison SC.** (2005a) Structure of SARS coronavirus spike receptor-binding domain complexed with receptor I2005. *Science* **309**:1864–1868
- Li W, Shi Z, Yu M, Ren W, Smith C, Epstein JH, Wang H, Crameri G, Hu Z, Zhang H, Zhang J, McEachern J, Field H, Daszak P, Eaton BT, Zhang S, Wang LF.** (2005b) Bats are natural reservoirs of SARS-like coronaviruses. *Science* **310**:676-679
- Li W, Zhang C, Sui J, Kuhn JH, Moore MJ, Luo S, Wong SK, Huang IC, Xu K, Vasilieva N, Murakami A, He Y, Marasco WA, Guan Y, Choe H, Farzan M** (2005c) Receptor and viral determinants of SARS-coronavirus adaptation to human ACE2. *EMBO J* **24**:1634–1643
- Li W, Sui J, Huang IC, Kuhn JH, Radoshitzky SR, Marasco WA, Choe H, Farzan M.** (2007) The S proteins of human coronavirus NL63 and severe acute respiratory syndrome coronavirus bind overlapping regions of ACE2. *Virology* **367**:367–374
- Lin HX, Feng Y, Wong G, Wang L, Li B, Zhao X, Li Y, Smaill F, Zhang C** (2008) Identification of residues in the receptor-binding domain (RBD) of the spike protein of human

- coronavirus NL63 that are critical for the RBD-ACE2 receptor interaction. *J Gen Virol* **89**:1015–1024
- Liu S, Xiao G, Chen Y, He Y, Niu J, Escalante CR, Xiong H, Farmar J, Debnath AK, Tien P, Jiang S** (2004) Interaction between heptad repeat 1 and 2 regions in spike protein of SARS-associated coronavirus: implications for virus fusogenic mechanism and identification of fusion inhibitors. *Lancet* **363**:938–947
- Lucas JM, True L, Hawley S, Matsumura M, Morrissey C, Vessella R, Nelson PS.** (2008) The androgen-regulated type II serine protease TMPRSS2 is differentially expressed and mislocalized in prostate adenocarcinoma. *J Pathol* **215**(2):118-125
- Mangasarian A, Foti M, Aiken C, Chin D, Carpentier JL, Trono D.** (1997) The HIV-1 Nef protein acts as a connector with sorting pathways in the Golgi and at the plasma membrane. *Immunity* **6**:67-77
- Maréchal V, Clavel F, Heard JM, Schwartz O.** (1998) Cytosolic Gag p24 as an index of productive entry of human immunodeficiency virus type 1. *J Virol* **72**(3):2208-2212
- Marra MA, Jones SJ, Astell CR, Holt RA, Brooks-Wilson A, Butterfield YS, Khattri J, Asano JK, Barber SA, Chan SY, Cloutier A, Coughlin SM, Freeman D, Girn N, Griffith OL, Leach SR, Mayo M, McDonald H, Montgomery SB, Pandoh PK, Petrescu AS, Robertson AG, Schein JE, Siddiqui A, Smailus DE, Stott JM, Yang GS, Plummer F, Andonov A, Artsob H, Bastien N, Bernard K, Booth T.F, Bowness D, Czub M, Drebot M, Fernando L, Flick R, Garbutt M, Gray M, Grolla A, Jones S, Feldmann H, Meyers A, Kabani A, Li Y, Normand S, Stroher U, Tipples GA, Tyler S, Vogrig R, Ward D, Watson B, Brunham RC, Krajden M, Petric M, Skowronski DM, Upton C, Roper RL.** (2003) The Genome sequence of the SARS-associated coronavirus. *Science* **300**:1399-1404
- Masters PS.** (2006) The molecular biology of coronaviruses. *Adv Virus Res* **66**:193–292
- Matsuyama S, Ujike M, Morikawa S, Tashiro M, Taguchi F.** (2005) Protease mediated enhancement of severe acute respiratory syndrome coronavirus infection. *Proc Natl Acad Sci U S A* **102**:12543-12547
- Matsuyama S, Taguchi F.** (2009) Two-step conformational changes in a coronavirus envelope glycoprotein mediated by receptor binding and proteolysis. *J Virol* **83**(21):11133-11141
- Matsuyama S, Nagata N, Shirato K, Kawase M, Takeda M, Taguchi F.** (2010) Efficient activation of SARS coronavirus spike protein by the transmembrane protease, TMPRSS2. *J Virol* [Epub ahead of print]
- McBride CE, Li J, Machamer CE** (2007) The cytoplasmic tail of the severe acute respiratory syndrome coronavirus spike protein contains a novel endoplasmic reticulum retrieval signal that binds COPI and promotes interaction with membrane protein. *J Virol* **81**:2418–2428

- Meier C, Aricescu AR, Assenberg R, Aplin RT, Gilbert, RJC, Grimes JM, Stuart DI.** (2006) The crystal structure of ORF-9b, a lipid binding protein from the SARS coronavirus. *Structure* **14**:1157-1165
- Molloy SS, Bresnahan PA, Leppla SH, Klimpel KR, Thomas G.** (1992) Human furin is a calcium-dependent serine endoprotease that recognizes the sequence Arg-X-X-Arg and efficiently cleaves anthrax toxin protective antigen. *J Biol Chem* **267**(23):16396-16402
- Molloy SS, Thomas L, VanSlyke JK, Stenberg PE, Thomas G.** (1994) Intracellular trafficking and activation of the furin proprotein convertase: localization to the TGN and recycling from the cell surface. *EMBO Journal* **13**:18-33
- Molloy SS, Anderson ED, Jean F, Thomas G.** (1999) Bi-cycling the furin pathway: from TGN localization to pathogen activation and embryogenesis. *Trends in Cell Biology* **9**:28-35
- Mossel EC, Wang J, Jeffers S, Edeen KE, Wang S, Cosgrove GP, Funk CJ, Manzer R, Miura TA, Pearson LD, Holmes KV, Mason RJ.** (2008) SARS-CoV replicates in primary human alveolar type II cell cultures but not in type I-like cells. *Virology* **372**:127-135
- Murakami M, Towatari T, Ohuchi M, Shiota M, Akao M, Okumura Y, Parry MA, Kido H.** (2001) Mini-plasmin found in the epithelial cells of bronchioles triggers infection by broad-spectrum influenza A viruses and Sendai virus. *Eur J Biochem* **268**(10):2847-2855
- Nagai Y. and Klenk HD.** (1977) Activation of precursors to both glycoproteins of Newcastle disease virus by proteolytic cleavage. *Virology* **77**:125-134
- Nakayama, K.** (1997) Furin - a mammalian subtilisin/kex2p-like endoprotease involved in processing of a wide variety of precursor proteins. *Biochemical Journal* **327**:625-635
- Nal B, Chan C, Kien F, Siu L, Tse J, Chu K, Kam J, Staropoli I, Crescenzo-Chaigne B, Escriou N, van der WS, Yuen KY, Altmeyer R.** (2005) Differential maturation and subcellular localization of severe acute respiratory syndrome coronavirus surface proteins S, M and E. *J Gen Virol* **86**:1423-1434
- Nash TC, Buchmeier MJ.** (1997) Entry of mouse hepatitis virus into cells by endosomal and nonendosomal pathways. *Virology* **233**(1):1-8
- Neumann G, Geisbert TW, Ebihara H, Geisbert JB, Daddario-DiCaprio KM, Feldmann H, Kawaoka Y.** (2007) Proteolytic processing of the Ebola virus glycoprotein is not critical for Ebola virus replication in nonhuman primates. *J Virol* **81**(6):2995-2998
- Neumann G, Noda T, Kawaoka Y.** (2009) Emergence and pandemic potential of swine-origin H1N1 influenza virus. *Nature* **459**(7249):931-939
- Nie Y, Wang P, Shi X, Wang G, Chen J, Zheng A, Wang W, Wang Z, Qu X, Luo M, Tan L, Song X, Yin X, Chen J, Ding M, Deng H.** (2004) Highly infectious SARS-CoV

- pseudotyped virus reveals the cell tropism and its correlation with receptor expression. Biochem Biophys Res Commun **321**:994–1000
- Nishimura Y, Kawabata T, Kato K.** (1988) Identification of latent procathepsins B and L in microsomal lumen: characterization of enzymatic activation and proteolytic processing in vitro. Arch Biochem Biophys **261**(1):64-71
- Ohnishi K, Sakaguchi M, Kaji T, Akagawa K, Taniyama T, Kasai M, Tsunetsugu-Yokota Y, Oshima M, Yamamoto K, Takasuka N, Hashimoto S, Ato M, Fujii H, Takahashi Y, Morikawa S, Ishii K, Sata T, Takagi H, Itamura S, Odagiri T, Miyamura T, Kurane I, Tashiro M, Kurata T, Yoshikura H, Takemori T.** (2005) Immunological detection of severe acute respiratory syndrome coronavirus by monoclonal antibodies. Jpn J Infect Dis **58**(2):88-94
- Opstelten DJ, Raamsman MJ, Wolfs K, Horzinek MC, Rottier PJ:** (1995) Envelope glycoprotein interactions in coronavirus assembly. J Cell Biol 131:339-349
- Paoloni-Giacobino A, Chen H, Peitsch MC, Rossier C, Antonarakis SE.** (1997) Cloning of the TMPRSS2 gene, which encodes a novel serine protease with transmembrane, LDLRA, and SRCR domains and maps to 21q22.3. Genomics **44**(3):309-320
- Peiris JS, Lai ST, Poon LL, Guan Y, Yam LY, Lim W, Nicholls J, Yee WK, Yan WW, Cheung MT, Cheng VC, Chan KH, Tsang DN, Yung RW, Ng TK, Yuen KY; SARS study group.** (2003a) Coronavirus as a possible cause of severe acute respiratory syndrome. Lancet **361**:1319-1325
- Peiris JSM, Chu CM, Cheng VCC, Chan KS, Hung IFN, Poon LLM, Law KI, Tang BSF, Hon TYW, Chan CS, Chan KH, Ng JS, Zheng BJ, Ng WL, Lai RW, Guan Y, Yuen KY.** (2003b) Clinical progression and viral load in a community outbreak of coronavirus-associated SARS pneumonia: a prospective study. Lancet **361**(9371):1767-1772
- Penninger J, Imai Y, Kuba K.** (2008) The discovery of ACE2 and its role in acute lung injury. Exp Physiol **93**(5):543-548
- Perlman S, Netland J.** (2009) Coronaviruses post-SARS: update on replication and pathogenesis. Nat Rev Microbiol **7**(6):439-450
- Poon LLM, Chu DKW, Chan KH, Wong OK, Ellis TM, Leung YHC, Lau SKP, Woo PCY, Suen KY, Yuen KY, Guan Y, Peiris JSM.** (2005) Identification of a novel coronavirus in Bats. J Virol **79**(4):2001-2009
- Prabakaran P, Xiao X, Dimitrov DS.** (2004) A model of the ACE2 structure and function as a SARS-CoV receptor. Biochem. Biophys. Res Commun **314**:235–241
- Pyrc K, Berkhout B, van der Hoek L.** (2007) Identification of new human coronaviruses. Expert Rev Anti Infect Ther **5**:245–253

- Qiu Z, Hingley ST, Simmons G, Yu C, Das Sarma J, Bates P, Weiss SR.** (2006) Endosomal proteolysis by cathepsins is necessary for murine coronavirus mouse hepatitis virus type 2 spike-mediated entry. *J Virol* **80**(12):5768-5776
- Rawlings ND, Barrett AJ.** (1993) Evolutionary families of peptidases. *Biochem J* **290**(1):205-218
- Rawlings ND, Barrett AJ.** (1994) Families of Serine Peptidases. *Methods Enzymol* **244**:19-61
- Rivers TM.** (1937) "Viruses and Koch's Postulates". *J Bacteriol* **33**:1-12
- Roberts A, Paddock C, Vogel L, Butler E, Zaki S, Subbarao K.** (2005) Aged BALB/c mice as a model for increased severity of severe acute respiratory syndrome in elderly humans. *J Virol* **79**(9):5833-5838
- Roebroek AJ, Schalken JA, Bussemakers MJ, van Heerikhuizen H, Onnekink C, Debruyne FM, Bloemers HP, Van de Ven WJ.** (1986a) Characterization of human c-fes/fps reveals a new transcription unit (fur) in the immediately upstream region of the proto-oncogene. *Molecular Biology Reports* **11**:117-125
- Roebroek AJ, Schalken JA, Leunissen JA, Onnekink C, Bloemers HP, Van de Ven WJ.** (1986b) Evolutionary conserved close linkage of the c-fes/fps protooncogene and genetic sequences encoding a receptor-like protein. *EMBO Journal* **5**:2197-2202
- Roebroek AJ, Creemers JW, Ayoubi TA, Van de Ven WJ.** (1994) Furin-mediated proprotein processing activity: involvement of negatively charged amino acid residues in the substrate binding region. *Biochimie* **76**(3-4):210-216
- Rota PA, Oberste MS, Monroe SS, Nix WA, Campagnoli R, Icenogle JP, Penaranda S, Bankamp B, Maher K, Chen MH, Tong S, Tamin A, Lowe L, Frace M, DeRisi JL, Chen Q, Wang D, Erdman DD, Peret TC, Burns C, Ksiazek TG, Rollin PE, Sanchez A, Liffick S, Holloway B, Limor J, McCaustland K, Olsen-Rasmussen M, Fouchier R, Günther S, Osterhaus AD, Drosten C, Pallansch MA, Anderson LJ, Bellini WJ.** (2003) Characterization of a novel coronavirus associated with severe acute respiratory syndrome. *Science* **300**:1394-1399
- Rota PA, Oberste MS, Monroe SS, Nix WA, Campagnoli R, Icenogle JP, Penaranda S, Bankamp B, Maher K, Chen MH, Tong S, Tamin A, Lowe L, Frace M, DeRisi JL, Chen Q, Wang D, Erdman DD, Peret TC, Burns C, Ksiazek TG, Rollin PE, Sanchez A, Liffick S, Holloway B, Limor J, McCaustland K, Olsen-Rasmussen M, Fouchier R, Gunther S, Osterhaus AD, Drosten C, Pallansch MA, Anderson LJ, Bellini WJ.** (2003) Characterization of a novel coronavirus associated with severe acute respiratory syndrome. *Science* **300**(5624):1394-1399
- Sainz B Jr, Rausch JM, Gallaher WR, Garry RF, Wimley WC** (2005) Identification and characterization of the putative fusion peptide of the severe acute respiratory syndrome-associated coronavirus spike protein. *J Virol* **79**:7195-7206

- Santos RA, Frezard F, Ferreira AJ.** (2005) Angiotensin-(1–7): Blood, heart, and blood vessels. *Curr Med Chem Cardiovasc Hematol Agents* **23**:383–391
- Sawicki SG, Sawicki DL, Siddell SG.** (2007) A contemporary view of coronavirus transcription. *J Virol* **81**:20–29
- Siddell S, Wege H, Ter Meulen V.** (1983) The biology of coronaviruses. *J Gen Virol* **64**(4):761–776
- Simmons G, Reeves JD, Rennekamp AJ, Amberg SM, Piefer AJ, Bates P** (2004) Characterization of severe acute respiratory syndrome-associated coronavirus (SARS-CoV) spike glycoprotein-mediated viral entry. *Proc Natl Acad Sci USA* **101**:4240–4245
- Simmons G, Gosalia DN, Rennekamp AJ, Reeves JD, Diamond SL, Bates P.** (2005) Inhibitors of cathepsin L prevent severe acute respiratory syndrome coronavirus entry. *Proc Natl Acad Sci USA* **102**:11876–11881
- Sims AC, Baric RS, Yount B, Burkett SE, Collins PL, Pickles RJ.** (2005) Severe acute respiratory syndrome coronavirus infection of human ciliated airway epithelia: role of ciliated cells in viral spread in the conducting airways of the lungs. *J Virol* **79**(24):15511–15524
- Siu YL, Teoh KT, Lo J, Chan CM, Kien F, Escriou N, Tsao SW, Nicholls JM, Altmeyer R, Peiris JS, Bruzzone R, Nal B.** (2008) The M, E, and N structural proteins of the severe acute respiratory syndrome coronavirus are required for efficient assembly, trafficking, and release of virus-like particles. *J Virol* **82**:11318–11330
- Skeggs LT, Dorer FE, Levine M, Lentz KE, Kahn JR.** (1980) The biochemistry of the renin-angiotensin system. *Adv Exp Med Biol* **130**:1–27
- Skehel JJ, Wiley DC.** (2000) Receptor binding and membrane Fusion in virus entry: the influenza hemagglutinin. *Annu Rev Biochem* **69**:531–569
- Snijder EJ, Bredenbeek PJ, Dobbe JC, Thiel V, Ziebuhr J, Poon LLM, Guan Y, Rozanov M, Spaan WJM, Gorbatenya AE.** (2003) Unique and conserved features of genome and proteome of SARS coronavirus, an early split-off from the Coronavirus Group 2 lineage. *J Mol Biol* **331**:991–1004
- Snijder EJ, van der Meer Y, Zevenhoven-Dobbe J, Onderwater JJ, van der Meulen J, Koerten HK, Mommaas AM.** (2006) Ultrastructure and origin of membrane vesicles associated with the severe acute respiratory syndrome coronavirus replication complex. *J Virol* **80**(12):5927–5940
- Song HC, Seo MY, Stadler K, Yoo BJ, Choo QL, Coates SR, Uematsu Y, Harada T, Greer CE, Polo JM, Pileri P, Eickmann M, Rappuoli R, Abrignani S, Houghton M, Han JH.** (2004) Synthesis and characterization of a native, oligomeric form of recombinant

- severe acute respiratory syndrome coronavirus spike glycoprotein. *J Virol* **78**:10328-10335
- Stadler K, Massignani V, Eickmann M, Becker S, Abrignani S, Klenk H-D, Rappuoli R.** (2003) SARS-Beginning to understand a new virus. *Nat Rev Mikrobiol* **1**(3):209-218
- Steinhauer DA.** (1999) Role of hemagglutinin cleavage for the pathogenicity of influenza virus. *Virology* **258**:1-20
- Stertz S, Reichelt M, Spiegel M, Kuri T, Martinez-Sobrido L, Garcia-Sastre A, Weber F, Kochs G.** (2007) The intracellular sites of early replication and budding of SARS-coronavirus. *Virology* **361**:304-315
- Stieneke-Gröber A, Vey M, Angliker H, Shaw E, Thomas G, Roberts C, Klenk H.D. Garten, W.** (1992) Influenza virus hemagglutinin with multibasic cleavage site is activated by furin, a subtilisin-like endoprotease. *Embo J* **11**:2407-2414
- Stoka V, Turk B, Turk V.** (2005) Lysosomal cysteine proteases: structural features and their role in apoptosis. *IUBMB Life* **57**(4-5):347-353
- Szabo R, Bugge TH.** (2008) Type II transmembrane serine proteases in development and disease. *Int J Biochem Cell Biol* **40**(6-7):1297-1316
- Szabo R, Wu Q, Dickson RB, Netzel-Arnett S, Antalis TM, Bugge TH.** (2003) Type II transmembrane serine proteases. *Thromb Haemost* **90**(2):185-193
- Turk B, Turk D, Turk V.** (2000) Lysosomal cysteine proteases: more than scavengers. *Biochim Biophys Acta* **1477**(1-2):98-111
- Thiel V, Ivanov KA, Putics A, Hertzig T, Schelle B, Bayer S, Weißbrich B, Snijder EJ, Rabenau H, Doerr HW Gorbalyena AE, Ziebuhr J.** (2003) Mechanisms and enzymes involved in SARS coronavirus genome expression. *J General Virol* **84**: 2305-2315
- Tipnis SR, Hooper NM, Hyde R, Karran E, Christie G, Turner AJ.** (2000) A human homolog of angiotensin-converting enzyme: Cloning and functional expression as a captopril-insensitive carboxypeptidase. *J Biol Chem* **275**:33238-33243
- Thomas G.** (2002) Furin at the cutting edge: From protein traffic to embryogenesis and disease. *Nat Rev Mol Cell Biol* **3**:753-766
- To KF, Lo AW.** (2004) Exploring the pathogenesis of severe acute respiratory syndrome (SARS): the tissue distribution of the coronavirus (SARS-CoV) and its putative receptor, angiotensin-converting enzyme 2 (ACE2). *J Pathol* **203**:740-743
- Tresnan DB, Levis R, Holmes KV.** (1996) Feline aminopeptidase N serves as a receptor for feline canine porcine and human coronaviruses in serogroup I. *J Virol* **70**:8669-8674

- Tripet B, Howard MW, Jobling M, Holmes RK, Holmes KV, Hodges RS.** (2004) Structural characterization of the SARS-coronavirus spike S fusion protein core. *J Biol Chem* **279**:20836–20849
- Tyrrell DA, Bynoe ML.** (1965) Cultivation of a Novel Type of Common-cold Virus in Organ Cultures. *Br Med J* **1**(5448):1467-1470
- Tyreill DAJ, Almeida JD, Berry DM, Cunningham CH, Hamre D, Hofstad MS, Mallucci L, McIntosh K.** (1968) Coronaviruses. *Nature London* **220**:650
- Vabret A, Dina J, Gouarin S, Petitjean J, Tripey V, Brouard J, Freymuth F.** (2008) Human (non-severe acute respiratory syndrome) coronavirus infections in hospitalised children in France. *J Paediatr Child Health* **44**:176–181
- Vabret, A., T. Mourez, S. Gouarin, J. Petitjean, and F. Freymuth.** 2003. An outbreak of coronavirus OC43 respiratory infection in Normandy, France. *Clin. Infect. Dis.* **36**:985–989.
- van der Hoek L, Pyrc K, Jebbink MF, Vermeulen-Oost W, Berkhout RJ, Wolthers KC, Wertheim van Dillen PM, Kaandorp J, Spaargaren J, Berkhout B.** (2004) Identification of a new human coronavirus. *Nat Med* **10**:368–373
- van der Hoek L, Sure K, Ihorst G, Stang A, Pyrc K, Jebbink MF, Petersen G, Forster J, Berkhout B, Überla K.** (2005) Croup is associated with the novel coronavirus NL63. *PLoS Med* **2**(8):e240
- van der Hoek L, Sure K, Ihorst G, Stang A, Pyrc K, Jebbink MF, Petersen G, Forster J, Berkhout B, Überla K.** (2006) Human coronavirus NL63 infection is associated with croup. *Adv Exp Med Biol* **581**:485-491
- van der Hoek L, Pyrc K, Berkhout B.** (2006) Human coronavirus NL63, a new respiratory virus. *FEMS Microbiol Rev* **30**(5):760-773
- van der Hoek L.** (2007) Human coronaviruses: what do they cause? *Antivir Ther* **12**:651–658
- van de Ven WJ, Voorberg J, Fontijn R, Pannekoek H, van den Ouwehand AM, van Duijnhoven HL, Roebroek AJ, Siezen RJ.** (1990) Furin is a subtilisin-like proprotein processing enzyme in higher eukaryotes. *Mol Biol Rep* **14**:265-275
- Vey M, Orlich M, Adler S, Klenk HD, Rott R, Garten W.** (1992) Hemagglutinin activation of pathogenic avian influenza viruses of serotype H7 requires the protease recognition motif R-X-K/R-R. *Virology* **88**(1):408-413
- Volchkov VE, Feldmann H, Volchkova VA, Klenk HD.** (1998) Processing of the Ebola virus glycoprotein by the proprotein convertase furin. *Proc Natl Acad Sci U S A* **95**(10):5762-5767

- Voss D, Pfefferle S, Drosten C, Stevermann L, Traggiai E, Lanzavecchia A, Becker S.** (2009) Studies on membrane topology, N-glycosylation and functionality of SARS-CoV membrane protein. *Virol J* **6**:79
- Wang W, Butler EN, Veguilla V, Vassell R, Thomas JT, Moos M Jr, Ye Z, Hancock K, Weiss CD.** (2008) Establishment of retroviral pseudotypes with influenza hemagglutinins from H1, H3 and H5 subtypes for sensitive and specific detection of neutralizing antibodies. *J Virol Method* **153**:111-119
- Watanabe R, Matsuyama S, Shirato K, Maejima M, Fukushi S, Morikawa S, Taguchi F.** (2008) Entry from the cell surface of severe acute respiratory syndrome coronavirus with cleaved S protein as revealed by pseudotype virus bearing cleaved S protein. *J Virol* **82**(23):11985-11991
- Weissenhorn W, Carfi A, Lee KH, Skehel JJ, Wiley DC.** (1998) Crystal structure of the Ebola virus membrane fusion subunit, GP2, from the envelope glycoprotein ectodomain. *Mol Cell* **2**(5):605-616
- Weissenhorn W, Dessen A, Calder LJ, Harrison SC, Skehel JJ, Wiley DC.** (1999) Structural basis for membrane fusion by enveloped viruses. *Mol Membr Biol* **16**(1):3-9
- Weissenhorn W, Hinz A, Gaudin Y.** (2007) Virus membrane fusion. *FEBS Lett* **581**(11):2150-2155
- Wise RJ, Barr PJ, Wong PA, Kiefer MC, Brake AJ, Kaufman RJ.** (1990) Expression of a human proprotein processing enzyme: correct cleavage of the von Willebrand factor precursor at a paired basic amino acid site. *Proc Natl Acad Sci U S A* **87**:9378-9382
- Wool-Lewis RJ, Bates P.** (1999) Endoproteolytic processing of the ebola virus envelope glycoprotein: cleavage is not required for function. *J Virol* **73**(2):1419-1426
- Wong SK, Li W, Moore MJ, Choe H, Farzan M. A** (2004) 193-amino acid fragment of the SARS coronavirus S protein efficiently binds angiotensin-converting enzyme 2. *J Biol Chem* **279**:3197-3201
- Wu XD, Shang B, Yang RF, Yu H, Ma ZH, Shen X, Ji YY, Lin Y, Wu YD, Lin GM, Tian L, Gan XQ, Yang S, Jiang WH, Dai EH, Wang XY, Jiang HL, Xie YH, Zhu XL, Pei G, Li L, Wu JR, Sun B.** (2004) The spike protein of severe acute respiratory syndrome (SARS) is cleaved in virus infected Vero-E6 cells. *Cell Res* **14**:400-406
- Wu K, Li W, Peng G, Li F.** (2009) Crystal structure of NL63 respiratory coronavirus receptor-binding domain complexed with its human receptor. *Proc Natl Acad Sci U S A* **106**(47):19970-19974
- Xiao X, Chakraborti S, Dimitrov AS, Gramatikoff K, Dimitrov DS** (2003) The SARS-CoV S glycoprotein: expression and functional characterization. *Biochem Biophys Res Commun* **312**:1159-1164

- Xu RH, He JF, Evans MR, Peng GW, Field HE, Yu DW, Lee CW, Luo HM, Lin WS, Lin P, Li LH, Liang WJ, Lin JY, Schnur A.** (2004) Epidemiological clues to SARS origin in China. *Emerg Infect Dis* **10**(6):1030-1037
- Xu Y, Lou Z, Liu Y, Pang H, Tien P, Gao GF, Rao Z** (2004) Crystal structure of severe acute respiratory syndrome coronavirus spike protein fusion core. *J Biol Chem* **279**:49414–49419
- Yamaoka K, Masuda K, Ogawa H, Takagi K, Umemoto N, Yasuoka S.** (1998) Cloning and characterization of the cDNA for human airway trypsin-like protease. *J Biol Chem* **273**(19):11895-11901
- Yang ZY, Huang Y, Ganesh L, Leung K, Kong WP, Schwartz O, Subbarao K, Nabel GJ.** (2004) pH-Dependent entry of severe acute respiratory syndrome coronavirus is mediated by the spike glycoprotein and enhanced by dendritic cell transfer through DC-SIGN. *J Virol* **78**:5642–5650
- Yang ZY, Kong WP, Huang Y, Roberts A, Murphy BR, Subbarao K, Nabel GJ.** (2004) A DNA vaccine induces SARS coronavirus neutralization and protective immunity in mice. *Nature* **428**:561-564
- Yao YX, Ren J, Heinen P, Zambon M, Jones IM.** (2004) Cleavage and serum reactivity of the severe acute respiratory syndrome coronavirus spike protein. *J Infect Dis* **190**:91-98
- Yeager CL, Ashmun RA, Williams RK, Cardellicchio CB, Shapiro LH, Look AT & Holmes KV** (1992) Human aminopeptidase N is a receptor for human coronavirus 229E. *Nature* **357**:420–422
- Ziebuhr, J.** (2004) Molecular biology of severe acute respiratory syndrome coronavirus. *Curr Opin Mikrobiol* **7**:412-419
- Zhong NS, Zheng BJ, Li YM, Poon, Xie ZH, Chan KH, Li PH, Tan SY, Chang Q, Xie JP, Liu XQ, Xu J, Li DX, Yuen KY, Peiris, Guan Y.** (2003) Epidemiology and cause of severe acute respiratory syndrome (SARS) in Guangdong, People's Republic of China, in February, 2003. *Lancet* **362**(9393):1353-1358

6. Anhang

Abkürzungsverzeichnis

%	Prozent
A	Alanin
Abb.	Abbildung
ACE	engl.: <i>angiotensin-converting enzyme</i>
ACE2	engl.: <i>angiotensin-converting enzyme 2</i>
ADAM17	engl.: <i>ADAM metallopeptidase domain 17</i>
ANG	Angiotensin
AS	Aminosäure(n)
AT1R	Angiotensin II Typ 1 Rezeptor
AT2R	Angiotensin II Typ 2 Rezeptor
Bat-CoV	Bat-Coronavirus
Bp	Basenpaare
bzw.	beziehungsweise
ca.	circa
CRR	cysteinreiche Region
CTSL	Cathepsin L
CUB	engl.: <i>Cls/Cir, urchin embryonic growth factor and bone morphogenic protein-1 domain</i>
D	Aspartat
DESC	engl.: <i>differentially expressed squamous cell carcinoma gene</i>
ELISA	engl.: <i>enzyme-linked immunosorbent assay</i>
Env	engl.: <i>envelope</i>
ER	Endoplasmatisches Retikulum
<i>et al.</i>	lat.: <i>et alteri</i> (und andere)
FRZ	engl.: <i>frizzled domain</i>
GP	Glykoproteinen
H	Histidin
HA	Hämagglutinin
HCoV-229E	humanes Coronavirus-229E
HCoV-NL63	humanes Coronavirus-NL63
HR	engl.: <i>heptad repeats</i>
HIV	humanes Immundefizienzvirus
Huh-7	humane hepatozelluläre Karzinomzelllinie 7

ICTV	engl.: <i>International Committee of Taxonomy of Viruses</i>
kb	Kilobasen
kDa	Kilodalton
L	Leader-Sequenz
LDLA	engl.: <i>low-density lipoprotein receptor domain class A</i>
MAM	engl.: <i>a meprin, A5 antigen and receptor protein phosphatase μdomain</i>)
MHV	Maus-Hepatitis-Virus
mRNS	<i>messenger</i> Ribonukleinsäure
N	Asparagin
N-Protein	Nukleokasid-Protein
Nef	engl.: <i>negative factor</i>
nm	Nanometer
NSP	Nichtstrukturprotein
ORF	engl.: <i>open reading frame</i> (offener Leserahmen)
PCR	engl.: <i>polymerase chain reaction</i> (Polymerase-Kettenreaktion)
pH	<i>potentia hydrogenii</i>
PMA	Phorbol-Myristat-Aacetat
R	Arginin
RAAS	Renin-Angiotensin-Aldosteron-System
RBD	Rezeptor-Bindungsdomäne
RNS	Ribonukleinsäure
S	Serin
S-Protein	Spike-Protein
SARS-CoV	engl.: <i>acute respiratory syndrome</i> -Coronavirus
SEA	engl.: <i>single sea urchin sperm protein, enteropeptidase, agrin domain</i>
SR	engl.: <i>scavenger receptor cysteine-rich domain</i>
SV5	Simian Virus 5
Tab.	Tabelle
TACE	engl.: <i>tumor necrosis factor-α converting enzyme</i>
TM	Transmembrandomäne
TRS	transkriptionsregulierenden Sequenzen
VLP	engl.: <i>virus like particle</i>
Vpu	engl.: <i>viral protein u</i>

WHO	engl.: <i>World Health Organization</i> , (Weltgesundheitsorganisation)
Wt	Wildtyp
z.B.	zum Beispiel

Danksagung

Herzlichen Dank an Stefan Pöhlmann für die Überlassung des Themas meiner Dissertation, die äußerst aufmerksame Betreuung, seine aufopfernde Art in der Lehre der Naturwissenschaft und die hilfreichen und kritischen Anmerkungen während des Schreibens. Zudem bedanke ich mich für seine Geduld, seine wertvolle Unterstützung und sein Engagement während der letzten Jahre.

Herrn Prof. Dr. T. Pietschmann danke ich herzlich für die Übernahme des Korreferats meiner Dissertation.

Herrn Prof. Dr. T. Schulz und dem ganzen Institut für Virologie danke ich für die immer währende Unterstützung.

Ich bedanke mich für die Kooperation im SARS-Verbund des BMBF, bei der Arbeitsgruppe von Prof. Dr. Christian Drosten (Susanne Pfefferle, Petra Herzog und Marcel Müller) und von Graham Simmons (Marcus Muench, Juliet Agudelo und Kai Lu).

Bei der ganzen Arbeitsgruppe SPÖ a.k.a. AG Schlemmer: Annika, Christina, Imke, Kerstin, Miriam, Steffi, Teddy bedanke ich mich für die mir erwiesene Unterstützung und Hilfe, die wundervollen Geburtstage (Picknick im FREIEN auf dem MHH-Gelände, das werde ich nie wieder vergessen!!!), die vielen durchlachten Stunden, die Kreuzworträtsel und die Kaffeepausen. Für die täglichen Minuten an der frischen Luft ;-) danke ich Imke. Die produktive und intuitive Zusammenarbeit mit Steffi hat einfach gepasst- danke Dir. Für die stets humorvolle Arbeitsatmosphäre bedanke ich mich bei euch beiden zutiefst. Besonders danke ich Imke, Kerstin, Steffi und Marcel für die Korrekturen meiner Arbeit.

Meinen Freunden, meinen Geschwistern und meiner Patentochter 'Helli' danke ich für die Bereicherung meines Lebens. Insbesondere bedanke ich mich bei meiner Schwester Nelly für ihre fürsorgliche Art während des Schreibens.

Lebenslauf

PERSÖNLICHE DATEN

Name	Ilona Glowacka
Adresse	Dieterichsstraße 16, 30159 Hannover
Geburtstag	30. Juni 1981
Geburtsort	Trzebiatow (Polen)
Staatsangehörigkeit	polnisch

AUSBILDUNG

09/2007- 02/2011	Promotion am Institut für Virologie, Medizinische Hochschule Hannover, Betreuer: Prof. Dr. S. Pöhlmann; Thema: Bedeutung von Wirtszellproteasen für die Infektion mit Severe Acute Respiratory-Coronavirus (SARS-CoV)
01/2007- 09/2007	Diplomarbeit am Institut für Virologie, Medizinische Hochschule Hannover, Betreuer: Prof. Dr. T.F. Schulz; Thema: Funktionelle Bedeutung von zwei konservierten Sequenzmotiven im K15 Protein des Kaposi Sarkoma- assoziierten Herpesvirus (KSHV)
10/2002- 09/2007	Biologiestudium an der Leibniz Universität Hannover, Diplom Hauptfach: Mikrobiologie; 1. Nebenfach: Molekularbiologie; 2. Nebenfach: Virologie, Vordiplom im Januar 2005
02/2006- 06/2006	Biotechnologie an der Landwirtschaftlichen Universität in Poznan, Polen, Stipendium des Deutschen Akademischen Austauschdienstes (DAAD): GoEast
06/2002	Abitur an der IGS Roderbruch Hannover

PRÄSENTATIONEN

Posterpräsentationen	Proteolytic activation of the 1918 influenza virus hemagglutinin. 19th Annual Meeting of the Society for Virology, 18-21 März, 2009, Leipzig, Deutschland SARS- and NL63-coronavirus interactions with angiotensin-converting enzyme 2: Determinants of pathogenicity? The XI th International Nidovirus Symposium, 22-27 Juni, 2008, Oxford, England
Vorträge	Differential downregulation of ACE2 by the spike proteins of SARS-coronavirus and human coronavirus NL63. Virologieseminar, Medizinische Hochschule Hannover, 17. März, 2010, Hannover, Deutschland Differential downregulation of ACE2 by the spike proteins of SARS-coronavirus and human coronavirus NL63. 5th European Meeting On Viral Zoonoses. 26-29 September, 2009, St. Raphaël, Frankreich SARS spike protein is cleaved by TMPRSS2 and cleavage decreases sensitivity to neutralization by antibodies. Virologieseminar, Medizinische Hochschule Hannover, 5. Juni, 2009, Hannover, Deutschland

Publikationen

Erstautor

Glowacka I, Bertram S, Herzog P, Pfefferle S, Steffen I, Muench MO, Simmons G, Hofmann H, Kuri T, Weber F, Eichler J, Drosten C, Pöhlmann S. Differential downregulation of ACE2 by the spike proteins of SARS-coronavirus and human coronavirus NL63. *J Virol.* 2010 Jan;84(2):1198-205.

Bertram S, Glowacka I, Blazejewska P, Soilleux E, Allen P, Danisch S, Steffen I, Choi SY, Park Y, Schneider H, Schughart K, Pöhlmann S. TMPRSS2 and TMPRSS4 facilitate trypsin-independent influenza virus spread in Caco-2 cells. *J Virol.* Oct;84(19):10016-25.

Glowacka I, Bertram S, Allen P, Soilleux E, Pfefferle S, Steffen I, Solomon Tsegaye T, He X, Drosten C, Pöhlmann S. Evidence that TMPRSS2 activates the SARS-coronavirus spike-protein for membrane fusion and reduces viral control by the humoral immune response. *J Virol.* [akzeptiert]

Simmons G, Bertram S, Glowacka I, Steffen I, Chaipan C, Hofmann H, Bates P, Pöhlmann S. Proteolytic activation of the SARS-coronavirus spike-protein: Evidence for an alternative cleavage site and for activation of cell-cell and virus-cell fusion by different host cell proteases. *J Virol.* [akzeptiert]

Koautor

Chaipan C, Kobasa D, Bertram S, Glowacka I, Steffen I, Tsegaye TS, Takeda M, Bugge TH, Kim S, Park Y, Marzi A, Pöhlmann S. Proteolytic activation of the 1918 influenza virus hemagglutinin. *J Virol.* 2009 Apr; 83(7):3200-11.

Kühl A, Münch J, Sauter D, Bertram S, Glowacka I, Steffen I, Specht A, Hofmann H, Schneider H, Behrens G, Pöhlmann S. No evidence for a restriction of retrovirus release by calcium-modulating cyclophilin ligand. *Nat. Med.* 2010 Feb;16(2):155-6.

Chaipan C, Steffen I, Tsegaye TS, Bertram S, Glowacka I, Kato Y, Schmökel J, Münch J, Gerardy-Schahn R, Pöhlmann S. Incorporation of podoplanin into HIV released from HEK-293T cells, but not PBMC, is required for efficient binding to the attachment factor CLEC-2. *Retrovirology.* 2010 May 19;7(1):47.

Pietrek M, Brinkmann MM, Glowacka I, Enlund A, Hävemeier A, Dittrich-Breiholz O, Kracht M, Lewitzky M, Saksela K, Feller SM, Schulz TF. The role of the Kaposi Sarcoma Herpesvirus K15 SH3 binding site in inflammatory signaling and B-cell activation. *J Virol.* Aug;84(16):8231-40.

Zhou Y, Lu K, Pfefferle S, Bertram S, Glowacka I, Drosten C, Pöhlmann S, Simmons G. A Single Asparagine-Linked Glycosylation Site of the SARS-Coronavirus Spike Glycoprotein Facilitates Inhibition by Mannose-Binding Lectin through Multiple Mechanisms. *J Virol.* 2010 Sep;84(17):8753-64.

Kühl A, Banning C, Marzi A, Steffen I, Bertram S, Glowacka I, Stürzl M, Guo J, Feldmann H, Behrens G, Schindler M, Pöhlmann S. The Ebola virus glycoprotein and HIV-1 Vpu employ different strategies to counteract the antiviral factor tetherin. *J Infect Dis.* [akzeptiert]

Reviews und Buchkapitel

Glowacka I, Bertram S, Pöhlmann S. Cellular Entry of the SARS Coronavirus: Implications for Transmission, Pathogenicity and Antiviral Strategies. *Molecular Biology of the SARS-Coronavirus: Viral Entry*, Lal SK (Edt), Springer 2010, ISBN: 978-3-642-03682-8

Choi SY, Bertram S, Glowacka I, Park YW, Pöhlmann S. Type II transmembrane serine proteases in cancer and viral infections. *Trends Mol Med.* 2009 Jul;15(7):303-12

Bertram S, Glowacka I, Steffen I, Kühl A, Pöhlmann S. Novel insights into proteolytic cleavage of influenza virus hemagglutinin. *Rev Med Virol.* 2010 Sep;20(5):298-310

Erklärung

Hierdurch erkläre ich, dass ich meine Dissertation mit dem Titel

**Bedeutung von Wirtszellproteasen für die Infektion mit dem Severe Acute
Respiratory Syndrome-Coronavirus (SARS-CoV)**

selbstständig verfasst und die benutzten Hilfsmittel und Quellen sowie gegebenenfalls die zu Hilfeleistungen herangezogenen Institutionen vollständig angegeben habe.

Die Dissertation wurde nicht schon als Masterarbeit, Diplomarbeit oder andere Prüfungsarbeit verwendet.

Ilona Glowacka

Hannover, den 26.11.2010